ADDIS ABABA UNIVERSITY

SCHOOL OF GRADUATE STUDIES DEPARTMENT OF EARTH SCIENCES

NUMERICAL GROUNDWATER FLOW MODELING OF THE KOBO VALLEY: NORTHERN ETHIOPIA

By

Getaneh Kinfu Hailu

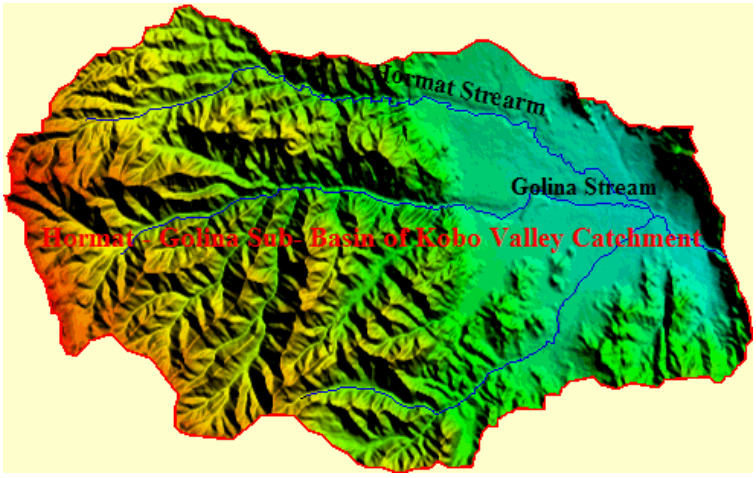

A Thesis Submitted to the School of Graduate Studies of Addis Ababa University in Partial Fulfillment of the Requirements for the Degree of Master of Science in Hydrogeology

June 2010

ADDIS ABABA UNIVERSITY
SCHOOL OF GRADUATE STUDIES DEPARTMENT OF EARTH SCIENCES

NUMERICAL GROUNDWATER FLOW MODELING OF THE KOBO VALLEY: NORTHERN ETHIOPIA

By

Getaneh Kinfu Hailu

A Thesis Submitted to the School of Graduate Studies of Addis Ababa University in Partial Fulfillment of the Requirements for the Degree of Master of Science in Hydrogeology

Advisor: - Tenalem Ayenew (Prof.)

June 2010

ADDIS ABABA UNIVERSITY

SCHOOL OF GRADUATE STUDIES DEPARTMENT OF EARTH SCIENCES

NUMERICAL GROUNDWATER FLOW MODELING OF THE KOBO VALLEY: NORTHERN ETHIOPIA

By

Getaneh Kinfu Hailu

A Thesis Submitted to the School of Graduate Studies of Addis Ababa University in Partial Fulfillment of the Requirements for the Degree of Master of Science in Hydrogeology

Approved by the Board of Examiners**:**

Dr. Balemwal Atenafu (Chairman) _____

Prof. Tenalem Ayenew (Advisor) _____

Ato Paulos Masresha (External Examiner) _____

Ato Sileshi Mamo (External Examiner) _____

ACKNOWLEDGMENTS

I am greatly indebted to my advisor Prof. Tenalem Ayenew, for his excellent guidance, encouragements, and unreserved advice throughout my research work. I highly appreciate his constructive comments and advise in every aspect of my thesis which helped me to come up with right direction of the research.

I would like to thank my instructor Dr. Seifu Kebede and all Earth Science Department of Addis Ababa University instructors for their support in the knowledge of Hydrogeology and Geology.

I greatly thank Ethiopian Water Technology Center (EWTEC) for offering me training on Groundwater modeling which encourages me to choose groundwater modeling for my research work.

I gratefully acknowledge all offices and persons who have given me data for my study. Ethiopian Ministry of Water Resources, National Meteorological Agency, Kobo-Girana Valley Development office and Metaferia Consulting Engineers.

I am most grateful to Mr. Fikadu Debalkie for his encouragement and advice.

I would like to express my deep gratitude to Jilalo Shemsu, Behailu, Kefyalew, Baye Gesese and his friend who helped me a lot during my fieldwork.

My deepest heart-felt gratitude go to my caring wife, Haddas Kebede, for her encouragement, support and love that played important role in my academic life. I also highly appreciate the patience she paid in caring our newly born daughter.

Finally yet importantly, I offer my deepest gratitude to my family, who were the founder of my life and non-stopped support in my career.

Table of Contents

List of tables

List of figures

List of appendices

List of acronyms

ASTER	Advanced Space borne Thermal Emission and Reflection Radiometer
CMB	Chloride Mass Balance
Co-SAERAR	Commission for Sustainable Agriculture and Environmental Rehabilitation in Amhara Region
d	Days
DEM	Digital Elevation Model
DWL	Dynamic Water Level
EIGS	Ethiopian Institute of Geological Survey
ET_o	Potential Evapotranspiration
GES	Geo-Engineering Service
GIS	Geographic Information System
ITCZ	Inter-Tropical Convergence Zone
KGVDP	Kobo-Girana Valley Development Project
m.a.s.l	Meter above sea lvel
MAE	Mean absolute error
ME	Mean error
MCM	Million Cubic Meters
RMS	Root mean square error
RVDP	Raya Valley Development Project
SCS	Soil Conservation Service
SRTM	Shuttle Radar Topographic Mission
SWL	Static Water Level
y	year

Abstract

The study aims to get better understanding of the groundwater flow system of the Hormat-Golina basin using numerical groundwater flow modeling under steady-state condition. The basin comprises inter-mountain valley (Kobo Valley) which is the most fertile irrigable land. The basin is part of the western escarpment of Afar Rift and measures about 811 km^2.

The study was ambitious in the sense that the modeling was conducted with limited data particularly for the highland volcanic part of the basin. Two aquifer units: the fractured basalt and the valley fill sediments aquifer were identified in the basin. The fractured basalt aquifer forms the highland part and underlies the alluvial sediments aquifer. The two-aquifer systems were assumed to be hydraulically connected. Deep groundwater circulation was assumed for the highland volcanic aquifer, because of the absence of shallow groundwater features such as springs and base flow of the rivers.

The groundwater flow system in the two aquifers of the basin was modeled using PMWIN *Pro* (Chiang et al., 1998) as pre-and post processor for MODFLOW (McDonald and Harbaugh, 1988). The model was run for steady-state conditions in unconfined aquifer. The grid cell size of the model was taken 250 x 250m and 500m x 500m for the valley part and the highland volcanic aquifer respectively. Model area and the layer top elevation were delineated by the ASTER DEM processing and use of topographic maps. The hydraulic conductivity values were determined from pumping test data analysis and literature review for the alluvial sediment aquifer and the fractured volcanic aquifer respectively. Recharge was estimated from water balance method.

The model was calibrated using observed hydraulic heads from 37 wells. The model was calibrated to the root mean square error (RMSE) of about 6m and it was sensitive to recharge and hydraulic conductivity. The model simulated water budget showed that the basin receives a total recharge of (in-flow) 48mmy^{-1} and discharge it to the river for steady state condition. Similarly, the model generated total in-flow for the highland volcanic aquifer and the alluvial sediments aquifers were 54mmy^{-1} and 52mmy^{-1} respectively. The model result showed that the valley fill sediment receives more in-flow from horizontal flux (40mmy^{-1}) than other recharge sources. In this study, the model was calibrated but not verified. Thus, the model results obtained should not be interpreted as a perfect simulation rather as system response for reasonable model input parameters.

1. Introduction

1.1 Background

For many years and even at present, utilization of water has preceded without a basic understanding of the hydrologic system and the water budgets. Even, those groundwater development projects that have been under implementation currently were planned based on limited data sources. This does not mean that the entire projects have planning limitations, as it needs its own investigation.

Groundwater is the sub-surface water that occurs beneath the water table in soils and geologic formations that are fully saturated (Freeze and Cherry, 1979). It is one of the most valuable natural resources, which supports human health, economic development, and ecological diversity. Because of its several inherent qualities (e.g., consistent temperature, widespread and continuous availability, excellent natural quality, limited vulnerability, low development cost, drought reliability), it has become an important and dependable source of water supplies in all climatic regions including both urban and rural areas of developed and developing countries (Todd, 2005). Of the 37 Mkm^3 of freshwater estimated to be present on the earth, about 22% exist as groundwater, which constitutes about 97% of all liquid freshwater potentially available for human use (Foster, 1998).

Ground water modeling is recognized nowadays as the best tool to support management of groundwater resources. Groundwater resource management of an aquifer system involves developing a quantitative understanding of the flow processes that operate within the aquifer. Three main futures must be considered: how water enters the aquifer system; how water passes through the aquifer system and how water leaves the aquifer system. Groundwater regime forecasting involves a study of modifications to the flow processes due to changes in any of these futures induced by natural and/or manmade processes.

The study area of this research is Kobo Valley catchment, situated south of Raya Valley in Northern part of Ethiopia. It covers a total area of 811 sq. kilometers and has a perimeter of 128km. The low-lying inter mountain valley part of the area is known by its

high groundwater potential and semi-arid climate. Currently, it is under groundwater source exploitation and investigation mainly for irrigation because of scarce surface water and low annual rainfall that vary seasonally. Most of the previous studies have been concerned more with resource development to meet users' need and alleviate the recurrent draught problem with low attention to the groundwater resource management. Such gaps can be seen even during the current field visit that the boreholes are not monitored, no meteorological stations on the highland part of the catchment and no surface water gauging stations over the area. However, safe groundwater abstraction and proper groundwater management is crucial for sustainability of the resource.

In this thesis, emphasis was given to numerical groundwater flow modeling of the Kobo Valley and the highland volcanic using MODFLOW- 2000 computer code for steady state condition. Thus, proper understanding of the response of the aquifer system to the applied stresses can help to manage the groundwater resources of the valley.

Groundwater modeling is an essential tool to evaluate the groundwater flow and quantifying its potential (Anderson and Woessner, 1992).

1.2 Objectives of the research

General objective

The primary objective of this study is to predict the variations in hydraulic head under different scenarios for planning of sustainable utilization of the groundwater resource by simulating the complex groundwater system using numerical groundwater flow model (Processing Modflow Pro) for steady state condition.

Specific objectives

The specific objectives of the research are:

- To obtain simulated groundwater budget.
- To develop simulated piezometric heads.
- To determine the sensitive parameter or parameters to the model.
- To study the role of boundary conditions on the model.

1.3 Research questions

To address the above objectives, the following research questions are posed:

- Does the conceptual model be transformed to a numeric model, which is capable to simulate the observed conditions of the aquifer system?
- Does the model provide reliable results?
- Do the simulated hydraulic heads match the observed heads?
- Can a steady state groundwater flow model of the area improve the understanding of flow patterns and predict the effect of future abstractions?

1.4. Methodology and materials used

To achieve the intended objective stated in section 1.2, appropriate methods were followed in three stages. The main stages of the activities are presented as pre-field, field work and post field stages (Figure 1.1).

Pre-field work

Previous works and data have been collected from different offices (Ministry of Water Resources, Metaferia Consulting Engineers, and Ethiopian Geological Survey) and were organized to prepare the research proposal. Then, following the appraisal of the proposal all the reliable secondary data were arranged to prepare database and base map of the study area. After identifying the gaps to be filled and data that need field verification, field preparation was conducted that involves acquisition of equipments such as groundwater level measuring device or deep meter and GPS. Literature review related to groundwater modeling was also included in this stage.

Fieldwork

A field trip was conducted to collect secondary data from different sources and primary data from the study area. The primary data includes, measuring groundwater levels, taking readings of borehole locations and elevation using GPS and altimeter, and field verification of the study area and determination of physical boundaries. Discharge of springs and the stream was measured by volumeters and floating method.

The field observation was focused on the description of the geology, lithology, geomorphologic setting, surface water divide, location of recharge and discharge areas. The secondary data such as borehole logs, pumping test data and hydrogeology feasibility report and well completion report were collected from Kobo-Girana Valley Development Project Office.

Post-field work

In this stage data processing and analysis was the main activity. Both the primary and secondary data were processed and analyzed to prepare database and conceptual model which was used for the input of the modeling process.

Geographic Information System (GIS) was used to enter store, retrieve, process and display spatial information in the form of maps or images. Advanced Space borne Thermal Emission and Reflection Radiometer (ASTER) DEM with 30m spatial resolution was processed to delineate the catchment surface water divide, visualize the geomorphology of the area, extract drainage patterns, to define the boundary of the valley, obtain surface elevations and to produce topographic cross- section line.

To analyze pumping test data in order to determine hydraulic parameters such as transmissivity and hydraulic conductivity, Aquifer test software v 3.5 was used. For the preparation of the aquifer top elevation, which is one of the model's input, Global Mapper and Surfer softwares were used.

1.5 Outline of the thesis

The content of the thesis is briefly outlined as follows;

Chapter one : Describes the introduction.

Chapter two : Discusses the review of previous studies.

Chapter three: Describes the study area.

Chapter four : Data processing and analysis.

Chapter five : Depicts the numerical modeling.

Chapter six : Deals with the pumping scenario analysis.

Chapter seven : Results and discussion.

Chapter eight : Conclusion and recommendations.

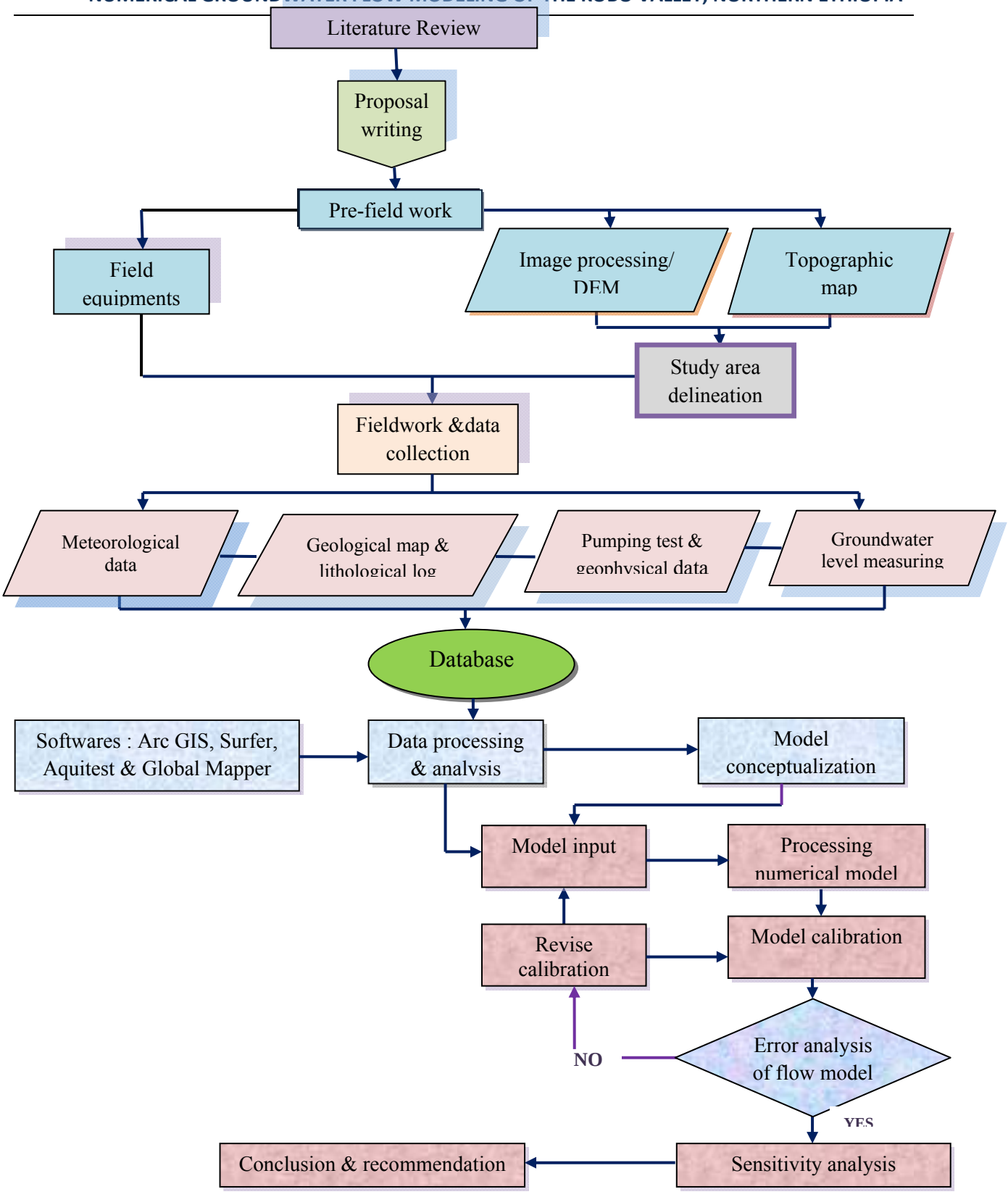

Figure 1.1. Flow chart of the methodology

2. Literature review

2.1 Review of previous study

The low-lying valley part of the area has been known as one of the most drought prone regions in Ethiopia. Historical analysis of rainfall data indicates that, the major part of the valley once every decade is a drought year on the average. In order to alleviate the drought and famine from the area and attain sustainable development, the Commission for Sustainable Agriculture and Environmental Rehabilitation in Amhara Region (Co-SAERAR) studied the Kobo-Girana valley for its groundwater potential and then by implement irrigation through groundwater source (Co-SAERAR & CECE P.L.C, 1999).

Co-SAERAR in 1997 has conducted geophysical surveys in the Kobo-Girana valley and the total alluvial sediment thickness estimated with the VES survey method was about 160 m, 130 m and 97 m in Kobo-Waja-Golesha, Alawuha and Girana basins, respectively. The current study area is part of the Kobo-Waja-Golesha basin.

The Ashengi groups of rocks underlying the alluvial deposits are weathered and highly fractured. It is expected to have a relatively high level of groundwater productivity (IGIP, Germany Consultant, 1997).

The deeply weathered and fractured zones of the volcanic rocks frequently exceed 100meters. Depth to groundwater varies from less than 20meters in the sediment deposit in the western part and along the river courses to over 100 meters in the volcanic rocks. The predominant groundwater flow direction is from west to east coinciding with topographic gradient. The hydraulic gradient of the Kobo basin is 0.012 (Co-SAERAR & CECE P.L.C, 1999).

The groundwater recharge of the Kobo-Robit basin was estimated from three different methods. These are surface water balance method using SCS model, groundwater level fluctuation rate, and Darcy's approach; and the results were 59.3 MCM, 64.8 MCM and 49.82 MCM respectively. The surface water balance method, despite its crude and lumped inputs was found relatively to be comprehensive and practical to estimate the valley's recharge (Co-SAERAR & CECE P.L.C, 1999).

Mesfin Aytenfisu and Engida Zemedagegnehu(2003) suggested that the conclusion made by Co-SAERAR has a limited application. This is because of, the feasibility report was prepared with limited and unreliable data, and the groundwater recharge of the basin was highly over estimated. Since the runoff was estimated from rainfall-runoff model according to Co-SAESAR (1999), the estimation of recharge by this method may not be reliable. In addition, the run- off from the mountainous areas is one of the components of recharges that recharge the groundwater of the valley fill. Estimation of recharge from groundwater level fluctuation can be computed, if there exists systematic water level measurements (daily, weekly, or monthly) of more than one hydrological year records and specific yield of the aquifer is known. However, in the Co-SAESAR (1999) feasibility report random data of measurements of old and recent static water level measurements of some non – operational wells are used. The Darcy approach is the appropriate method to calculate the recharge of the alluvial fill of Kobo basin since relatively there is substantial data for calculation compared to the other methods. The mean annual dynamic groundwater recharge of Hormat-Golina basin of Kobo valley unconsolidated sediment aquifer (alluvial) as subsurface seepage from the western volcanic aquifer and infiltration from rivers was estimated 34.38 MCM/year and 1.8 MCM/year respectively.

It was concluded that the seepage of runoff from the mountainous area at the foot of the escarpment is considerable (RVIDP, Hydrogeology report 1998). If the seepage from runoff is considerable then the water level fluctuation should be considerable during the observed rainy season of August-October 2001. Different to the previous assumption, the major component of recharge to the unconsolidated sediment aquifer of the valley is sub-surface inflow from the western highlands fractured volcanic aquifer.

The total thickness of the sediment aquifer varies from few meters in the extreme west to more than 170 meters in the central part; the material is relatively coarser and thinner in the west and is finer and thicker in the east. The frequency distribution of transmissivity shows that the mean and median are 488 and 428 m^2d^{-1} respectively indicates a normal distribution within the valley. The transmissivity values were computed from the relationship of the aquifer permeability (obtained from four test boreholes) and weighted

average resistivity values of the unconsolidated sediment aquifer. The Hormat-Golina groundwater system flow in southeast direction with a hydraulic gradient of about 0.01 on the western part and it decreases highly to the east along the Golina stream outlet. In the most part of the valley, the groundwater is shallow depth varying from 10-30 meters (Mesfin Aytenfisu and Engida Zemedagegnehu, 2003).

Recharge estimation using Cl mass balance has given recharge rates of 60.07 mm/year for the western plateau and 52.00 mm/year for the graben fill sediments and adjoining escarpment. A total of 192.78 MCM/yr dynamic groundwater resource is estimated for the graben sedimentary aquifer; 123.89 and 68.9 MCM/yr for Raya and Kobo valleys, respectively (Sileshi Mamo, 2007).

According to Sileshi Mamo (2007), hydrogeological units of the Raya-Kobo were classified into aquifers of high, low, and very low productivity. The recent unconsolidated fluvio-lacustrine sediments and the slightly to moderately jointed and highly weathered basalt are classified as aquifers of high and low productivity respectively. The later was classified based on the data of very low discharging springs and relatively low yield shallow boreholes drilled for community water supply. No transmissivity data are available for the volcanic aquifer.

2.2 Groundwater Modeling

A groundwater model may be defined as a simplified version of the real groundwater system that approximately simulates the excitation- response relations of the groundwater system. The real system is very complicated and difficult to use it directly for the purpose of planning and making management decisions. The simplification is introduced in the form of a set of assumptions that express our understanding of the nature of the system and its behavior. These assumptions will tend to smooth out the effect of various heterogeneities. Because the model is a simplified version of the real system, there exists no unique model for a given groundwater system (Bear, J. & Verruijt, A., 1994).

A computer program or code solves a set of algebraic equations generated by approximating the partial differential equations (governing equation, boundary

conditions, and initial conditions) that form the mathematical model (Anderson & Woessner, 1992).

With the introduction of computers and their application in the solution of numerical models, physical models and analogs have become laid off as tools for predicting future groundwater regimes. The selection of the appropriate model to be used in any particular case depends on the objective or objectives of the investigation and the available resources. The later include time, budget, skilled manpower, high capacity computers and codes (Bear, J. & Verruijt, A., 1994).

Groundwater models are an attempt to represent the essential features of the actual groundwater system by means of a mathematical counterpart (Todd & Mays, 2005). These models have a capacity to test and quantify the consequences of various errors and related model-based forecasts.

Groundwater models according to Todd are physically based mathematical models derived from Darcy's law and the law of conservation of mass. Various established solution techniques based upon either finite difference or finite element approximations, or a combination of both, are available for solving the governing equations of the model. The accuracy of the solutions (model predictions) is dependent upon the reliability of the estimated model parameters and the accuracy of the prescribed boundary conditions.

The finite difference method requires a rectangular element shaped discretization of the aquifer and the finite element method consists of a triangular discretization. Discretization is the process of subdividing the continuous hydrogeologic units into discrete segments or cells. Finite element method is easy to define the boundaries of irregularly shaped aquifers and to ensure that node points coincide with monitoring wells or varies types of geographic features. The mathematical basis for finite element methods is more complex than for the finite difference method (Todd & Mays, 2005).

There are several ways to classify groundwater flow models, models can be transient or steady state and one, two, or three spatial dimension. Steady state flow occurs when at any point in a flow field the magnitude and direction of the flow are constant with time (Anderson and Woessner, 1992).

Selecting the appropriate conceptual model for a given problem is one of the most important steps in modeling process. The key data requirements in the process of conceptualization include data about hydro-stratigraphic units, surface water bodies, physical and hydraulic boundaries, recharge and discharge zones. The most common numerical methods to solve flow problems are finite differences and finite elements. Finite-difference grids are easy to understand and require less input data than finite-element grids (Anderson and Woessner, 1992). The finite difference method, as applied in the computer code MODFLOW, was used in this study. The code is based on the physical theory of groundwater movement Darcy's law and the continuity equation. The program supports seven additional packages, which are integrated with the original MODFLOW (Chiang and Kinzelbach, 2001).

Once the conceptual model is translated into a numerical model in the form of governing equations, with associated boundary and initial conditions, a solution can be obtained by transferring it into a numerical model and writing a computer program (code) for solving it. This includes, design of grid, setting boundary and initial conditions and preliminary selection of values for aquifer parameters. The input parameters include model grid size, layer elevations, boundary conditions, hydraulic conductivity, recharge, and additional model input for steady state condition. Model calibration consists of changing values of model input parameters in an attempt to match field conditions within some acceptable criteria (Anderson and Woessner, 1992). Sensitivity analysis is useful in determining which parameter or parameters most influence the model results. These parameters will be emphasized in the future data collection attempting to improve model accuracy.

3. General description of the study area

3.1. Location

The studied area is located in Northern part of Ethiopia some 570 km north of the capital Addis Ababa. It is bounded within the limits of $11^0$55'40'' to $12^0$10'11'' north latitude and $39^0$22'30'' to $39^0$46'44'' east longitude (Figure 3.1).

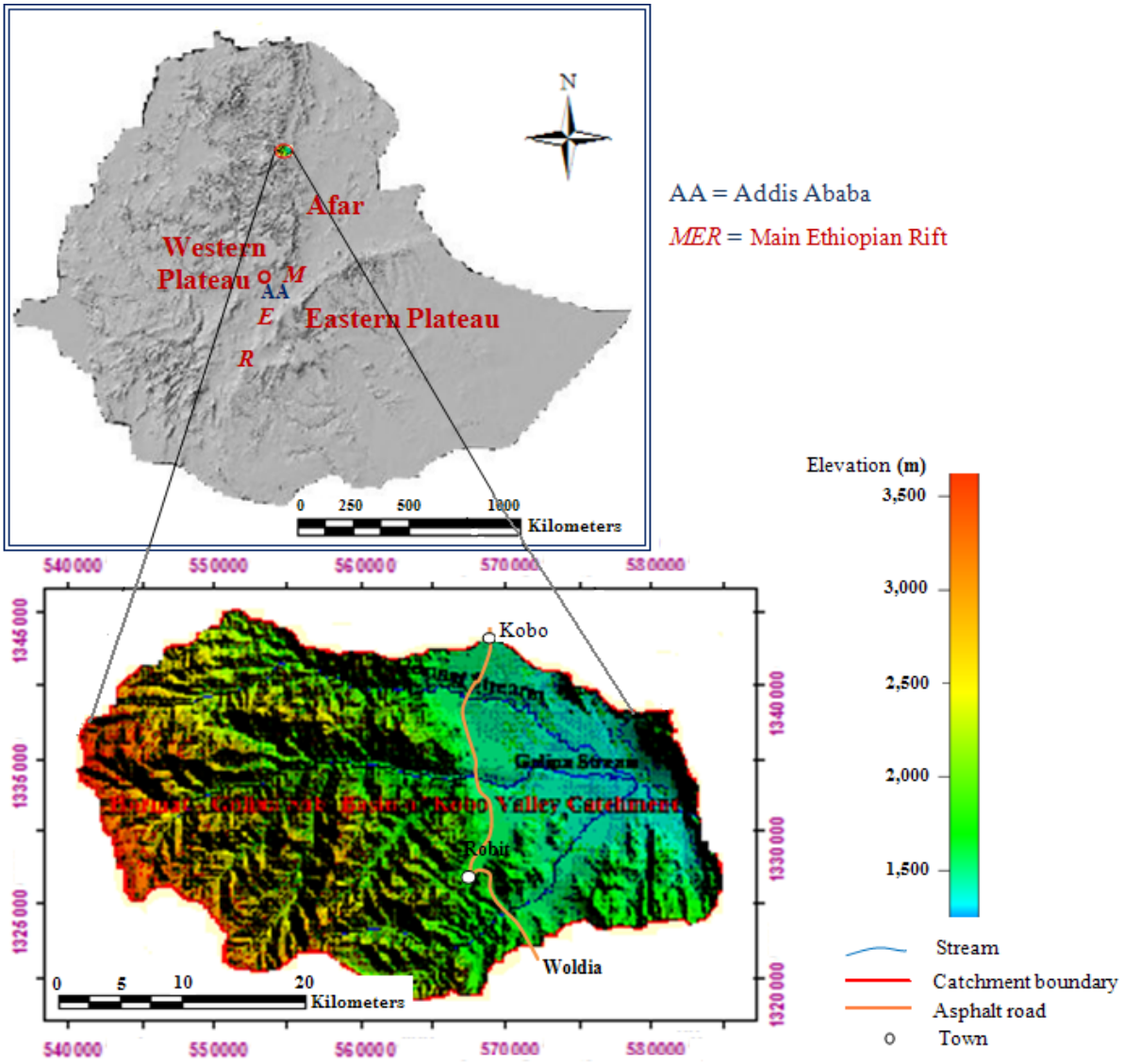

Figure 3.1. Location map of the study area

It covers a total area 811 km^2 and named Hormat – Golina basin. The largest portion of the area is highly dissected topographic high which accounts 65% and the remaining portion covers a valley and its escarpment. The valley part commonly called Kobo Valley. It is bounded by highly rugged mountains of Lasta in the west, Zobel Mountains in the east, Raya Valley in the north and volcanic ridges in the south. It is considered as part of interconnected valleys of the Ethiopian rift system.

3.2 Topography

The studied catchment has three types of physiographic features: the planer inter-mountains valley part, the valley escarpment, and highly dissected highlands. There is a large topographic difference between the valley and the highland. The lowest elevation is the outlet of Golina stream (1304m a.m.s.l) and the highest is Aboyi Gara mountain (3974 m a.m.s.l).The average altitude of the valley floor ranges from 1355 m a.m.s.l. to 1610 m a.m.s.l, while the mountain ridges range from 1610m a.m.s.l. to 3600 m a.s.l.(Figure 3.2).

The valley is characterized by a graben-like structure bounded by north- south trending mountains in the west and east of the valley. The chain of mountains bordering the valley on the western part are marked by highly dissected steep slope deep gorges and canyons, because of east-west and north-south trending faults that might be associated with marginal rift system. It is covered with low-density bushes that enhance a large amount of runoff. Since the area receives highly variable rainfall, runoff generated from the western mountains cause intermittent flooding of the valley floor adjacent to the streams draining the area during the rainy season (Figure 3.3).

3.3 Drainage

The Hormat – Golina basin has an open surface water drainage system that opens to Afar at Golina outlet. It is part of the Denakil dry basin. The basin is bordered by the Tekeze river basin to the west, the Raya valley to the north, the Alwuha basin to the south and the Golina dry basin to the east. Three main streams that originate from the western highlands drain the basin. These are Golina, Hormat and Kelkelit streams. Among the

prevailing streams, only Golina is perennial and others are intermittent carrying floodwater only during the rainy seasons. It collects all the run-off water in excess of recharge to the valley portion and discharge it into the Afar depression through the gap at south-east of the valley (Figure 3.4). Golina has a very limited base flow and Hormat has significantly low seepage flow through the streambed sediment during the field visit (end of February 2010).

The drainage density is high in the western highlands and, low in the valley floor and eastern highlands. All streams and ravines carry large volumes of sediments from the mountains in the rainy seasons and deposit on the valley plain.

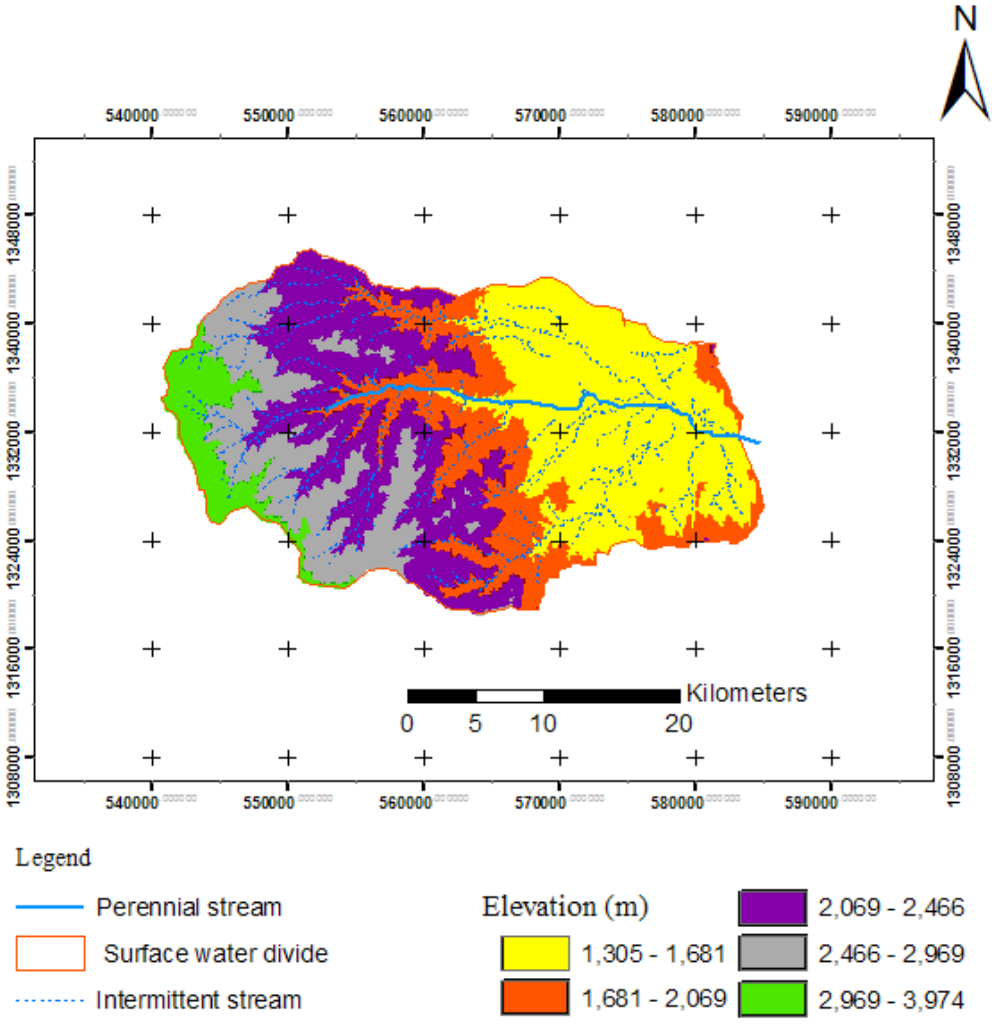

Figure 3.2. Simplified topographic map of the studied basin

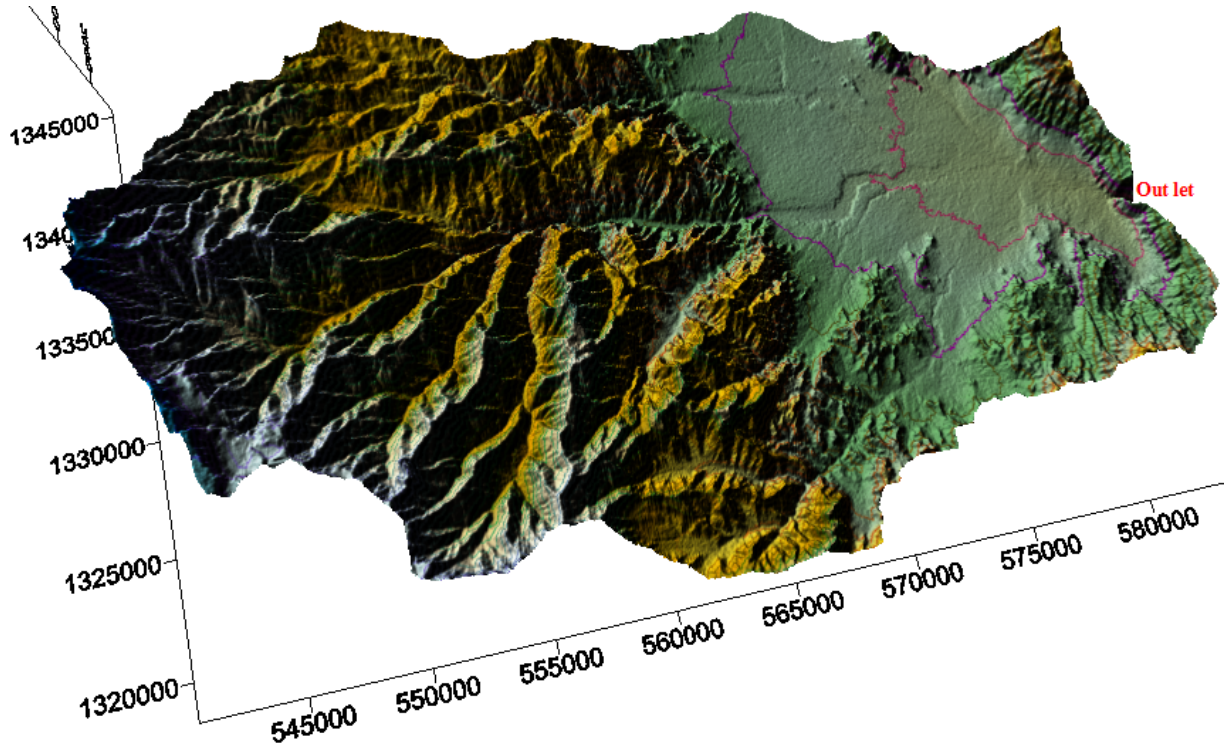

Figure 3.3. Three-dimensional view of the area.

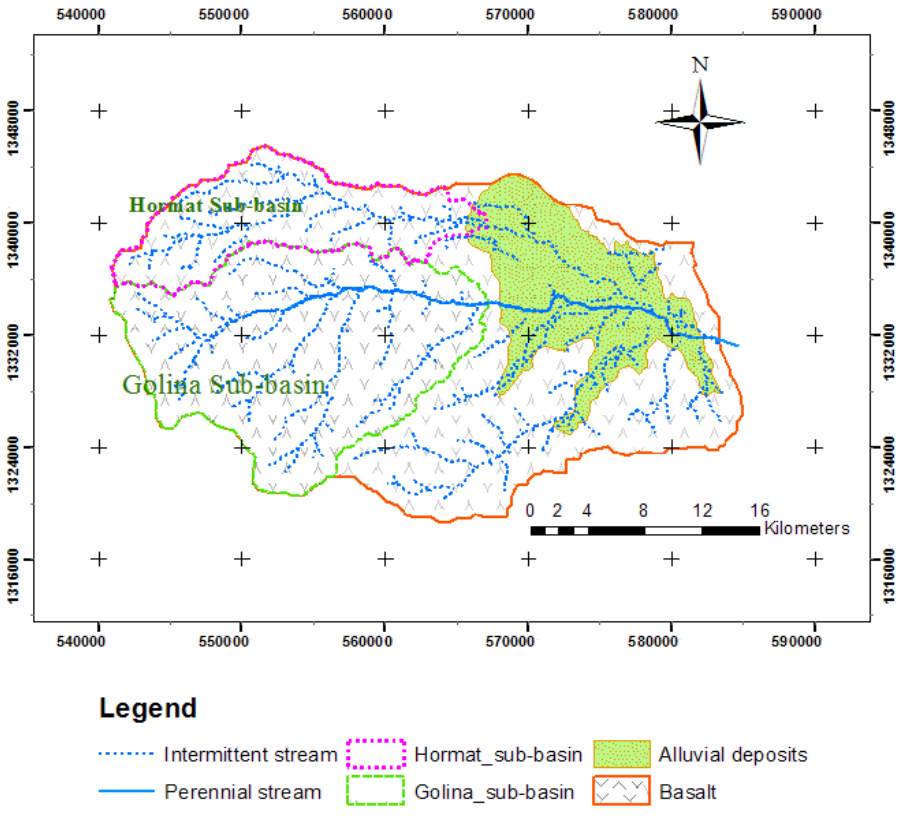

Figure 3.4. Drainage map

3.4 Climate

The position of the Inter- Tropical Convergence Zone (ITCZ), seasonal variations in pressure system and air circulation, results in the seasonal distribution of rainfall over the area. This low-pressure area of convergence between tropical easterlies and equatorial westerlies causes equatorial disturbances (Daniel Gemechu, 1977). The climate is sub-humid in the highlands and semi-arid in the valley plain. The average annual temperature in the valley plain ranges from 17.5°C to 26°C. The average monthly temperatures in Kobo area range from 18.7°C in December to about 26°C in June (See Appendices 1.2 – 1.3).

Orographic effects modify the distribution of rainfall over the area. Moreover, its distribution certainly correlated with altitude. Two rainy seasons have been experienced. The main rainy season often extends from end of June through end of September and the small rainy season from end of March to mid of April. The rest of the months are generally dry. The mean annual rainfall of the watershed is estimated to be about 798.4 mm. About 80% of the annual rainfall amount occurs during the main rainy season. The plain valley part of the area receives an average annual rainfall of 700 mm. the quantitative description of the climatic variability was discussed in chapter four.

3.5 Land use and land cover

Land use is important in the hydrological and groundwater studies, because it is a prominent factor affecting the recharge. Four types of land cover units were identified based on interpretation from satellite images, aerial photographs and field observations. These are forest, agricultural area, woodland, and bare-land. Agricultural area and woodland are the dominant land use units (Figure 3.5).

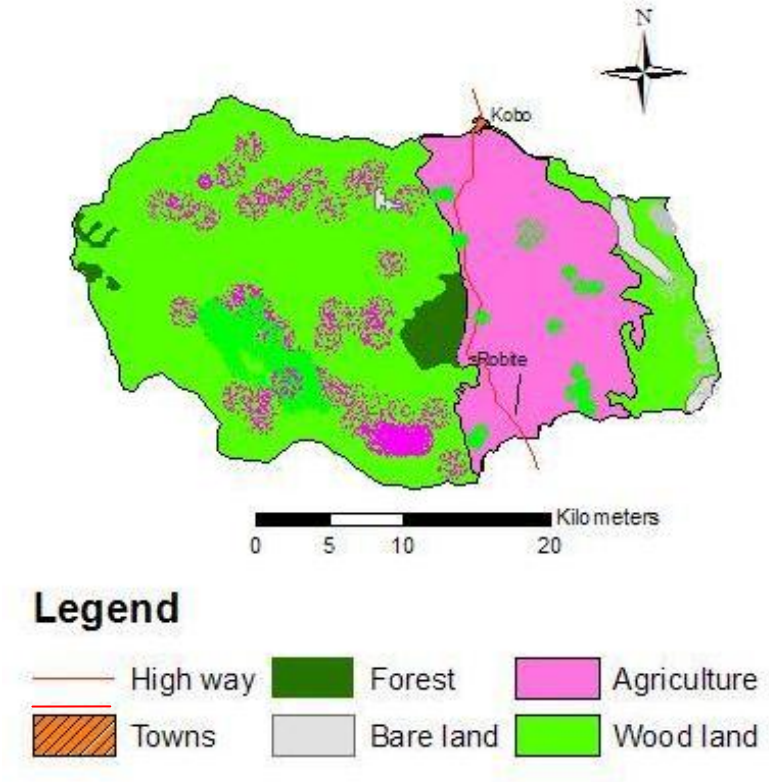

Figure 3.5 Land cover and land use classification

3.6 Geology and hydrogeology

3.6.1 Geology

Regional geology

In northern Ethiopia and Yemen, volcanism started during the Oligocene with the emplacement of a thick continental flood basalt pile. These basaltic highlands now encircle the Afar depression. Most of these flood basalts were extruded over a short time period (possibly 1-2 Ma) 30 Ma and significantly predate the main extensional phases (Pik et al., 1999).

The Ethiopian flood basalts (or traps) cover an area of about 600,000 km2 with a layer of basaltic and felsic volcanic rocks. The thickness of this layer is highly variable but

reaches 2km in some regions. The volcanic and shallow intrusive rocks have a total volume of about 350,000 km3 (Mohr, 1983b; Mohr and Zanettin, 1988 cited in Dessie Nadew, 2003).

New structural and geochronological date (Cukstins et al., 2002; Wolfenden et al.,2004, In press) have shown that basin formation commenced between 29 and 26 Ma in the Southern Red Sea rift, while rifting in the northern most Main Ethiopian rift (MER) Initiated around - 11 Ma. Initial crustal extension within the Southern and central MER commenced between 18 and 15 Ma (Welde Gabriel et al., 1990; Ebinger et al., 2000). Thus, the MER, which is northern most sector of the East African rift system, propagated northward from the Turkana rift at – 25 Ma (Dereje Ayalew et al., 2005).

Inter-layered with the flood basalts, particularly at upper stratigraphic levels, are felsic lavas and pyroclastic rocks of rhyolitic, or less commonly trachytic compositions (Dereje Ayalew et al., 1999).

Except along its margins and in major river valleys, the entire Ethiopian volcanic plateau currently stands above 2000m in altitude. According to Jestin and Hucho (1992) and Menzies et al. (1992), the uplift took place concurrently with or very soon after eruption of the flood basalts (30 Ma) and since that time the high altitudes have been maintained. It is most unlikely that this uplift is due to the thermal or compositional influence of Oligocene plume, which should have dissipated by now. Instead, the present elevation of the plateau is normally attributed to dynamic support from a thermally anomalous up welling portion of the present upper mantle (Bruno Kieffer et al., 2003).

Local geology

The studied area is a basin at the western edge of the Danakil basin. The main lithological units in the study area are basaltic rocks that form the western highlands and escarpments, Rhyolite which form the eastern ridge (Zobel ridge) overlying the basalt and the alluvial deposits that originate from these basalts on the valley floor (Figure 3.6).

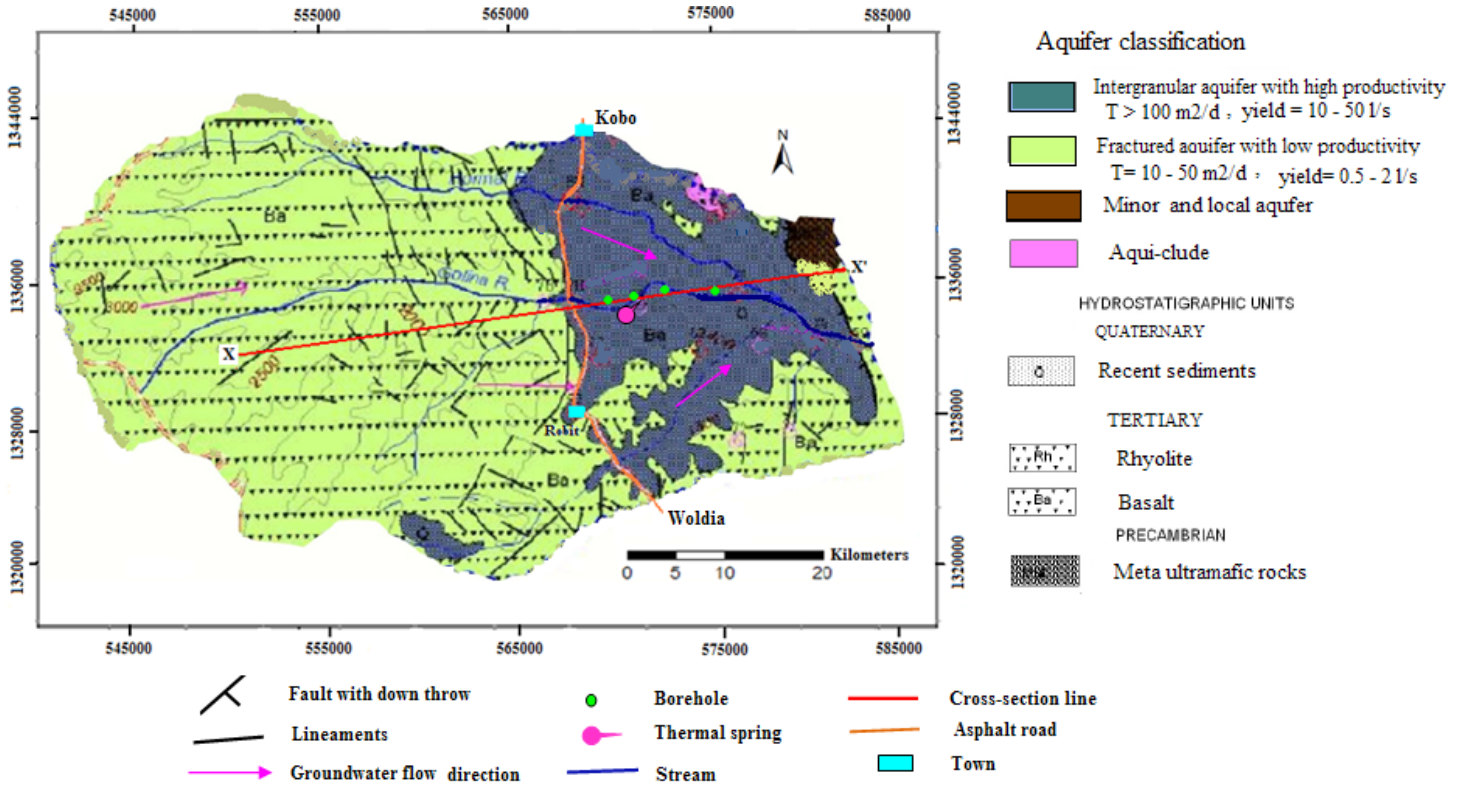

Figure 3.6. Simplified hydrogeological map (modified after Sileshi Mamo, 2007).

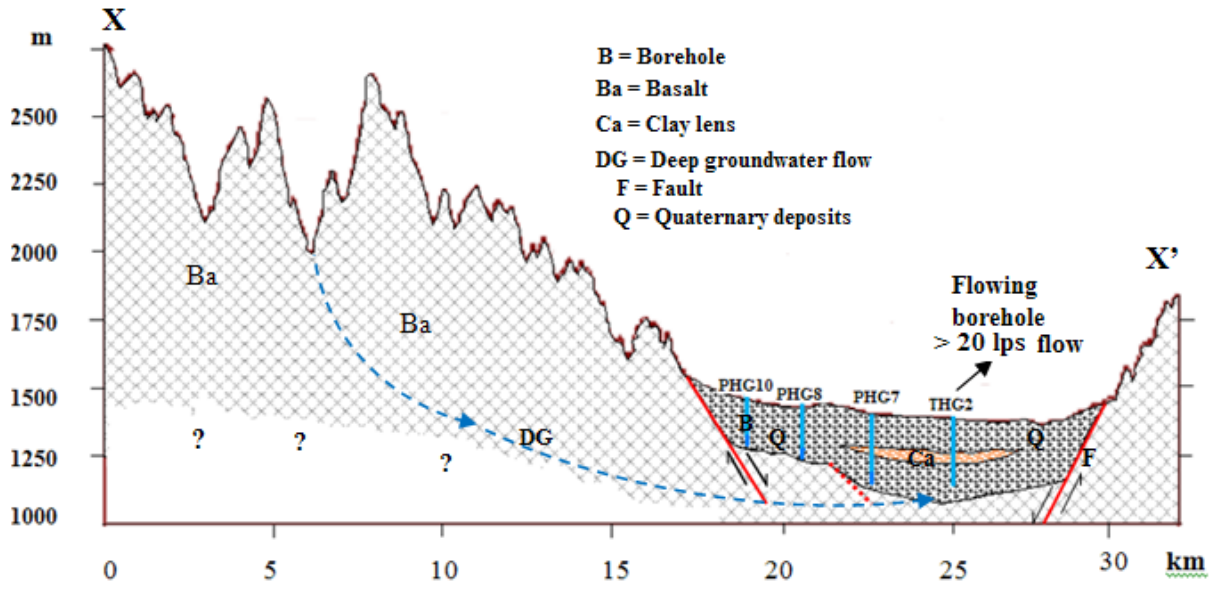

Figure 3.7. Hydrogeological cross-section (West – East).

The Basaltic rocks

According to the geological map of Ethiopia published in 1996, the basalts in the study area are grouped into the pre-oligcene stage Ashange basalt. The name Ashange basalt applies to strongly weathered basalts without clear stratification which lie below the major pre –Oligocene (?) unconformity having a thickness of several hundreds of meters (Zebetin et al., 1980 cited in Dessie Nadew, 2003).

The basaltic rocks that form the western highlands and escarpments of the area are characterized by fine grained and light to dark greenish gray, light pinkish fine grained, and dark olivine, plagioclase, pyroxene and hornblende porphyry basalt layers. It is slightly to moderately fractured and highly weathered in the upper part. Aphanitic basalt dykes intrude this formation at places. Owning to a number of fractures, faults and lineaments, it is possesses highly rugged topographic terrain.

The basaltic rock in the eastern highlands show slightly to moderately weathering and well fractured. It is overlain by slightly fractured and weathered Rhyolite.

The Rhyolite unit

The Rhyolite is often light pink with K-feldspar, plagioclase, quartz and some mafic minerals porphyry, and at places it is quartz, K-feldspar and plagioclase porphyry. Light pink, fine-grained outcrop was seen with basalt xenoliths above the basalt, at the outlet of Golina stream to Afar (Sileshi Mamo, 2007).

The Alluvial deposits

The alluvial deposits make up the low-lying valley part of the study area and constitute 25 % of the total catchment area. Braided streams and rivers that drain the western highly dissected steep slope highlands and surface runoff along either side of the valley (Kobo valley) escarpment and early damming effect of the eastern ridge were believed to be the source for the formation of the alluvial deposits. The sediments are unconsolidated and basaltic in composition. This unit is mapped as Quaternary alluvial deposits with thickness ranging from 5 m to 150 m on the geological map of Ethiopia published in 1996.

The valley part is considered as an intermountain trough-like structure that originated from local tectonic development attributed to the regional East African rift system (Gershanovich, 2000). The graben is filled with sediments, which drift out of the basaltic rocks on the western and eastern highlands, mainly due to weathering and erosion of the rocks. The colluvial sediments on the sides and feet of the highlands, especially on the west, are very coarse grained and highly permeable. These deposits are largely composed of gravels and cobbles with sands and silts as matrix. The sediments are poorly sorted and sub-angular in shape because they may not have transported far distance from their origin. Adjacent to the colluvial, there are alluvial deposits that are mainly transported by surface run-off along streams and rivers during the rainy seasons. The alluvial sediments are relatively fine, well sorted and sub-rounded to spherical shaped. They are dominantly composed of sands and silts with some proportion of fine gravel, especially adjacent to the streams and rivers in the study area. Towards the centre of the valley floor, finer proportions like clay, silt, and sand dominate the sediments (Co-SAESAR 1999).

Recent sediments consist of fluvio-lacustrine deposits, which are at places covered by channel and fan deposits, and by not well-developed colluvial deposits at the foot of the eastern escarpment. These sediments cannot be separately mapped unlike the previous classification made by Co-SAESAR, which gave lateral contacts among different units that are not in place, and this is not logically correct. The fluvio-lacustrine deposit seems to have been deposited due to damming of proto river during faulting that gave rise the eastern escarpment (Sileshi Mamo, 2007).

Data from borehole lithological logs and geophysical surveys in the valley floor has indicated that the valley fill is composed of intercalating layers of gravel, gravely sand, sand, silty sand, clay, and silty clay.

Geologic structures

Most of the fractures and dykes have nearly N-S, and E-W oriented strike and dip sub-vertically.

The study area and its surroundings are structurally similar to the steep fault scheme of western Afar margin (Zanettin et al, 1978) (Figure 3.8). Most lineaments that were

traced from aerial photographs were oriented nearly in the N–S and E–W directions (Figure 3.6). The N-S striking faults are responsible for the easterly tilting and throw of block in that direction. However, the E-W striking faults result to southerly tilting and minor throws of blocks. Most of the rivers and streams that flow in the E-W direction from the highland areas are indications of lineaments oriented in that direction.

In general, the fracture pattern in the study area does not signify a single direction while the dominant strike directions are NNW-SSE and NNE-SSW (Dessie Nadew, 2003).

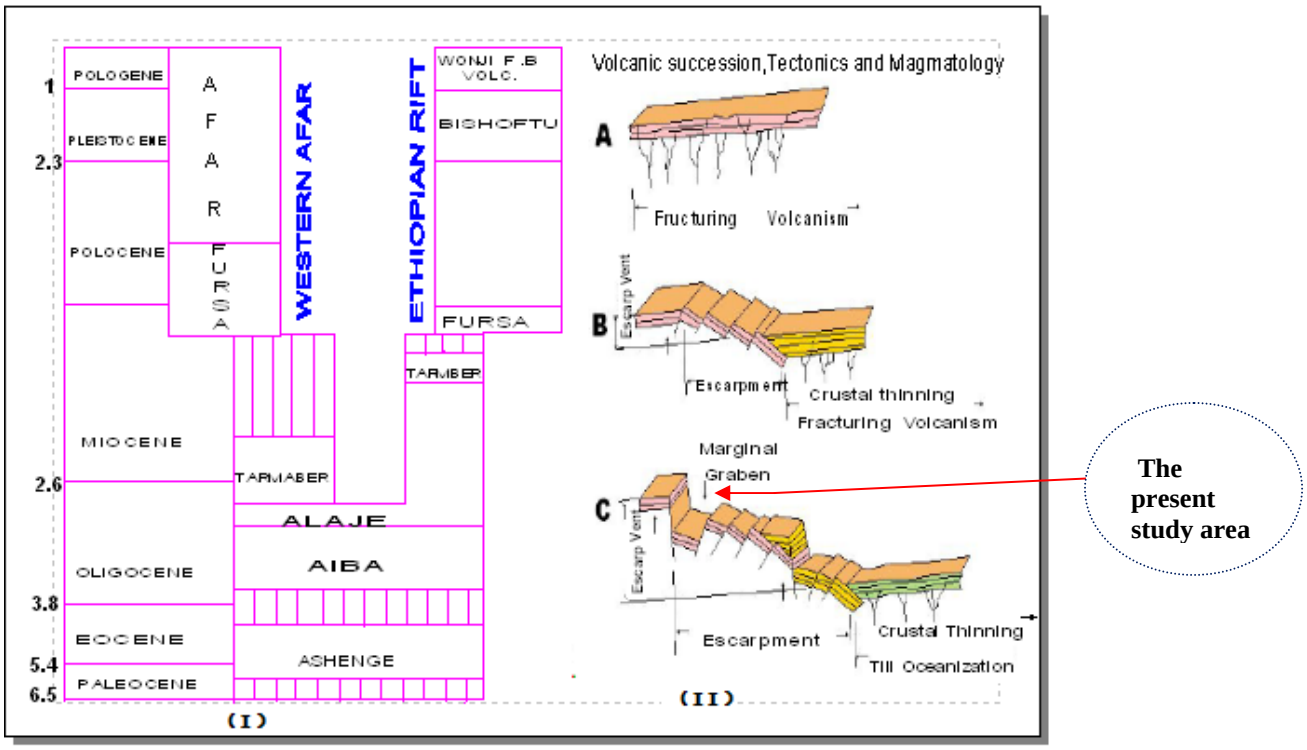

Figure 3.8 (I) Schematic Stratigraphic Section of the Tertiary Volcanic in Ethiopia (Zanettin et.al, 1978)
(II) Tectonic and Volcanic Evolution of the Western Margin of Afar A to C (Zanettin et.al, 1978)

A) The fracturing, magmatic injection and Volcanism are restricted to increasingly narrower belts.
B) The width and height of the escarpment increase while the Rift narrows.
C) The narrowing of the Rift is opposed by thinning of the crust.

3.6.2 Hydrogeology

Based on the lithologic units described before in section 3.6.1, two main hydrogeologic units or aquifers were identified in the study area (Figure 3.6). These are the Quaternary alluvial deposits and the upper fractured and weathered basalt. According to Freeze and Cherry, an aquifer is saturated geologic material that is sufficiently permeable to yield water in significant quantities to a well or spring, where as a confining units has low permeability that restricts the movement of ground water and limits the usefulness of the unit as a source of water supply.

The Quaternary alluvial deposits

Aquifers of unconsolidated or non-indurate materials, such as alluvial, glacial or Aeolian deposits, are among the most common sources of groundwater. In alluvial or glacial deposits, buried valleys or old streambeds offer the best groundwater potential. These are ancient stream beds or valleys, primarily consisting of sand and gravel that have been covered by finer sediments. Because of erosion, bed- rock tends to be depressed below unconsolidated sediments of ancestral streams (Bouwer, 1978).

This unit occupies the valley part of the basin and own varying thickness. The thickness was determined from VES and drilling data. It is considered as an aquifer if it is composed of layers of sand, gravel, pebbles, and boulders. Unlikely, previous studies suggested that the entire alluvial deposits as an aquifer. The average aquifer thickness reaches 90 m with maximum thickness of 150 m at VES-30/THG3 borehole area close to the Golina-Kelkelit interfluves area across which close to the Golina-Hormat confluence at THG2 borehole. The minimum thickness the aquifer part of this unit is some 30m. Generally, the maximum aquifer thickness of this unit lies across the center of the valley and its minimum lies close to the western escarpment and around volcanic hills within the valley (Figure 3.7).

Evidences from lithologic and resistivity logs of the drilled boreholes verify that there could be shifting position of stream channels and ever-changing depositional velocities, which are responsible for characteristic textural variability especially along the mainstream courses. Such processes locally generate much heterogeneity in the distribution of hydraulic properties of the alluvial aquifers. Freezee and Cherry (1979)

stated that braid rivers generally occur in settings where the sediment available for transport has considerable coarse-grained sand or gravel and where velocities are large because of steep regional topographic slopes. Shifting positions of channels and bars and changing velocity can result in extensive deposits of bedded sand and gravel with minor zones of silty or clayey sediments filling in abandoned channels. The silty and/or clayey depositional horizons/lenses are thick at the center and close to the outlet valley. Aquifers of the alluvial origin are the main important sources of groundwater in the area.

The groundwater potential varies within the valley plain because of differences in the grain size, grain pack geometry, and thickness.

In this unit, depth to groundwater level varies from flowing condition to a depth of 40 m below ground surface. The flowing condition is attributed to recharge from higher head and local confining effect. It is observed at the center of the valley. The deep level is along the western flank of the valley where the sediment thickness is minimal. The western part of the aquifer has generally unconfined groundwater condition, whereas the southeastern part is characterized mostly by semi-confined to confined conditions.

Based on the analysis result from pumping test data, the hydraulic conductivity values range from 1 to 31 md^{-1}. The boreholes were tested from 15 to 80 ls^{-1}.

The basaltic unit

The upper most fractured and weathered part of this unit is identified as the second important aquifer in the study area. It covers more than 70% of the area. However, its importance as aquifer limited to fractured zones particularly at the foot of the hills, along valleys and beneath the alluvium sediments. There are few productive boreholes, which tap groundwater from the volcanic aquifers. They possess a depth of <100m and located at the foot of western escarpment of the valley. Their productivity varies from place to place depending on the availability of local recharge, degree and depth of weathering and fracturing. No pumping test data was acquired for these boreholes to determine aquifer hydraulic parameters. The yield of the boreholes is not more than 2.5 ls^{-1}. This unite is believed to be one of the groundwater recharge source for the valley fill alluvial sediments.

4. Analysis and model input data preparation

4.1 Meteorological data analysis

4.1.1 Rainfall

Rainfall records of five stations had been considered to describe the rainfall regime of the studied basin. All stations are aligned linearly in north-south direction, whereas the eastern and western highland parts of the basin have no stations. Stations network inadequacy was observed in its spatial distribution for aerial averages, for the catchment as a whole and for water balance studies in particular. All the stations except Kobo station are located out of the study area. Missing data is a common case for the stations. However, the selected stations for ten years (1996 to 2005) have adequate data that could be used for the purpose of this study (see Appendix 1). The average of monthly meteorological data of these ten years was taken for analysis (Table 4.1). The mean annual precipitation has a bimodal distribution with most of the rainfall occurring during the months July to September while there is a short rainy season from March to April. The other months are generally dry (Figure 4.1). Korem and Maichew were the only gauging stations in the western highlands that nearly close to the studied catchment. Korem reported a maximum annual rainfall depth of 1356mm and the minimum annual rainfall depth (465mm) was reported at Waja gauging station, located within Raya valley floor north of this catchment. Since, the three stations (Kobo, Waja and Alamata) are closely and evenly spaced on the floor of Raya- Kobo valley, arithmetic mean method was applied to determine the aerial depth of precipitation for the valley part of the study area. The weighted mean of the precipitation was calculated using equation 4.1, which resulted in 738mm of mean annual rainfall for the valley part/ Kobo valley (Table 4.1).

$$P_A = \frac{\sum_{i=1}^{n} P_i}{n} \qquad (4.1)$$

P_A : mean annual rainfall for the Kobo valley (mm)
P_i : measured precipitation at a given station and time (mm)
n : number of rain gauges

Table 4.1 Mean monthly rainfall distribution (mm) / 1996 – 2005

Station	Jan	Feb	Mar	Apr	May	Jun	Jul	Aug	Sep	Oct	Nov	Dec	Annual
Kobo	53	29	27	59	47	19	152	202	60	41	24	21	734
Waja	35	14	46	66	37	14	124	214	40	30	20	19	659
Alamata	63	11	62	76	39	15	164	256	47	32	31	25	821
Korem	37	8	61	90	67	34	224	290	87	65	33	24	1022
Maichew	26	8	52	74	56	35	145	223	79	59	22	16	778

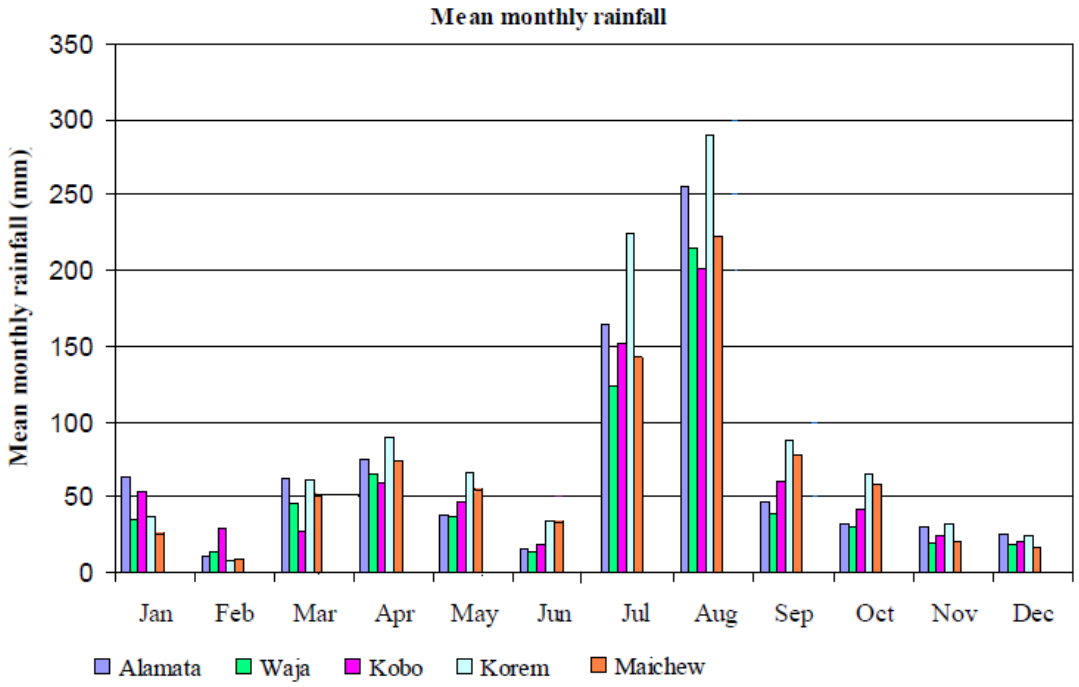

Figure 4.1. Mean monthly rainfall of the stations (1996- 2005)

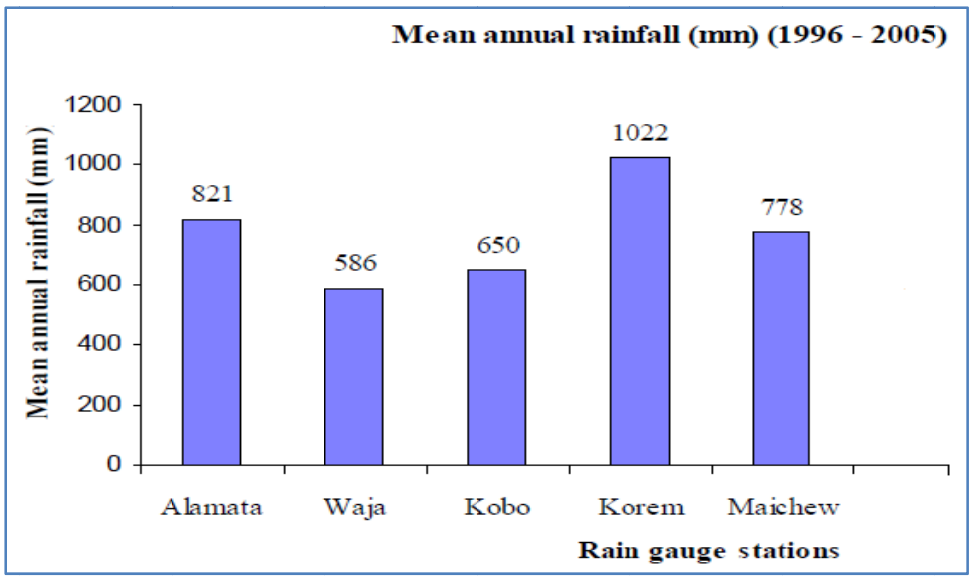

Figure 4.2 Mean annual rainfall of the stations.

The distribution of rainfall in relation to altitude in the vicinity of studied area shows the least correlation because of orographic effect and some may attribute to data quality (Figure 4.3). Therefore, estimation of the rainfall distribution based on altitude – rainfall relationship may not be applicable.

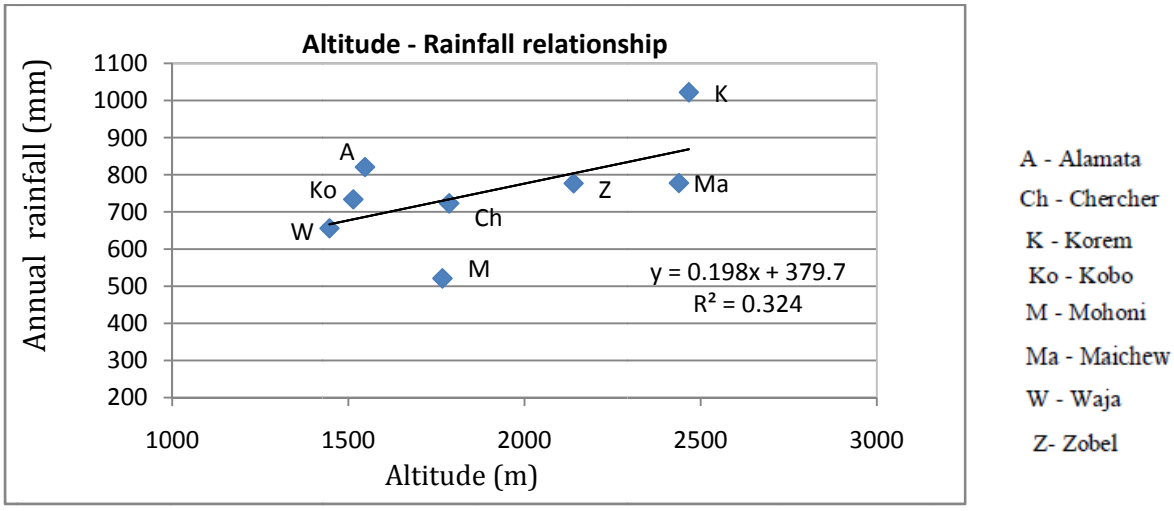

Figure 4.3. Rainfall – altitude relationship (1996 to 2005).

4.1.2. Temperature

Kobo and Korem stations were used to see the climatic variation in the lowland/ valley and highland parts of the studied catchment respectively. The average monthly maximum temperature of both stations show that highest record in June and lowest in January (Figure 4.4). The difference in their maximum temperature is about 9 ^{0}C. The maximum temperature in Korem station ranges from 19 to 25 ^{0}C and in Kobo station from 27 to 34.5 ^{0}C. The record for all the stations is attached in the Appendix 1.2.

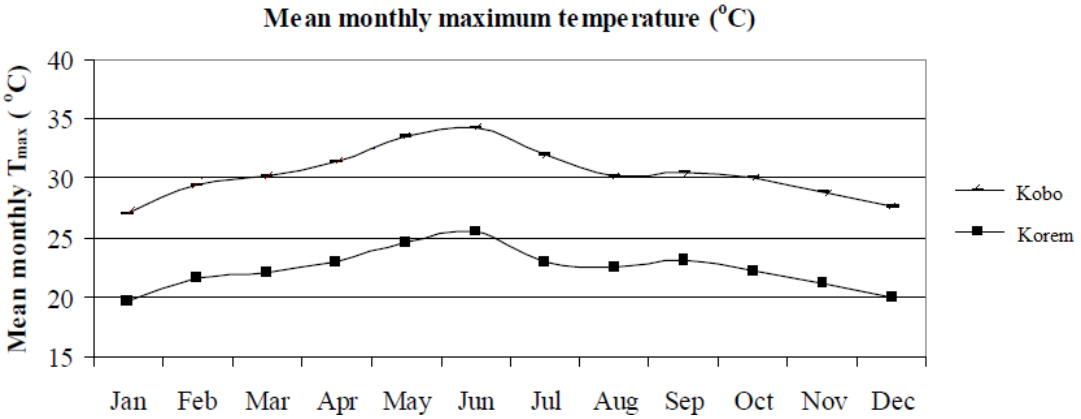

Figure 4.4. Mean monthly maximum temperature of Kobo and Korem stations.

As shown in the Figure 4.5, the average monthly minimum temperature for Kobo and Korem stations have lowest values of 11 ^{0}C and 4 ^{0}C in the month of December and highest values of 19 ^{0}C and 10 ^{0}C in the month of June respectively. Although, they show significant difference of average monthly temperature, the trend of the temporal variation is similar at both places. See the record in Appendix 1.3.

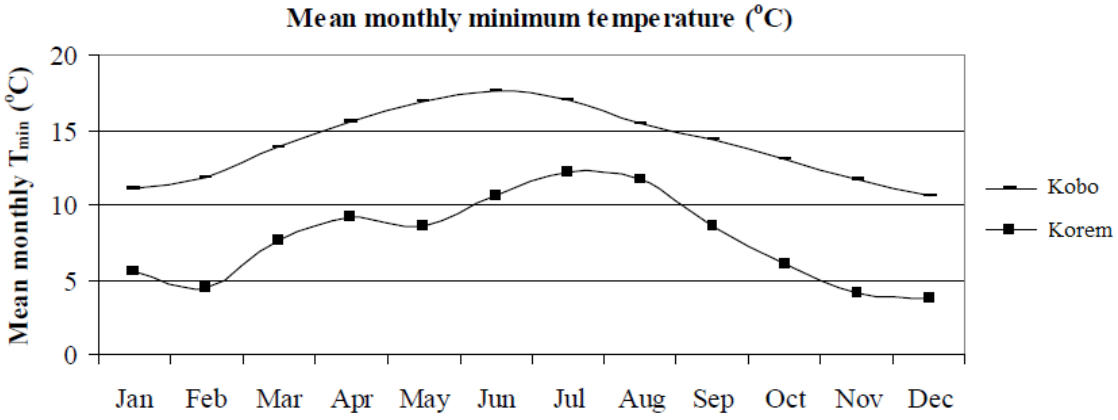

Figure 4.5. Mean monthly minimum temperature for Kobo and Korem stations.

4.1.3. Relative humidity (RH)

The relative humidity data is available for stations of Kobo and Maichew. At Kobo, the data were recorded at 1200, 1800 and 0600 local times (Figure 4.6) and the mean monthly values ranges from 30% in June to some 57% in January. It ranges from 41.5 to 70% for Maichew station. The recorded lists are attached in the Appendix 1.4.

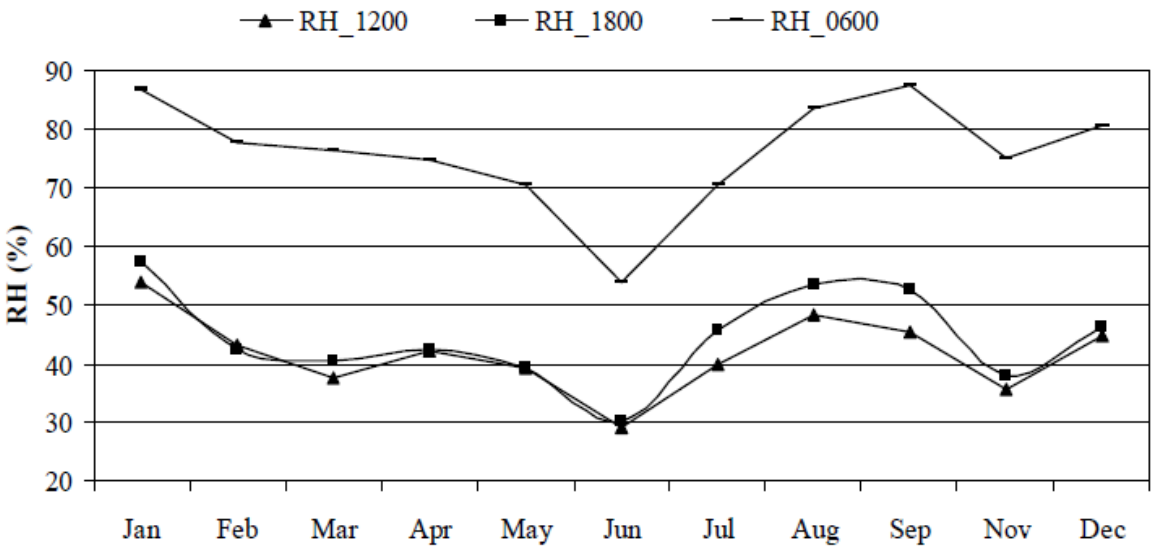

Figure 4.6. Mean monthly relative humidity at Kobo station taken at 1200, 1800, and 0600 local time.

4.1.4. Wind speed

Wind is expressed by its direction and velocity. Wind direction refers to the direction from which the wind is blowing. To compute evapotranspiration, wind speed is the relevant variable. Its mean value vary between 1 ms^{-1} in September to 2.04 ms^{-1}in March at Kobo. For Maichew station, it varies between 1.1 ms^{-1} in January and 3.25 ms^{-1} in July (Figure 4.7). (See Appendix 1.6.)

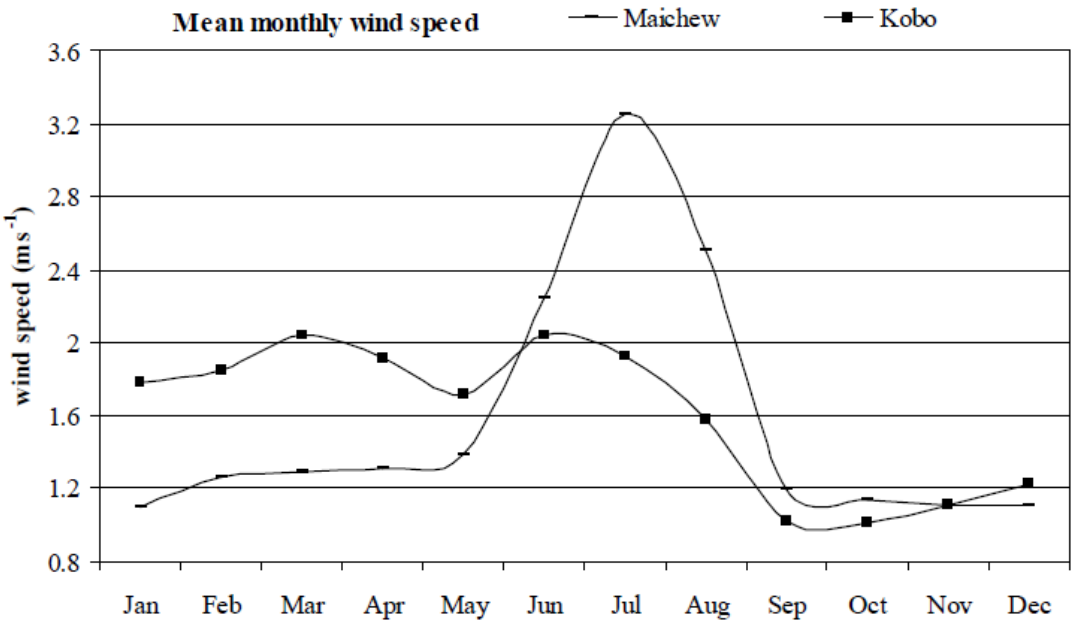

Figure 4.7. Mean monthly wind speed at Kobo and Maichew stations.

4.1.5. Solar radiation

Solar radiation governs the rate of evaporation by changing large quantities of liquid water into water vapor. Consequently, the evapotranspiration process is determined by the amount of energy available to vaporize water. Sunshine hour duration data are available for Kobo and Maichew stations. Mean sunshine hours determined for the Kobo station was above 8.0 hours in the months of October to December and March to May. In the other months, it decreases up to 5.3. It goes up beyond 8 for the month of April and May, where as for the remaining moths it decreases to a minimum of 5.0 which is in July. The mean monthly sunshine durations at Kobo and Maichew stations were 7.6 and 7.2 hours respectively. (See Appendix 1.7).

4.1.6. Evapotranspiration (ET_O)

Evapotranspiration is the process in which water is returned back to the atmosphere by a combination of evaporation and transpiration. Potential evapotranspiration is the water loss that will occur under given climatic condition without deficiency of water supply whereas actual evapotranspiration is the amount of water that actually returns to the atmosphere depending on the availability of water.

Potential evapotranspiration

Potential evapotranspiration is one of the most difficult components of the hydrological cycle to estimate. However, it can be estimated from weather data. Different methods have been developed to estimate the potential evapotranspiration, from point-measured data (Allen et al., 1998). For the purpose of this study, the Penman- Monteith and Hargreaves methods were used to estimate the potential evapotranspiration. The Penman-Monteith method integrates the effect of factors such as altitude, aerodynamics, geographic location, and solar radiation for computation. Hydro- meteorological data of ten years (1996 – 2005) were used as input for computation. The FAO CROPWAT software developed by United Nations Food and Agriculture Organization (FAO) was used to estimate the potential evapotranspiration. It uses the (FAO56) Penman-Monteith equation. The Penman- Monteith method was applied for the Kobo and Maichew stations which have relatively better meteorological data. Since the other stations have no wind speed and sunshine hour duration data, Hargreaves equation was used, that employ only temperature and extraterrestrial radiation (R_a) data. The mean air temperature in the Hargreaves equation was calculated as an average of maximum and minimum temperature and Ra is computed from information on location of the site and time of the year. Thus, air temperature is the only parameter that needs to be measured.

The mean monthly precipitation for Kobo station varies from 19mm in June to 201mm in August with annual precipitation of 734mm. The estimated annual ET_O for this station was 1752mm (Table 4.2). It is calculated based on the Penman-Monteith method. This value is by far larger than the annual precipitation. The monthly ET_O at Kobo ranges from 118mm in December to 180mm in June. The average temperature also varies between 19 ^{0}C in December and 26.5 ^{0}C in June (Figure 4.8).

Table 4.2. Computed ET_O of Kobo station using Penman-Monteith equation.

Month	T_{max} (°C)	T_{min} (°C)	Humidity (%)	Wind Speed (Kmd^{-1})	Sun Shine (Hours)	R_n ($MJm^{-2}d^{-1}$)	ET_o (mmd^{-1})	ET_o monthly
Jan	26.2	12.8	60.2	153.8	7.8	18.2	3.8	119.0
Feb	28.7	12.4	56.2	159.8	7.4	19.2	4.4	122.6
Mar	29.8	15.3	46.4	176.3	8.4	22.0	5.3	165.5
Apr	31.2	16.9	49.7	165.9	8.2	22.1	5.5	164.1
May	33.2	17.2	41.4	147.7	8.6	22.4	5.7	176.4
Jun	34.5	18.5	31.7	176.3	6.6	19.2	6.0	180.3
Jul	32.1	18.1	39.3	166.8	5.3	17.4	5.3	164.6
Aug	30.6	16.8	51.8	136.5	6.0	18.6	4.8	147.6
Sept	30.8	15.2	52.9	88.1	6.7	19.3	4.4	131.7
Oct	29.6	13.0	42.2	87.3	8.5	21.0	4.4	136.4
Nov	28.5	11.9	40.8	95.9	9.3	20.6	4.2	124.8
Dec	27.0	10.9	40.4	105.4	8.5	18.8	3.8	118.7
Average	30.2	14.9	46.1	138.3	7.6	19.9	4.8	1752.0

Penman-Montheith equation was used in Eto Calculations with the values for Angstrom's Coefficients: a = 0.25 and b = 0.5

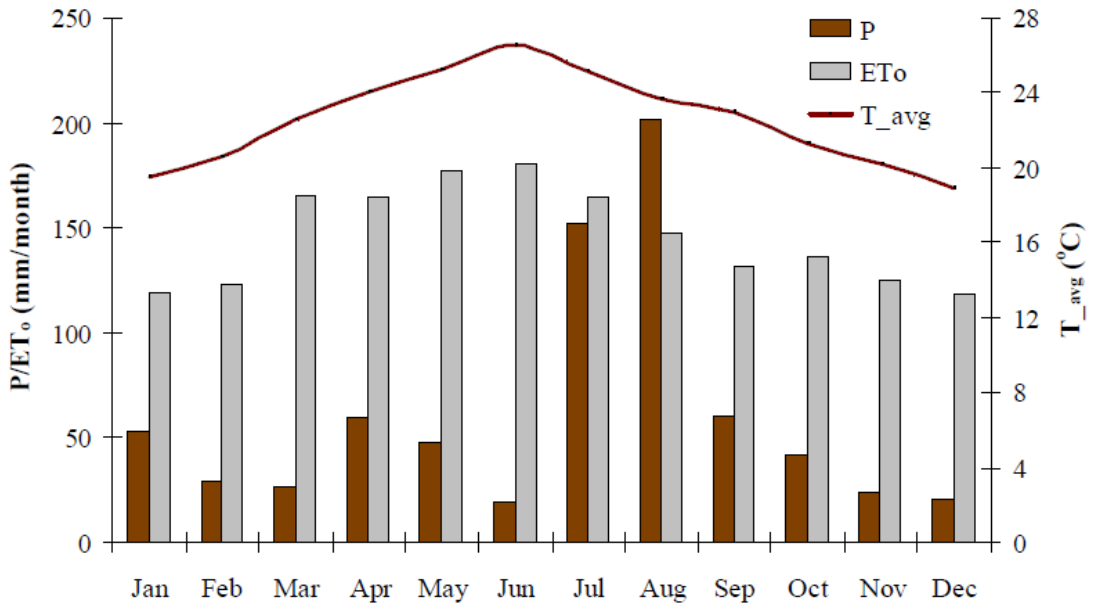

Figure 4.8. Precipitation (P), potential evapotranspiration (ET_O) and average monthly temperature (T_avg) for Kobo station (1996 to2005).

Maichew station is found at distance from the studied basin on the western highlands of Raya Valley. It has greater annual precipitation (796mm) and lower potential evapotranspiration (1378mm) as compared to Kobo station. As shown in Figure 4.9 its monthly precipitation ranges from 8mm in February to 223mm in August. Both the ET_o and average temperature have their minimum values in December and maximum values in June (Table 4.4).

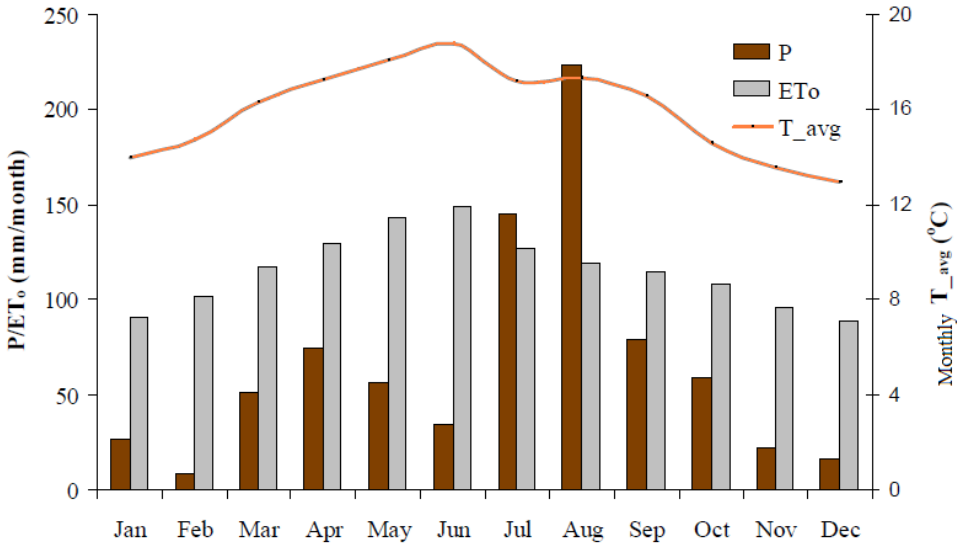

Figure 4.9. Precipitation (P), potential evapotranspiration (ET_O) and average monthly temperature (T_avg) of Maichew station (1996 to2005).

The result of the Penman – Monteith showed that the annual potential evapotranspiration for Kobo and Maichew are 1752 and 1387 mm respectively. In order to see the variation of these results, Hargreaves equation was also used to calculate the ET_o. The results from Hargreaves equation are about 8% more than the Penman-Monteith results (Table 4.3).

Table4.3Annual ET_o (mmy^{-1}) computed from Penman-Monteith and Hargreaves methods

	Kobo	Maichew	Alamata	Korem	Waja
Annual ET_o Hargreaves	1896	1410	1960	1511	1939
Annual ET_o Penman-Monteith	1752	1387			

Table 4.4. Calculated ET_O of Maichew station using Penman-Monteith equation.

Month	T_{max} (°C)	T_{min} (°C)	Humidity (%)	Wind Speed (Kmd^{-1})	Sun Shine (Hours)	R_n ($MJm^{-2}d^{-1}$)	ET_o (mmd^{-1})	ET_o monthly
Jan	20.2	7.7	66.3	95.0	7.0	17.1	2.9	90.5
Feb	21.8	7.7	56.3	108.9	8.3	20.3	3.7	102.2
Mar	22.5	10.0	61.0	111.5	7.0	19.8	3.8	117.2
Apr	23.4	11.1	57.0	113.2	8.2	22.2	4.3	129.0
May	24.2	11.9	49.9	120.1	8.8	22.9	4.6	142.6
Jun	24.8	12.8	41.5	193.5	7.2	20.1	5.0	149.4
Jul	22.2	12.3	62.6	280.8	5.0	16.9	4.1	127.1
Aug	22.0	12.7	66.6	216.0	5.3	17.5	3.8	119.0
Sept	22.5	10.7	61.8	102.8	6.8	19.5	3.8	114.6
October	20.8	8.5	61.8	98.5	7.5	19.5	3.5	108.2
Nov	20.2	7.0	59.1	95.9	7.8	18.5	3.2	96.0
Dec	19.3	6.7	65.7	95.9	7.7	17.6	2.9	89.0
Average	22.0	9.9	59.1	136.0	7.2	19.3	3.8	1387.0

Penman-Monteith equation was used in ET_O calculations with the values for Angstrom's Coefficients: a = 0.25 and b = 0.5.

Actual evapotranspiration

Actual evapotranspiration is the amount of water that actually returns to the atmosphere depending on the availability of water.

Due to the absence of gauging stations in the western highlands of the studied basin, the FOA New-Local climate estimator (New_LocClim v. 1.03) software was used to estimate the annual precipitation and temperature of this part studied area. Jürgen Grieser developed this application in July 2005. New LocClim is a tool for spatial interpolation of agro-climatic data. New LocClim is also capable of producing climate maps of the average monthly climate conditions (8 variables) taken from the agro-climatic database of the Agromet Group of the Food and Agriculture Organization of the United Nations.

For the purpose of this interpolation, nine gauging stations with their data from FAO database were used. These stations include: Alamata, Maichew, Adishoho and Betemera north of the studied area whereas Woldia, Haik, Desie and Combolcha south of the area and Debre-Tabor west of the studied area. Except Debre-Tabor station, all lie along the western edge of the Afar rift. (See Appendix 1.7).

Accordingly, seven points were selected spatially within this data gap area and their annual precipitation and temperature data were estimated using New_LocClim by applying nearest-neighbor method. To improve the quality of the results, it was corrected with the observed data of Korem and Maichew stations. Since the estimated results are more or less similar, the mean of these values was used for the calculation of the actual evapotranspiration for the highland part of the studied area. The estimated average annual precipitation and temperature from New_LocClim estimator are 906mm and 14 ^{0}C respectively (See Appendix 1.8 – 1.9).

The Turc, Langbein and Wundit empirical formula was used to estimated the mean areal actual evapotranspiration of both the valley and highland parts of the studied basin. The formula estimates the mean actual evapotranspiration for a given river basin based on precipitation and temperature records and the relation is given by:

$$\bar{E} = \frac{\bar{P}}{\sqrt{0.9 + \frac{(\bar{P})^2}{[L(t)]^2}}} \qquad (4.2)$$

Where,

$\bar{E}$: mean annual evapotranspiration (mm)

$\bar{P}$: mean annual precipitation (mm)

t : mean annual temperature (^{0}C)

$L(t) = 300 + 25t + 0.05t3$

The inputs used in the above equation 4.2 to calculate the mean annual actual evapotranspiration for the western highlands and valley parts of the studied basin and the obtained results are show in the Table 4.5.

Table 4.5. Mean annual actual evapotranspiration values of the studied area calculated using Equ. 4.2

Part of the study area	Average altitude range (m)	Area coverage (km^2)	Mean annual precipitation (mm)	Mean annual temperature (^{0}C)	Mean annual actual evapotranspiration (mm)
The valley floor and escarpment	1335 - 1880	284	738	23	689
The highland area	1880 - 3600	527	855	14	543

4.2 Groundwater recharge estimation

Groundwater recharge is defined as the entry into the saturated zone of water made available at the water table surface together with the associated flow away from the water table within the saturated zone (Freeze & Cherry, 1979). Quantifying the rate of recharge to aquifer is the most difficult of all measures in the evaluation of groundwater resources. Estimation of groundwater recharge requires modeling of the interaction between all the important processes in the hydrological cycle such as precipitation, infiltration, surface runoff, evapotranspiration, soil moisture and groundwater level variations (Jyrkama and Sykes, 2007).

There are many sources of recharge to groundwater systems. These include recharge from precipitation, rivers, irrigation losses, urban water sources and inter-aquifer flows. Learner et al., (1990), have defined principal recharge mechanisms from these sources as direct, localized and indirect (cited in Tenalem Ayenew, 1998).

In many cases, combination of the various types of recharge will occur (Simmers, 1997). This also leads to different recharge estimation techniques (e.g. direct measurement, water balance methods, Darcian approaches, tracer techniques, empirical methods). The existence of different combinations of groundwater recharge makes the quantification process difficult (Tenalem Ayenew, 1998).

As it is mentioned above in the section 4.1 of this chapter, meteorological data limitation together with absence of hydrological data within this basin made the estimation of groundwater recharge very tough. In this study, recharge was estimated using water balance method through dividing the studied basin into two zones: the mountains highland area and the valley floor including its escarpment. The classification is based on the prevailing climatic conditions, topographic features and the conceptualized groundwater system of the basin (Figure 4.10).

The highland area

This part of the basin is characterized by steeply cut deep gorges and highly rugged topographic surfaces with sharp tips (Figure 3.3). Lithologically, it is composed of basalts

of the Ashenge group (geological map of Ethiopia, 1996). The basalts show weathering and fracturing that resulted in the formation of relatively thin soil cover over the slopes.

The estimated average annual precipitation and actual evapotranspiration of this area are 855mm and 543mm respectively (Table 4.5). Although, the area possesses highly elevated mountain ridges, it receives likely moderate rainfall amount due to orographic effect.

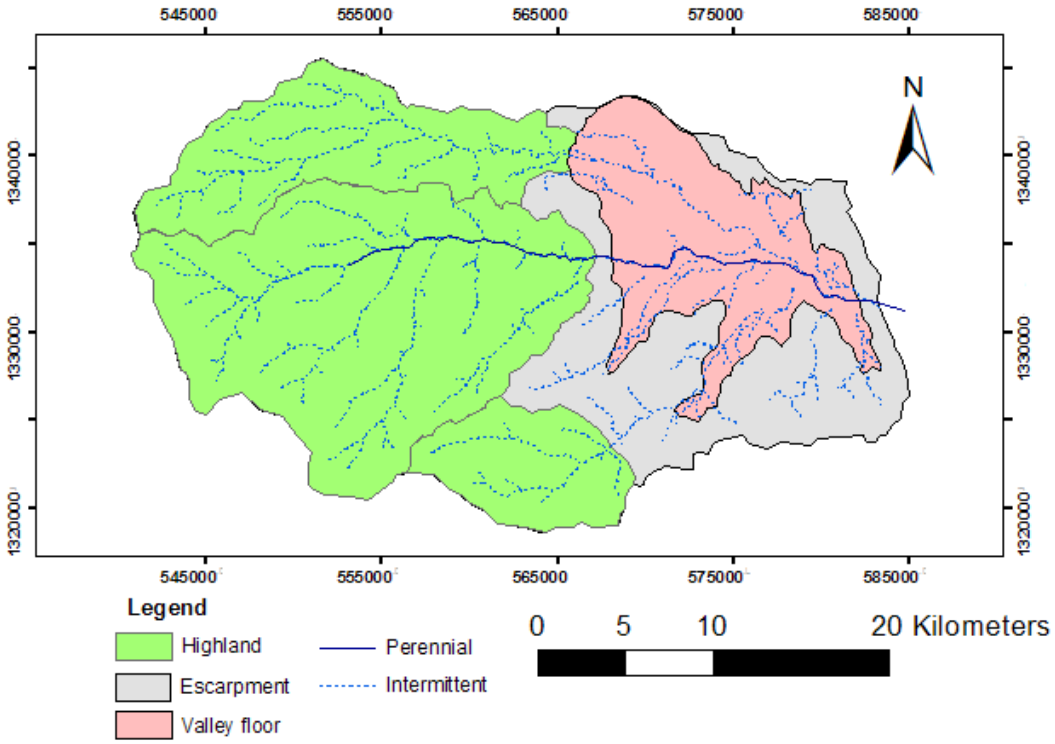

Figure 4.10. Simple classification of the basin for the purpose of recharge estimation.

At relatively short distances from the drainage divides, the base flow is perennial and therefore the recharge has to be substantial. Recharge events also have to be frequent because there is no evidence for deep significant storage of groundwater sustaining base flow over long dry periods. However, a small proportion of the recharge contributes to a deeper groundwater flow system which discharges in the valleys further downstream in the plateaux and escarpments (Tenalem Ayenew, 1998).

Similar to the above observation the starting point of perennial streams in the basin is at the foot of high mountains which are the major drainage divides. The base flow increases

downstream owning seepages from adjacent valley sides. Moreover, there are very small discharge seepage springs that are used for community water supply emerge along the local slopes.

The surface runoff over this part of the area will be expected to be the highest as it is evidenced from the geomorphologic features, drainage network and vegetation cover (Figure 4.11). To estimate the amount of runoff generated from the highland part is also another limitation as there is no measured hydrometric (river discharge) data in the area.

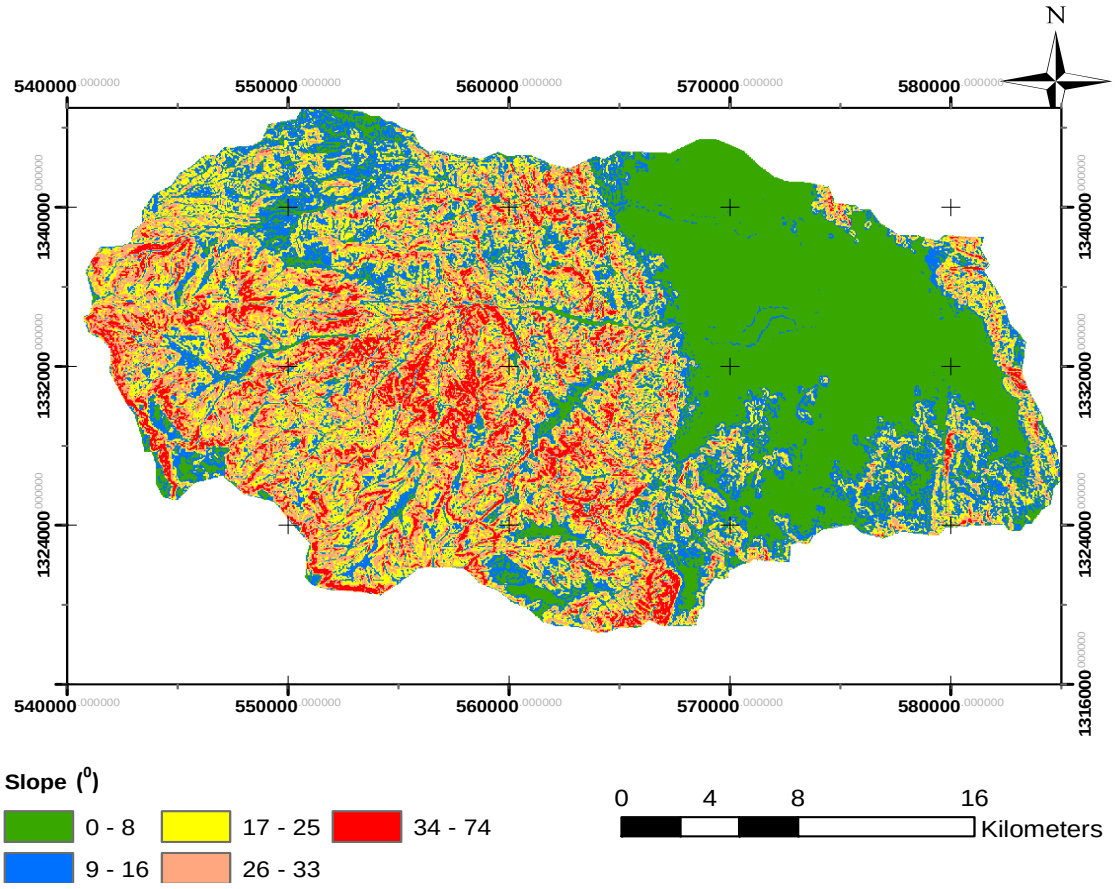

Figure 4.11. Slope map illustrating the topographic gradient.

However, the runoff coefficient was adopted from the nearby Hayq–Ardibo inter-mountain lakes catchment, which has some similarity with the present study area.

The mean runoff coefficient for Hayq–Ardibo catchment is 0.3(Molla Demlie, 2007). Accordingly, the estimated runoff amount for the highland part of the studied catchment was calculated using the estimated annual precipitation for highland area.

$$\text{Runoff}_{(\text{Highland})} = \text{Runoff coefficient ®} \times \text{Annual precipitation}_{(\text{Highland})} \quad (4.3)$$

Thus, the groundwater recharge for the highland area can be calculated using simple water balance method;

$$P = ETa + Sr + R + S \quad (4.4)$$

Where, P : Annual precipitation (mm)

ETa : Annual Actual evapotranspiration (mm)

Sr : Annual Surface runoff (mm)

R : Recharge to groundwater (mm /year)

S : Soil moisture content (mm)

By considering that thick soil cover was not develop over such topographic terrain, the soil moisture content was assumed negligible for the highland area. The estimated recharge is shown on Table 4.6.

The valley floor

The valley floor including its escarpment receives relatively low annual precipitation (738mm) and has high annual actual evapotranspiration (689mm). Recharge in this area is generally assumed to very minimum from direct precipitation. However, the valley floor gets recharge from runoff along escarpments and stream leakage which flow down the highlands. The runoff from the highland area flow out to the valley floor along two mainstream channels, Golina and Hormate streams, and few along Keleklit stream.

To estimate the amount of recharge to the valley fill sediment deposits from runoff, the escarpment part of the valley (source) is delineated and the amount of runoff generated was estimated based on the runoff coefficient of previous studies. However, to compute the amount of recharge from the river leakage and seepage from volcanic aquifer is the

most difficult process (Figure 4.12). The recharge from river leakage might be estimated, if the streams draining the area are gauged at the inflow and at the out let of the valley.

Thus, the amount of recharge to the valley floor can be estimated in two ways;

- The direct recharge which is surplus of evapotranspiration and soil moisture considering that insignificant runoff over the valley plain,
- The indirect recharge from runoff along the valley escarpment

The direct recharge was calculated using the above equation 4.4 and the soil moisture content was adopted from Co-SAESAR (1999) which was computed from SCS model, while the indirect recharge was assumed 50% of the runoff from the valley escarpment. According to RVPD (1998), the runoff coefficient for the escarpments was estimated between 0.13 to 0.22.

In this study, for the estimation of recharge from the escarpment runoff, 15% of the precipitation was considered. Recharge for the escarpment area was assumed 2% of the annual precipitation. The estimated recharge values of the basin are shown below on Table 4.6.

Table 4.6. The estimated annual groundwater recharge

Part of the study area	Average altitude range (m)	Area ($km^{2)}$	Mean annual P (mm)	Mean annual T (0C)	Mean annual actual Et (mm)	Estimated annual runoff (mm), 30% & 15 % of precipitation were assumed for highland and escarpment respectively	Soil moisture content (mm/yr)	Direct R (mm/yr)	Indirect R (mm/yr) from runoff*
The Valley floor	1340 - 1590	140	738	23	689		22	27	17
The valley escarpment	1610 - 2100	144	738	23	689	49		15	
The highland	1900 - 3600	527	855	14	543	256		56	

*** It is localized to the foot of the escarpment area**

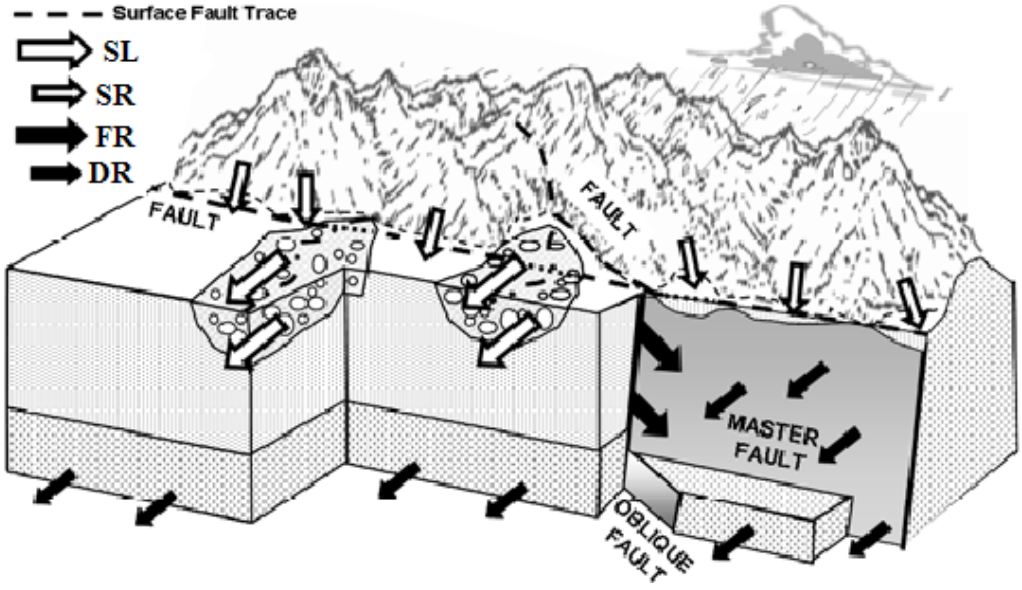

Figure 4.12. Schematic diagram illustrating mountain front recharge (MFR) components (modified after Wilson and Guan, 2004).
SL = Recharge from streambed leakage, ***SR*** = Recharge from surface runoff along steep front slopes (valley escarpment) via ephemerals, ***FR*** = Sub-surface flow through the structures (faults and fractures), ***DR*** = Sub-surface diffuse flow at the interface of the volcanic aquifer and the sediments of the basin aquifer.

4.3 Pumping test data analysis

Through proper pumping test data collection, analysis and interpretation adequate information about the groundwater condition would be generated. Since, direct observation of groundwater movement is impossible, mathematical analysis offers a convenient and reliable way to predict what happens to water in the ground. It is therefore, imperative to derive simple mathematical expressions for describing the flow region of water in the subsurface.

In this study, the analysis of the pumping test data was conducted to determine the aquifer hydraulic parameters such as transmissivity and hydraulic conductivity, which later used as one of the model input parameters. The aquifer parameters are important as they give an understanding of the groundwater flow in the system. Kruseman and de Ridder (1992), suggested that generally all the analytical methods assumed the aquifer is homogenous and isotropic, groundwater flow is horizontal and Darcy's law is valid,

discharged at constant rate, fully penetrating well of very small diameter and geologic formations are horizontal and have infinite horizontal extent. Geo Engineering Service (GES, 2003) and Metaferia Consulting Engineers (MCE, 2009) were conducted some pumping test analysis for the alluvial aquifer of the studied area.

The data processing was also includes screening and correction of the pumping test data. The data had to be corrected for external influences, which are independent of the test.

Initially the behavior of drawdown curve was compared with the various model curves to identify the aquifer type where the particular borehole was sunk. Further, the result was also compared with the borehole log. The model that comprises best fit with real system is then selected for the calculation of the physical properties of the aquifer. The analysis was done using Aquifer Test v.3.5 software.

The aquifers in the study area are mainly Quaternary alluvial deposits, and fractured and weathered basalts. Totally 50 boreholes were inventoried in this study and almost all were sunk in the alluvial sediments aquifer with the exception of very few boreholes which are located in the volcanic aquifer. However, most of the early constructed boreholes have incomplete data. For the purpose of this study, pumping test data of 19 large diameter (12''∅) boreholes were analyzed. All the boreholes were sunk in the alluvial aquifer. Among these boreholes, 10 of them have observation well. The boreholes have relatively complete pumping test data, deeper in depth and well distributed over the valley plain. However, to have result that is more representative over the area particularly the valley plain, pumping test analysis results of previous studies were used.

The pumping test data show that the constant test was conducted for 72 hours for most of the boreholes. Before calculating the hydraulic parameters, the aquifer type was identified by comparing with the theoretical models that are developed for a specific aquifer type (confined or unconfined). Consequently, comparison of recorded drawdown with various theoretical models with the log-log plots and semi-log plots of the drawdown versus time were used. Moreover, borehole lithologic logs were also

considered in the identification of the aquifer type. Based on the comparison the aquifer type for the corresponding borehole was assigned as follows.

Unconfined aquifer for boreholes: PHG1, PHG2, PHG4, PHG5, PHG6, PHG7, PHG8, PHG9, PHG10, PK1, PK2, TK7, PK6, PK7, PK8 and PK9 and Confined aquifer for boreholes: PHG3, THG2 and THG4.

From the spatial distribution of the boreholes, the alluvial deposits have locally show two aquifer types. The unconfined aquifer type which covers most of the western part of the valley and semi-confined to confined type which is localized near the center of the valley plain. Evidences from drilled boreholes and VES data have shown thick sediment deposits near the center of the valley.

Recovery test help to verify the accuracy of the pumping data and assist to confirm the results of the aquifer parameters determined by the constant rate test. Recovery data are more reliable than pumping data for the reason that no pumping is involved during this test and hence no water level reading problems associated with the pumping action is encountered. Theis recovery method is applicable to data from single well recovery tests conducted in confined, leaky or unconfined aquifers (Kruseman and de Ridder, 1992).

Once the aquifer type is identified, the appropriate method of analysis was selected for computing the aquifer hydraulic parameters. Hence, Thies and Neuman methods were applied for confined and unconfined aquifers respectively. For the recovery data, Thies recovery method was used. The results of the analysis are shown on Table 4.7. The time – drawdown curves are attached in the Appendices 2.

There are three boreholes that tap the volcanic aquifer within the studied basin. The only data that was obtained from the boreholes is drilled depth which is relatively shallow, depth to water level and discharge. Therefore, it was found difficult to calculate the hydraulic parameters for the volcanic aquifer. Because of such limitation the hydraulic parameters for the volcanic aquifer was adopted from literature and the boreholes sunk on similar aquifer located out of the study area. The Transmissivity values of the volcanic aquifer from the boreholes located in adjacent catchment (Raya) show 3.68 to 70 m^2d^{-1} (Dessie Nadew, 2003).

Table 4.7 Hydraulic parameters of the alluvial sediment aquifer.

No	Well ID	Location			Observ. Well	Depth (m)	SWL (m)	DWL (m)	Q (l/s)	DD (m)	T_{av} (m^2d^{-1})	K_{av} (md^{-1})	S	Sy
		X	Y	Z										
1	PK1	568066	1340931	1491	**PK1-OB1**	170	25.54	34.54	55	9	280	3.04		0.22
2					**PK1-OB2**	151	25.68	34.22	55	8.54				0.27
3	PK2	568476	1341101	1488		137	23.56	39.13	80	15.6	341	4.06		0.57
4	TK7	569334	1341467	1475	**TK7-OB1**	160	14.27	18.96	50	4.69	486.5	3.99		0.26
5	PK6	569299	1341890	1481		145	17.52	32.55	40	15	198	2.61		0.29
6	PK7	569892	1341651	1474	**PK7-OB1**	203	20.34	23.55	40	3.21	577.5	7.41		0.06
7	PK8	569814	1341065	1469		181	17.98	37.16	50	19.2	168	1.43		0.37
8	PK9	569485	1341610	1475		145	23.85	29.76	50	5.91	768.5	8.35		0.19
9	PHG1	567688	1338578	1487		129	24.35	29.24	50	4.89	1245	13.53		0.55
10	PHG2	567801	1337977	1479	**PHG2-OB1**	150	18.92	19.41	45	0.49	3145	44.9		0.28
11	PHG3	568356	1337982	1473		156	16.63	25.89	50	9.26	513.5	4.94	0.031	
12	PHG4	566854	1339244	1507	**PHG4-OB1**	128	27.96	32.39	45	4.43	1411.5	22.75		0.31
13	PHG5	571398	1335248	1432		155	21.5	40.01	57	18.51	244	8.13		0.25
14	PHG6	571821	1334963	1426	**PHG6-OB1**	178	20.13	25.85	58.5	5.72	1017	23.1		0.29
15	PHG7	572289	1334951	1419		180	17.53	33.04	51.6	15.51	255	4.7		0.2
16	PHG8	570553	1334124	1447		147	20.61	37.93	46.4	17.32	267.5	5.6		0.22
17	PHG9	570089	1333952	1456	**PHG9-OB1**	158	21.67	27.25	53.5	5.58	1427	29.8		0.3
18	PHG10	569560	1334010	1462		146	25.1	30.88	59.5	5.78	1412	31.4		0.25
19	THG1	576123	1336656	1384	**THG1-OB1**	118	16.21	31.02	32	14.81	350.7	11.7		0.18
20	THG3	575801	1333260	1385	**THG3-OB1**	212	3.1	16.61	57	13.51	571	9.51	0.0012	
21	THG4	575471	1331124	1408		175	5.2	12.47	62	7.27	906.5	16.8	0.0018	
22	HG-1	568171	1339140	1480		112	20.59	41.49	51	20.9	225	2.3		
23	HG-2	569552	1339024	1461		91	15.1	30.6	51	15.5	433	6.2		
24	HG3	569659	1338130	1455		111	21	59.1	20	38.1	25.06	0.84		
25	HG4	569354	1339493	1466		109	17.55	33.21	51	15.66	259.2	7.2		
26	HG11	571055	1335915	1437		116.5	14.4	35.17	50	20.77	230.54	5.52		
27	HG12	572295	1335804	1417		110.3	16.3	30.72	50	14.42	218.45	5.2		
28	HG13	571683	1336365	1425		110.6	18.26	31.61	50	13.35	239.62	5.7		
29	HG14	571067	1336466	1436		108.5	16.66	29.53	50	12.87	318.24	7.58		
30	Zeleke1	570187	1338097	1452		113	20.4	37.9	50	17.5	276			
31	Zeleke2	570658	1337490	1446		110.5	19.05	38.53	50	19.48	345			
32	TW1	568755	1329590	1367		114	58.78	62.69	7	3.91	236			
33	TW3	579090	1332043	1375		81	13.3	38.01	29	24.71	140			

SWL – Static water level **, DWL –** Dynamic water level**, Q –** Constant pumping rate**,**
DD – Draw down, **T_{av} –** Average Transmissivity**, K_{av} –** Average Hydraulic conductivity **,**
S – Storativity**, Sy –** Specific yield

5. Numerical groundwater flow modeling

5.1 Introduction

For groundwater modeling, collection and assemblages of relevant hydrogeological data have to be made. This process includes identifying hydrostratigraphic units, estimating transmisivity values, defining system boundaries, preparation of groundwater contours, etc.

There are two areas of hydrogeology where we need to rely on models of real hydrogeological system: to understand why a flow system is behaving in a particular observed manner and to predict how a flow system is behaving (Fetter, 2001). There are several ways to classify groundwater flow models, models can be either transient or steady state and one, two or three spatial dimension. Steady state flow occurs when at any point in a flow field the magnitude and direction of the flow are constant with time (Anderson and Woessner, 1992).

Proper understanding of the hydrogeologic system and realistic model inputs are imperative in order to have confidence in model simulation results. In this study most of the existing hydrogeological data such as hydraulic conductivity, transmissivity, aquifer thickness, groundwater heads, etc are limited to the valley part. This chapter focused on the simulation of groundwater flow system in the Hormate – Golina basin using groundwater flow modeling. The basin comprises low-lying valley and mountainous highland areas. The highlands particularly the western part is believed to be the recharge area for the valley part. The aquifer system was modeled using PMWIN *Pro* (Chiang et al., 1998) as pre –and post – processor for MODFLOW (McDonald and Harbaugh, 1988) assuming steady-state conditions. The aquifer was modeled under unconfined condition represented by a single layer with varying thickness. The grid cell size of the model was determined based on the existing hydrogeological data. Accordingly, a grid cell size of 250m x 250m and 500m x 500m were used for areas with sufficient data and data limited respectively. Model area and the elevations of the top layer were delineated by the ASTER DEM optimization and use of the topographic maps. Aquifer properties were assigned based on the results of the pumping test data analysis. Recharge to the major

component of the system were considered to take place as direct infiltration of precipitation for the entire model area and further inflow from the surrounding hills for the valley part. Simplified water balance method was employed to estimate the recharge. Optimized parameters such as hydraulic conductivity and recharge are spatially distributed over the model area. A combination of trial and error and automatic methods were used to calibrate the model using the observed hydraulic head.

5.1.1. The modeling process

To ensure that the modeling study is conducted correctly, it is important to use a proper modeling methodology. This is also increase confidence in the results of the model (Anderson and Woessner, 1992). The modeling protocol suggested by Anderson and Woessner (1992) was followed to come up with good result (Figure 5.1).

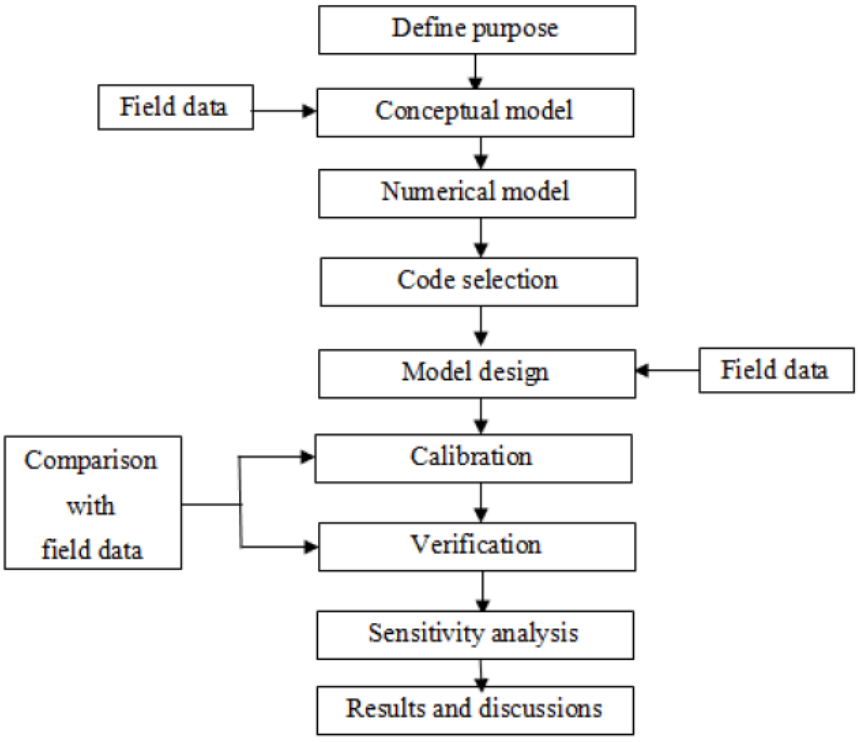

Figure 5.1. Steps in modeling protocol (after Anderson and Woessner, 1992).

5.2. Conceptual model

Developing the appropriate conceptual model for a given problem is one of the most imperative steps in the modeling process. Over simplification may lead to a model that lacks the required information, while under simplification may result in the lack of data required for model calibration and parameter estimation. A conceptual model describes how water enters an aquifer system, flows through the aquifer system and leaves the aquifer system. Briefly, it describes the hydrologic system with respect to aquifer properties, flow characteristics and boundary conditions. According to Anderson and Woessner (1992) there are three steps in building a conceptual model: defining hydrostratigraphic units, preparing a water budget and defining the flow system.

Although, there was very limited data particularly for the highland part, a simplified conceptual model was developed for the groundwater flow system in Hormat- Golina basin. To develop the conceptual model, some simplifying assumptions were made. The assumptions include: the model consists of a single layer, the model is two dimensional, the aquifer is unconfined with varying thickness and, the groundwater flow is horizontal.

In principle the groundwater flow and contaminant transport in porous medium domain are three-dimensional. However, when considering regional problems, one should note that because of the ratio of aquifer thickness to horizontal length, the flow in the aquifer is practically horizontal. The horizontal dimension may be from tens to hundreds of kilometers with a thickness of tens to hundreds of meters (Bear, 1979).

Simplification is important because complete reconstruction of the filed system is not feasible. The conceptual model should be simplified as much as possible while it is still remains complex enough to represent the system behavior (Anderson and Woessner, 1992). In this study, to simplify the complex nature of the basin, a simplified conceptual hydrogeological model of the groundwater system was developed based on information about geology, hydrogeology and hydrology.

The groundwater flow system comprises the subsurface water, the porous geologic media containing the water, the flow boundaries, the sources (outcrop areas, streams for

recharge to the aquifer), and the sinks (springs, inter-aquifer flow, and wells for flow from the aquifer) (Todd & Mays, 2005). The groundwater flow through the volcanic rocks that cover the highland part of the studied basin is mainly localized to the fractured and faulted zones. It is more likely through those structures that the groundwater flows from the highland to the low laying valley fill alluvial deposits and the underlying fractured volcanic rocks. Thermal spring that emerged on the valley floor might justify such conditions (Figure 4.12).

The hilly topography produces numerous subsystems within the major flow system. Water that enters the flow system in a given recharge area may be discharged in the nearest topographic low or it may be transmitted to the regional discharge area in the bottom of the major valley (Freeze and Cherry, 1979). From theoretical point of view, the deep groundwater flow system from the highlands should be of importance (Tenalem Ayenew, 1998).

For the modeling purpose, the system is considered in a steady- state throughout the year. Deep groundwater flow condition from the recharge highland area to the valley floor was assumed. As a result, the aquifer bottom elevation was also assumed erratic. The simplified conceptual groundwater system of the basin is shown in Figure 5.2.

5.2.1. Boundary conditions

Boundary conditions are constraints imposed on the model grid that express the nature of the physical boundaries of the aquifer being modeled. Boundary conditions have great influence on the computations of heads within the model area. Anderson and Woessner (1992) defined three types of mathematical conditions used to represent hydrogeological boundaries:

- Specified head boundaries (Dirichlet conditions)
- Specified flow boundaries (Neuman conditions)
- Head-dependent flow boundaries (Cauchy or mixed conditions)

Boundary conditions are mathematical statements specifying the dependent variable (head) or the derivative of the dependent variable (flux) at the boundaries of the problem

domain. In steady-state simulation, the boundaries largely determine the flow pattern. Therefore, correct selection of boundary conditions is a critical step in model design (Anderson and Woessner, 1992).

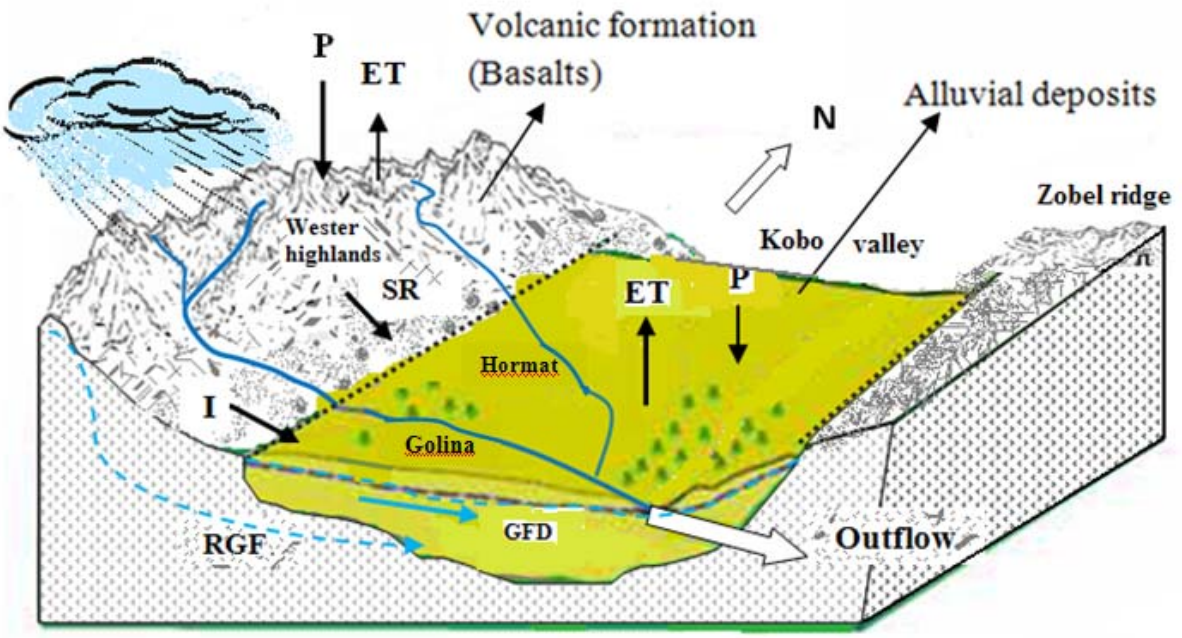

Figure 5.2. Schematic diagram illustrating the simplified conceptual model.

P = Precipitation , ET = Evapotranspiration , I = Infiltration, SR = Surface runoff without defined channel, RGF = Regional groundwater flow path, GFD = Groundwater flow direction

The basin is bounded by chain of volcanic mountains that are major drainage divide in the west, steep slope volcanic mountains that have north and south aspects in the north-west and south, Zobel mountains in the east, volcanic inselberg in the north-east and Raya valley in the north. The basin has only one outlet to the Afar depression in the southeast. The topographic divides primarily define the lateral model boundaries. Apart from the northern boundary, in these areas it can be assumed that groundwater and surface water divides coincide, and therefore a no-flow boundary has been assumed. From the boreholes data that tap the alluvial sediments aquifer, it has been assumed inflow boundary in the northern part particularly near kobo town. The groundwater exits the system in the form of base flow through a gap at southeast of the Kobo valley

(Figure 5.4). The drain package was applied along the lower reach of the Golina river, which cuts through the eastern ridge at 'Golina Ber', in order to simulate the groundwater discharge through the outlet. The out let has a width of about 20m and cuts through the basaltic rock.

5.2.2. Stratigraphic units

Identification of hydrostratigraphic units is crucial in determining the number of layers controlling groundwater flow within the system. A hydrostratigraphic unit is comprised of geological units of similar hydrogeological properties. Numerous geological units may be grouped together or a single formation may be subdivided into different aquifers and aquitards (Anderson and Woessner, 1992).

As it was discussed above in section 3.6.2, in the basin two main lithologic units were defined as aquifers based on field observation, collected data and previous studies. These are the valley fill alluvial deposits and the fractured and weathered basalt. However, the available hydrogeologic data are limited to the valley floor only. Few boreholes data, which tap the volcanic aquifer, show that there is significant difference in aquifer hydraulic properties between these two units.

The transmissivity of the alluvial aquifers in the marginal grabens vary from 0.5 to more than 500 m^2/day. The volcanic rocks making up the mountains are characterized by transmissivity ranging from 1 to 100 m^2/day. The thermal waters in the marginal grabens are depleted in $\delta^{18}O$ and δD contents and show similar values to that of the groundwater from the plateau in the west, indicating the main source of recharge to the thermal waters is groundwater inflow from the mountain body (Seifu Kebede et. al, 2007).

The above isotopic evidences and the present field study suggest that the two-aquifer systems are hydraulically connected. High discharge flowing borehole (THG2), which flows more than 20 ls^{-1} at 1.5m above the ground surface may attributed to groundwater source with high head (highland) in addition to the local confining effect.

Accordingly, in the model design the two aquifers are simulated as a single layer with laterally varying hydraulic properties (Figure 3.7).

5.2.3. Sources and sinks of the model area

For the studied basin, the primary groundwater source is direct recharge from precipitation for both the highland mountains area and the valley floor. However, the valley floor gets additional recharge from surface runoff along the escarpments and from stream leakages that drain the highlands. The primary output or sink is groundwater outflow in the form of base flow (Figure 5.2).

Recharge

Groundwater recharge processes and estimated results are discussed in section 4.2 of the previous chapter. To estimate the amount of recharge, the basin was divided into three zones: the highland area, the escarpment and the valley floor. It was estimated based on water balance method (Figure 5.3). There are no recharging wells in the study area. The recharge from excess irrigation was assumed to be negligible, because the current irrigation system uses drip and sprinkler method.

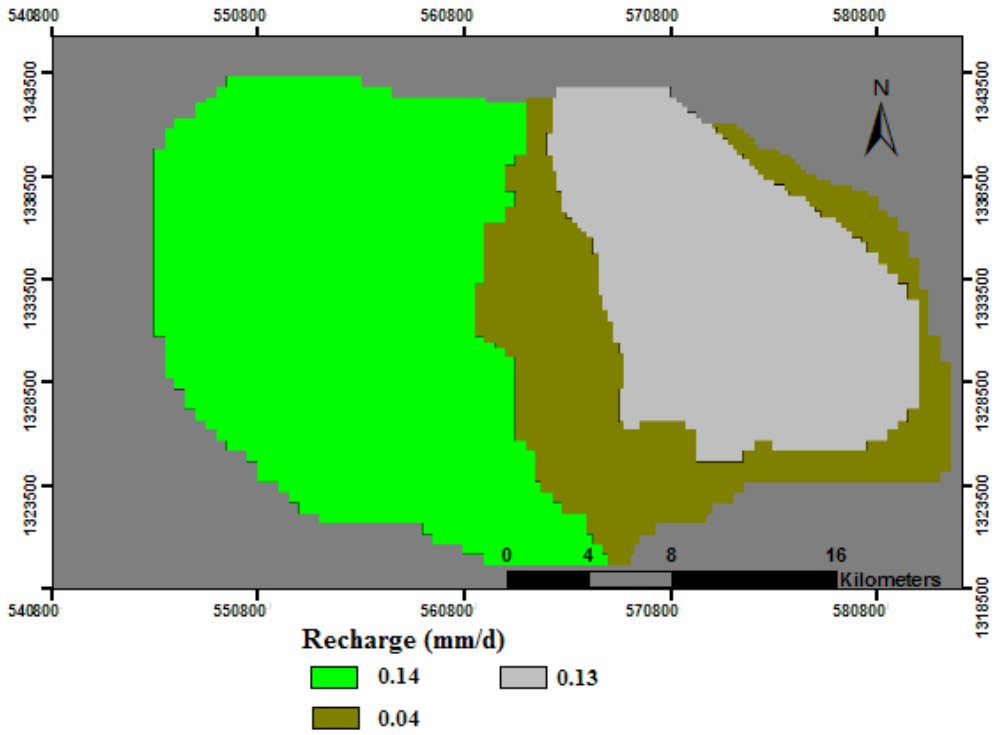

Figure 5.3. Estimated recharge zones.

Groundwater outflow/sinks

The ways of groundwater discharge from the aquifer system is mainly by discharge to streams. The main stream (Golina) that drains the western highlands gets its base flow from the volcanic aquifer and losses some amount when it reaches the valley floor (the alluvial deposits). However, near the out let to Afar it gains some amount as it was evidenced from increased flow during field visit. On the other hand, the Hormat stream collects some seepage flows from the western highlands and loses into the alluvial sediments along the stream course.

Evapotranspiration from the groundwater system can be assumed to be negligible, since there is no significant groundwater discharge areas such as marshes, swamps, and/or lakes within the basin.

Groundwater has been abstracted for water supply and irrigation purpose particularly in the valley part of the basin. However, there is no recorded data regarding the abstraction rate and duration of pumping from the wells. Based on the information from KGVDP office, Kobo town water supply office and operators who work at well pumping stations, and from the field inventory, the amount of water abstracted from the wells was estimated to be 2.68 Mm^3y^{-1} (Table 5.1).

Table 5.1 The estimated amount water abstracted from boreholes per annual

Well ID	Discharge (ls^{-1})	Jan (25 d x 6hrs)	Feb (25 d x 12hrs)	Mar (25 d x 16hrs)	Apr (25 d x 16hrs)	May (25 d x 14hrs)	Jun (25 d x 12hrs)	m^3/annual	m^3/day
Irrigation boreholes (water used per crop season)									
HG1	50	27000	54000	72000	72000	63000	54000	342000	937
HG2	50	27000	54000	72000	72000	63000	54000	342000	937
HG6	50	27000	54000	72000	72000	63000	54000	342000	937
HG7	50	27000	54000	72000	72000	63000	54000	342000	937
HG8	28	15000	30000	40000	40000	35000	30000	190000	521
HG10	34	18300	36600	48800	48800	42700	36600	231800	635
TW1	7	3750	7500	10000	10000	8750	7500	47500	130
Water supply boreholes (Kobo town)									
K33	40	40 x 8hrs x 365d						420480	1152
K34	40	40 x 8hrs x 365d						420480	1152

d = average pumping days per month, hrs = pumping hours per day

Therefore, the main mechanism of groundwater discharge from the basin is in the form base flow along Golina river. Since, this river is not gauged and possesses both processes (gaining and losing) along its course within the basin; a river package was used to simulate the interaction between the river and the aquifer.

The river package is designed to simulate the effect of flow between rivers and aquifers based on the following relations:

$$QRIV = CRIV(HRIV - h) \quad \text{For } h > RBOT \qquad (5.1)$$

$$QRIV = CRIV(HRIV - RBOT) \quad \text{For } h <= RBOT \qquad (5.2)$$

$$CRIV = \frac{KLW}{M} \qquad (5.3)$$

Where:

QRIV = rate of leakage between the river and aquifer [$L3T^{-1}$]

CRIV = hydraulic conductance of the river bed [$L2T^{-1}$]

HRIV = head in the river [L]

h = hydraulic head in cell [L]

RBOT = elevation of the bottom of the riverbed [L]

K = hydraulic conductivity of the riverbed material [LT^{-1}]

L = length of the river within a cell [L]

W = width of the river [L]

M = thickness of the riverbed [L]

In the data collection, areas where access is difficult to measure the river, it was inferred from aerial photos, images and immediate nearby data. The hydraulic conductivity was also adopted from literature.

Drain package

At the out let of the basin, the volcanic rock through which the river cuts was assumed to have relatively very low permeability. Therefore, leakage from riverbed to the bedrock

channel will be negligible. For such reasons the drain package is more convenient and was used in the model to simulate the groundwater outflow in the form of base flow at the outlet of the basin.

Drain package is different from river package in that the flow is directed only from the aquifer towards the drain and it stops when the head in the aquifer drops below the elevation of the drain. The rate of flow entering the drain (QD) is calculated from the following equation 5.4 (McDonald and Harbaugh, 1988):

$$QD = CD\,(h - d) \qquad \text{For } h > d \qquad (5.4)$$

$$CD = \frac{KLW}{M} \qquad (5.5)$$

Where:

K = equivalent to hydraulic conductivity of the drain material [LT^{-1}]

L = length of the drain within the cell [L]

W = the width of the stream within the cell [L]

M = the thickness of the stream bed material [L]

h = aquifer hydraulic head [L]

d = elevation of the drain [L]

The value of CD was adjusted during calibration process, L is approximated to the length of the cell, W was estimated to be 20 m, and M was estimated to be 2.5m. There is no any such recorded data and it was impossible to be accurate on a detailed level.

5.2.4. The model area

The model area was delineated by processing ASTER DEM using GIS and use of topographic maps. It was defined along the surface water divide. The grid cell size of the model was determined based on the existing hydrogeological data. Accordingly, a grid cell size of 250m x 250m and 500m x 500m were used for the valley floor and the highland parts of the basin respectively. A total of 806-km^2 area of the basin was modeled (Figure 5.4).

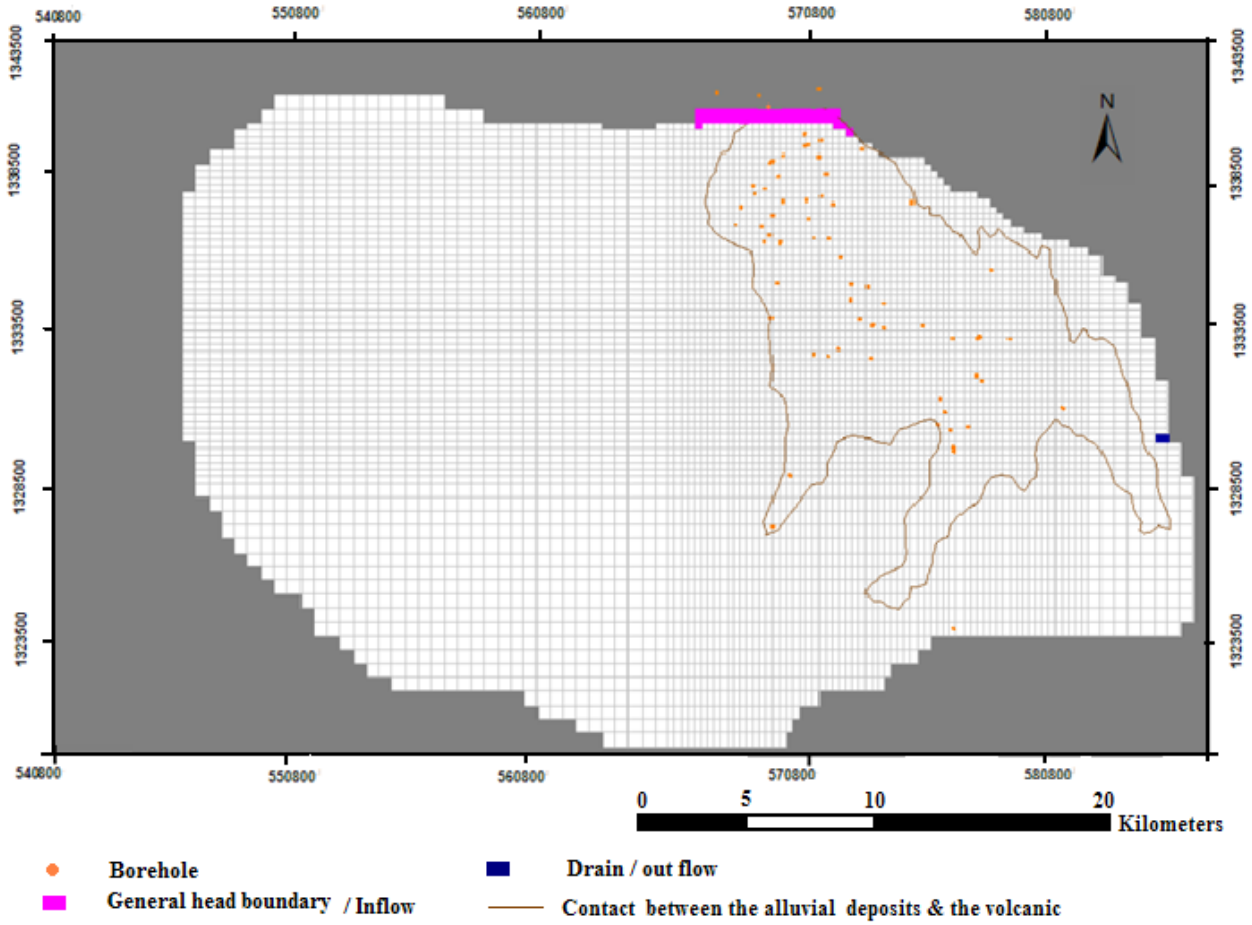

Figure 5.4. Discretization of the model area.

5.2.5. Aquifer geometry

The extent of the aquifer was inferred from limited available hydrogeological data and hydrogeological cross-section (X – X'). Since, unconfined aquifer was assumed, the aquifer top elevation was assigned surface elevation, which was extracted from the ASTER DEM using Surfer grid slicing method. The bottom elevations of the aquifer were inferred, by assuming that the two aquifers (the volcanic and the alluvial deposits) are hydraulically connected. As a result, the aquifer bottom elevations were varied depending on the surface elevation (Figure 3.7). The average aquifer length and width are 36 km along E – W and 22 km along N – S respectively.

5.3. Numerical model

Numerical model development allows for a detailed analysis of the movement of water through the hydrologic units that constitute the groundwater flow system. The groundwater flow through the highland volcanic aquifer and the valley fill unconsolidated deposits of the basin were simulated using the U.S. Geological Survey modular three – dimensional finite- difference groundwater flow model, MODFLOW (McDonald and Harbaugh, 1988). This numerical modeling was performed using the interface of Processing Modflow *Pro* (*PMWIN Pro*), Version 7.0.17 (Chiang and Kinzelbach, 2001) as code environments for the data input and output management. *PMWIN Pro* supports MODFLOW- 2000, PEST- ASP, different packages, and models/programs. It is founded on the physical theory of groundwater movement: Darcy's law and the continuity equation. The steady- state groundwater flow is simulated based on the following governing differential equation under two- dimensional aerial view (Anderson and Woessner, 1992).

$$\frac{\partial}{\partial X}\left(K_x \frac{\partial h}{\partial X}\right)+\frac{\partial}{\partial Y}\left(K_y \frac{\partial h}{\partial Y}\right)+R=0 \qquad (5.6)$$

Where:

Kx and Ky = Components of the hydraulic conductivity along x, and y axes [LT^{-1}]

R = Flux per unit volume representing sources/sinks term [T^{-1}]

h = Hydraulic head [L]

5.3.1. Data input for the model

The model input data were processed and analyzed in chapter four. The data were feed to the model in accordance to how the computer code runs to simulate the input data. The model was assumed to simulate the developed conceptual model. After defining the model extent and boundary conditions, the aquifer top elevation (processed DEM) was imported into the model. Whereas, the aquifer bottom elevation was assigned from the cross-sections. The cross –sections are selected, in such a way that the volcanic and the alluvial aquifers are hydraulically connected (Figure 3.7). The hydraulic conductivity values from the pumping test analysis of the alluvial aquifer were used as initial values

for this aquifer in the model input by making different zones along the valley floor. However, the hydraulic conductivity values for the volcanic aquifer were adopted from literature depending on the nature of geology and hydrogeology of the area. Since the area is part of the rift margin, where there are prominent faulting and fracturing, the hydraulic conductivity values were assumed to decrease away from the escarpment (Figure 5.5). The estimated recharge values were distributed as initial values in the model area after making in to three zones (Figure 5.3).

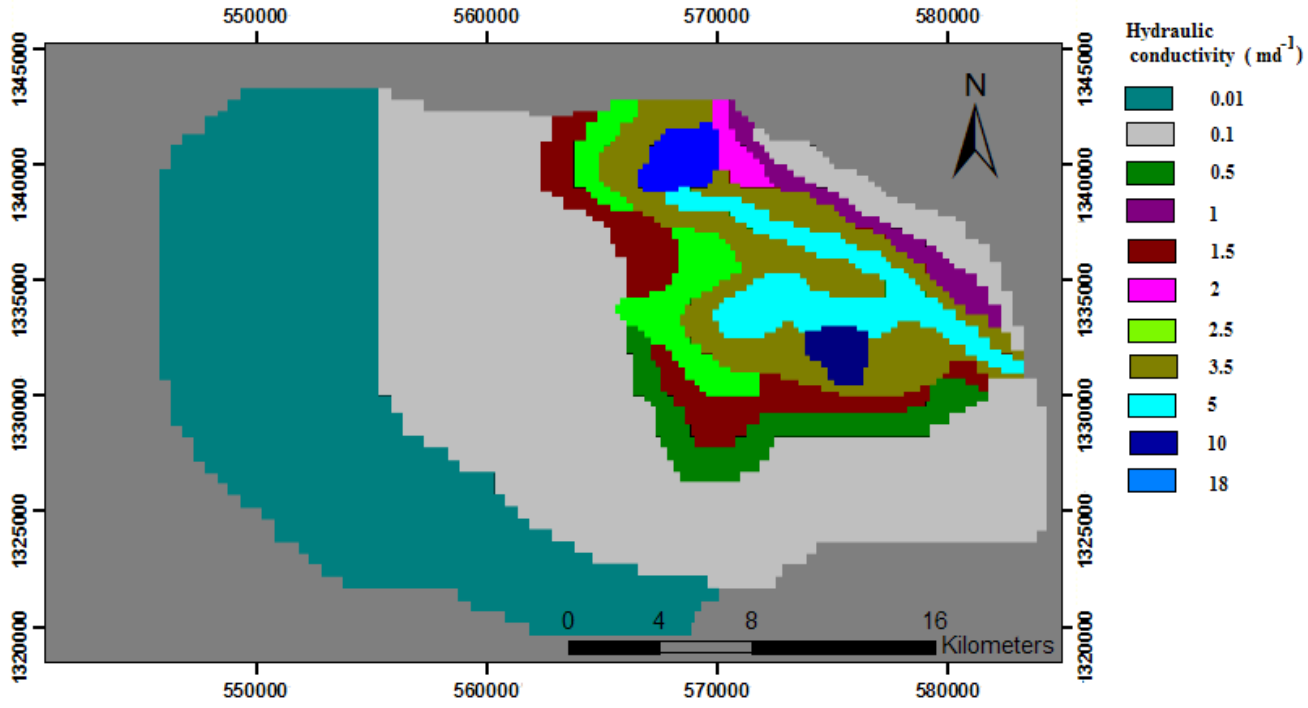

Figure 5.5. Hydraulic conductivity values used as initial model input.

More than 35 borehole coordinates and observed water levels were organized and imported into the model for the calibration purpose.

5.3.2. Model execution and calibration

Model execution includes the entry of organized input data into the selected computer code, and interpretation of the model results. Model results were compared with the

calibration target and if the error in the simulated results is acceptable, the model is considered as calibrated; if the level of error is unacceptable, the input parameter values are adjusted within a reasonable ranges and the model is run again until acceptable results are achieved. The model runs with the interactive method.

5.3.3. Calibration target and uncertainty

The calibration target was to match the hydraulic heads simulated by the model with the observed heads. In this study, the hydraulic heads obtained from groundwater level measurement data were used as calibration values. The hydraulic heads were obtained from water level records measured during drilling. It should be noted that most of the measured head data and the uncertainty of the model are associated with errors due to the following reasons:

- Some of the water level measurements were taken from the pumping wells, without monitoring well.
- The water level measurements are single time measurement (taken during drilling time).
- The water level measurements are from both the unconfined and semi-confined aquifer type which may result in significant head change between two points within short distance .
- Measurement errors related to measuring device and operator/user.
- Errors due to averaging ground surface elevations from digital elevation models (DEM).

Despite the above limitations the observed groundwater levels are limited to the valley floor only. Because of the absence of wells and high discharge springs that emerge along the valley escarpment and nearby the existing access on the highland volcanic made the available groundwater level data not to represent the entire model area. All the mentioned uncertainties together with data limitation made the calibration not only uncertain in some part of the model but also constitute a challenging and tough task. The standard deviation of the groundwater level below ground surface showed a value of about 6m. By considering this value together with the cumulative effect of the above uncertainties in

the input data, it was reasonable to assume a RMS error of 6m as predefined calibration target. Thirty-five boreholes were selected for calibration of the steady- state model (Figure 5.4). Initially, the model was calibrated for the condition without abstraction, which helps to observe the model reliability in generating field condition when it is subjected only to the natural stresses. In order to see the effect of abstraction on the model calibrated hydraulic heads and on the overall water budget of the basin, the estimated abstracted water from the wells (2.68 Mm^3y^{-1}) was used (Table 5.1).

5.3.4. Trial- and- error calibration

Trial- and – error calibration was the first technique to be used and is still the technique preferred by most users (Anderson and Woessner, 1992). It is the process of manual adjustment of input parameters until the model simulates the measured heads within range of the error criteria. The model was calibrated for steady- state conditions, assuming constant recharge and steady discharge neglecting seasonal fluctuations. Calibration was conducted through trial and error by varying aquifer hydraulic conductivity, recharge and river bed material conductance values. During the calibration, the parameter values and their zones were modified manually and trial runs were carried out until the model result was close to the pre-defined error criterion. The best-fit results were achieved after the model area was divided into different zones of the respective parameters. Since the available hydrogeological data are limited to the alluvial deposit aquifer, more hydraulic conductivity zones were extrapolated in this region whereas for the volcanic aquifer relatively a homogenous condition was assumed (Figure 5.5). Despite of very limited hydro-meteorological data in the basin, three recharge zones were defined based on different assumptions, as it was discussed in chapter four, section 4.2. The procedure followed for the trial- and-error calibration is shown in Figure 5.6.

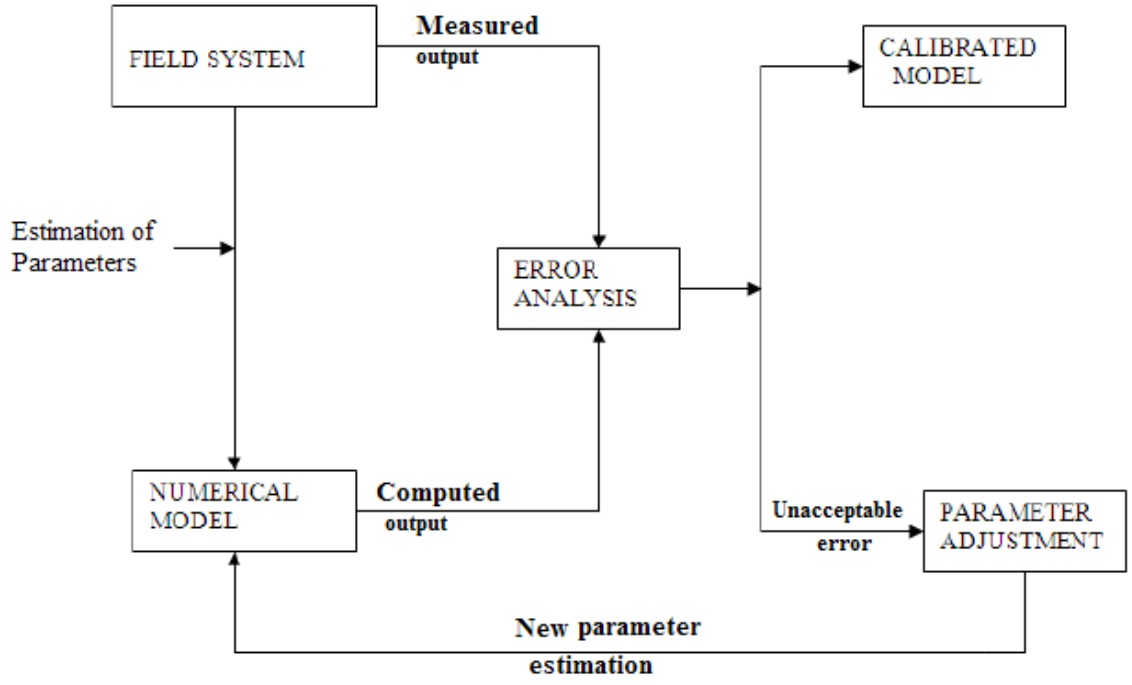

Figure 5.6. Trial and error calibration procedures (adapted from Anderson and Woessner, 1992)

5.3.5. Evaluation of calibration

The results of the calibration should be evaluated both qualitatively and quantitatively (Anderson and Woessner, 1992). The mean of the observed and simulated heads differences was used to quantify the average error in the calibration process. The three ways of expressing the average difference between simulated heads (h_s) and measured heads (h_m) are the mean error (ME), the mean absolute error (MAE) and the root mean square error (RMS). The objective of the calibration is to minimize these error values.

$$\mathbf{ME} = \frac{1}{n}\sum_{i=1}^{n}\left(\mathbf{h_{m,i} - h_{s,i}}\right) \qquad (5.7)$$

The mean difference between measured heads and simulated

$$\mathbf{MAE} = \frac{1}{n}\sum_{i=1}^{n}\left|\left(\mathbf{h_{m,i} - h_{s,i}}\right)\right| \tag{5.8}$$

The mean of the absolute value of the differences in the measured and simulated heads

$$\mathrm{RMSE} = \sqrt{\frac{1}{n}\sum_{i=1}^{n}\left(h_{m,i} - h_{s,i}\right)^2} \tag{5.9}$$

The average of the squared differences in measured and simulated heads

The above error measures can only be used to evaluate the average error in the calibrated model. The RMSE is usually thought to be the best measure of error if errors are normally distributed. The maximum acceptable value of the calibration criterion depends on the magnitude of the change in heads over the problem domain (Anderson and Woessner, 1992).

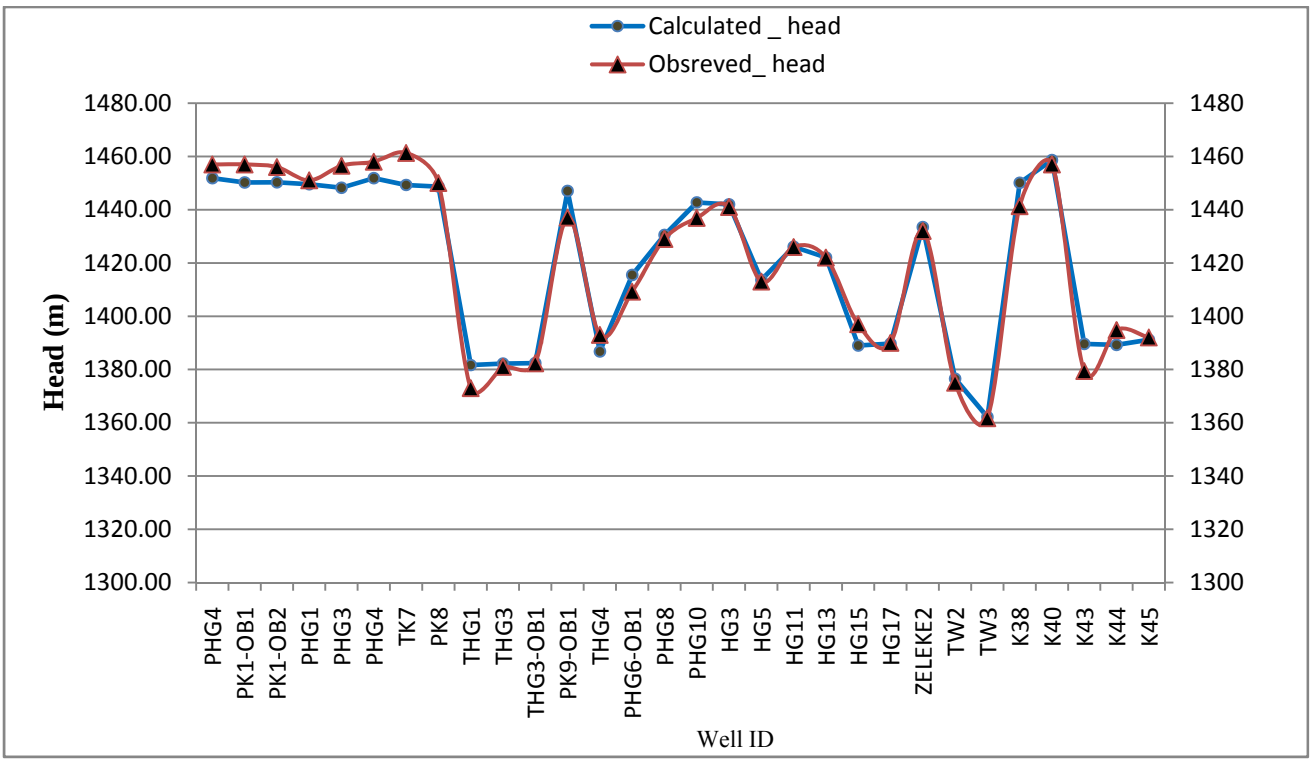

Figure 5.7. Graphical comparison between the observed and simulated heads.

Model generated scatter diagram showing the calibrated fit between the observed and simulated heads is shown in Figure 5.8. The scatter plots are visually examined whether points in a plot show deviation from the straight line in a random distribution or have systematic deviation, where systematic deviation of the plots can indicate systematic error in adjusting the parameter values. The scatter plot shows a correlation coefficient of 0.97 and RMSE of 5.7m.

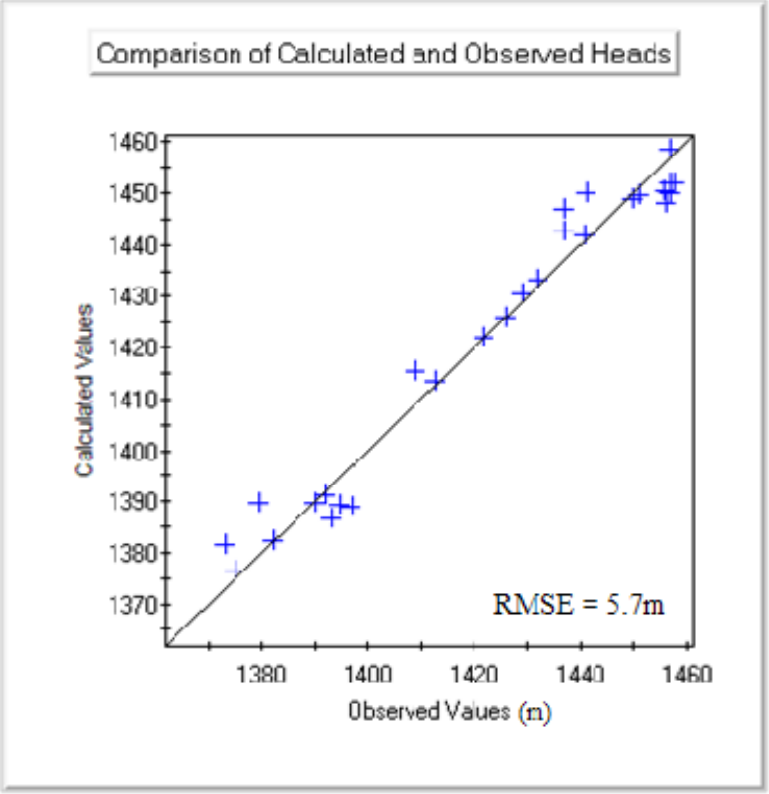

Figure 5.8. The scatter diagram showing the comparison of measured and simulated heads

The differences in simulated and observed heads are shown in Appendix 3. The summary of the error analysis for the calibrated model is shown in Table 5.2.

Table 5.2 Error summary for the calibrated model

Type of error measure	Value (m)
ME	0.3
MAE	4.2
RMSE	5.7

While, the above three error measure types can only show the average error value but not the distribution of the errors in the model area. Therefore, comparison of contour maps of simulated and measured heads and scatter plots of the residual error were used to make qualitative analysis of the spatial distribution of errors.

The residual water level error is the difference between the observed/measured heads and the simulated heads. As it is shown in Figure 5.9, about 60% of the simulated water levels are within 5m head error and the rest are almost within 10m head error. Generally, from the residual head error distribution plot one can may suggest that there should be little bias in model simulation for the entire model area.

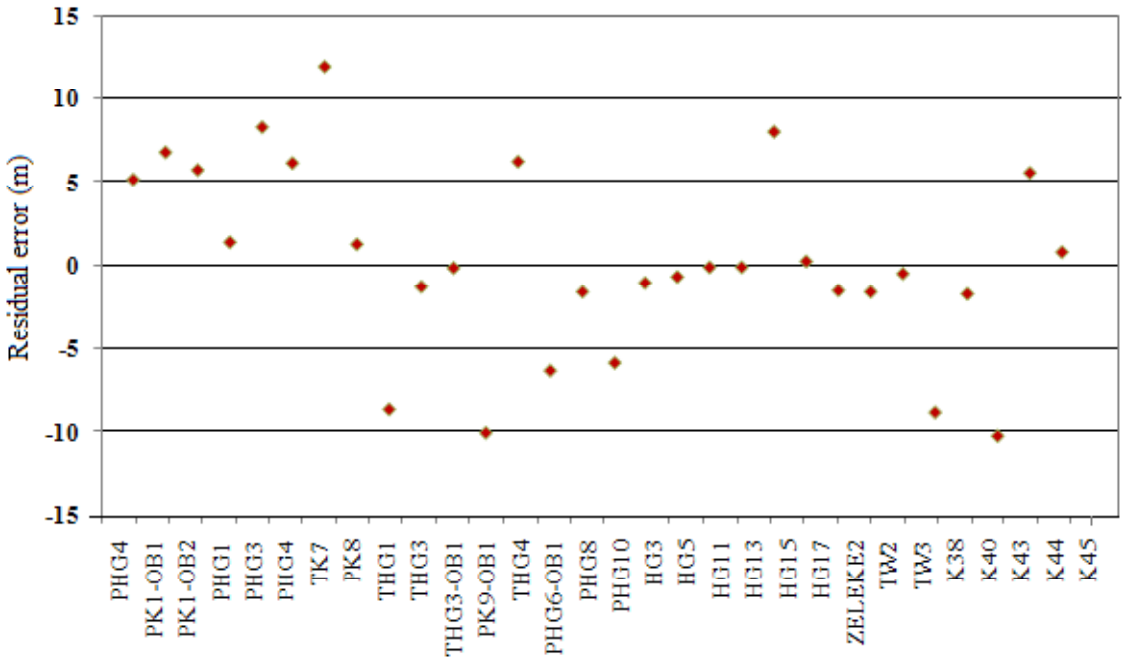

Figure 5.9. A scatter plot showing residual head error distribution .

The contour map of the hydraulic heads was assumed to represent the top of the groundwater surface in an aquifer. It helps to observe the groundwater flow direction and groundwater recharge and discharge areas. The observed and the simulated head contour maps were overlaid to see whether the model results agree with the actual field condition (Figure 5.10). The groundwater flow directions more or less agree with the conceptualized flow direction. The groundwater flow direction in the volcanic highlands shows a general trend of west to east and later converged towards the basin out let in the

alluvial sediments aquifer. The steep hydraulic gradient in the west most part of the basin may attributed to the assumed relatively low values of hydraulic conductivity and very high topographic gradient.

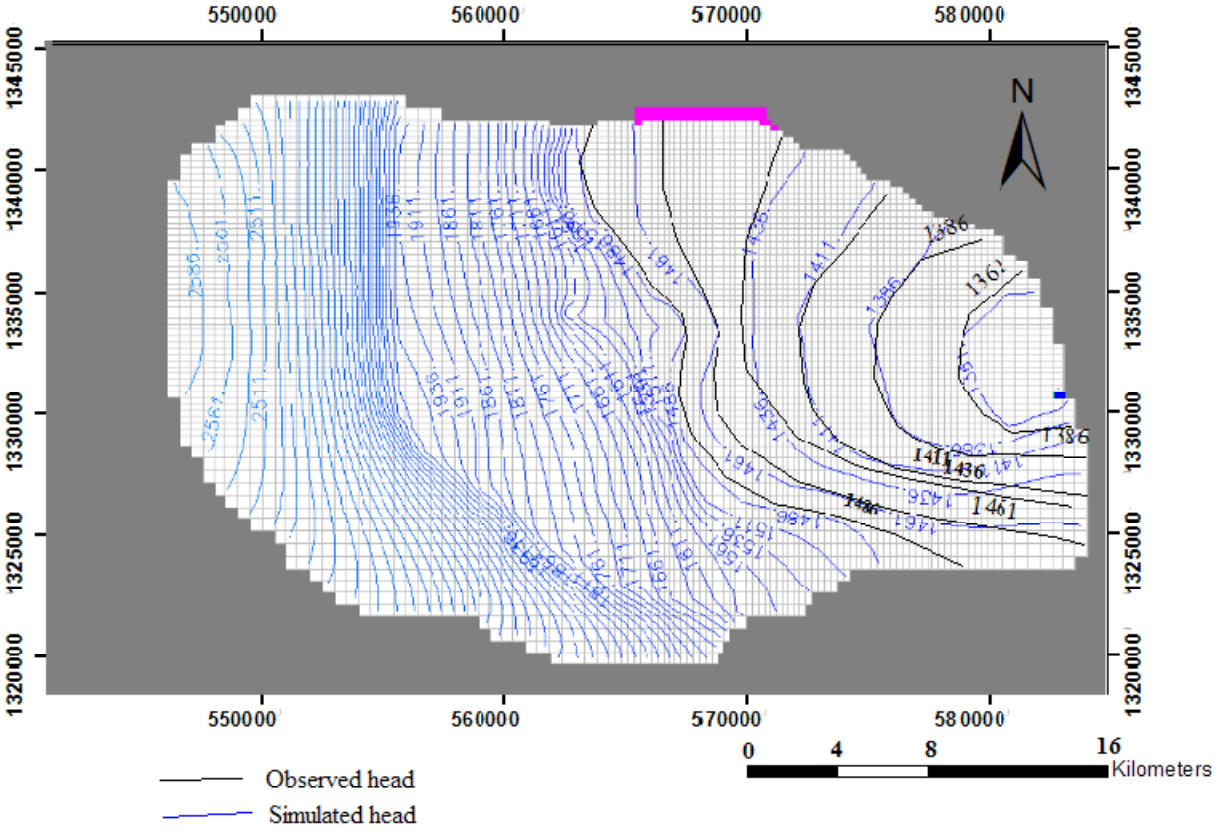

Figure 5.10 Contour map of model simulated and measured hydraulic heads

5.4. Water budget of the model domain

In direct way of checking, the amount of residual error in the solution is to compare the total simulated inflows and outflows as computed by the water budget of the entire domain. The water budget modeling is one of the methods to quantify the amount of water that flows through the aquifer system. The basic equation for a water budget under steady state condition is that sum of inputs to the aquifer equals sum of outputs from the aquifer.

$$\sum \text{Inputs} = \sum \text{Outputs} \tag{5.9}$$

In the model area, the inflow term includes the recharge, river leakage and head dependent boundary whereas, the outflow term includes drains and river leakage under natural condition. The water budget is calculated by water budget tool in MODFLOW. The model result shows both inflow and outflow are in balance which is consistent with the steady-state modeling theory (Table 5.2).

Table 5.3 Water budget of the entire model domain in Mm3y-1

FLOW TERM	IN	OUT	IN - OUT
Drains	0.0	0.2	-0.2
Recharge	17.8	0.0	17.8
River leakage	20.1	38.1	-17.9
Head dependent boundary	0.4	0.0	0.4
Total	38.2	38.2	0.0
Discrepancy [%]	0.00		

Table 5.4 Water budget of the entire model domain in mmy-1

FLOW TERM	IN	OUT	IN - OUT
Drains	0.00	0.24	-0.24
Recharge	22.34	0.00	22.34
River leakage	25.29	47.86	-22.57
Head dependent boundary	0.47	0.00	0.47
Total	48.10	48.10	0.00
Discrepancy [%]	0.00		

The model simulated water budget result shows that the main groundwater outflow components are discharge to the river and flow out as a drain (Table 5.3). The model calibrated total recharge rate of the basin is 48.10 mmy^{-1}, whereas the recharge estimated using water balance method was 51 mmy^{-1}. Despite of the limited data used to estimate the recharge using the water balance method, it agrees with the recharge estimated by the model calibration.

Moreover, MODFLOW can also computes the water budgets of the user-defined sub-regions. Accordingly, the model area was divided in to two zones: the volcanic aquifer

and the alluvial sediments aquifer. The results of the water budget of the sub- regions are shown in Table 5.4 and 5.5.

Table 5.5 Water budget of the highland volcanic aquifer in Mm3y-1

FLOW TERM	IN	OUT	IN - OUT
Horizontal exchange	5.96	28.60	-22.64
Recharge	12.80	0.00	12.80
River leakage	11.96	2.14	9.82
Head dependent boundary	0.02	0.00	0.02
Total	30.74	30.74	0.00
Discrepancy [%] 0.00			

Table 5.6 Water budget for the valley fill sediments and the underlying top most fractured zone in Mm3y-1

FLOW TERM	IN	OUT	IN - OUT
Horizontal exchange	36.83	13.33	23.50
Recharge	3.34	0.00	3.34
River leakage	7.23	34.38	-27.15
Head dependent boundary	0.32	0.00	0.32
Total	47.71	47.71	0.00
Discrepancy [%] 0.00			

The model calibrated water budget of the sub-regions as it is shown in Table 5.4 and 5.5, indicate that the calibrated total recharge for the highland volcanic aquifer and the low-lying valley part are 30.74 and 47.71 Mm^3y^{-1} respectively. As it was discussed in chapter four the recharge estimated by the water balance method for the highland volcanic and the valley floor were 29.13 Mm^3y^{-1} and 7.28 Mm^3y^{-1} respectively. Based on the comparison of the two results, the waster balance estimated recharge for the highland volcanic agrees with the model-calibrated recharge, while the recharge estimated by the water balance method for the valley part of the basin shows a significant difference with the total model calibrated recharge value. This is mainly because of the water balance method does not consider the horizontal groundwater flux from the highland volcanic aquifer which is the most important component of recharge in the model simulation result.

5.5. Sensitivity analysis

Sensitivity analysis is the measure of uncertainty in the calibrated model caused by uncertainty in aquifer parameters and boundary conditions. Sensitivity analysis was performed by systematically changing the calibrated values of conditions (Anderson and Woessner, 1992). The main objective of a sensitivity analysis is to understand the influence of various model input parameters and hydrological stresses on the aquifer system and to identify the most sensible parameter(s), which will need a special attention in future studies. By running the calibrated model for the respective changed values of the input parameter and comparing the result with the calibrated head, the parameter(s) sensitive to the model was established. The parameter values were varied within a reasonable range. Thus, it is important step in modeling studies.

The response of the calibrated model to changes in model parameters of hydraulic conductivity and recharge was examined. During model run, when the effect of one parameter was being tested, the other parameters were kept unchanged from the calibrated value. The amount of changes in heads from the calibrated solution was used as a measure of the sensitivity of the model to that particular parameter. The sensitivity analysis was associated with stressing the calibrated model differently from the calibrated conditions.

The calibrated values of hydraulic conductivity and recharge were varied by using multiplier factors: 0.4, 0.6, 0.8, 1.2 and 1.4. The changed values were used as input in order to evaluate the model's sensitive parameter(s) (Figure 5.11). Figure 5.11 depicts that the model is sensitive to both recharge and hydraulic conductivity. The model is highly sensitive with decrease of the calibrated recharge and hydraulic conductivity values and relatively less sensitive with increasing these values which result in lower RMS error.

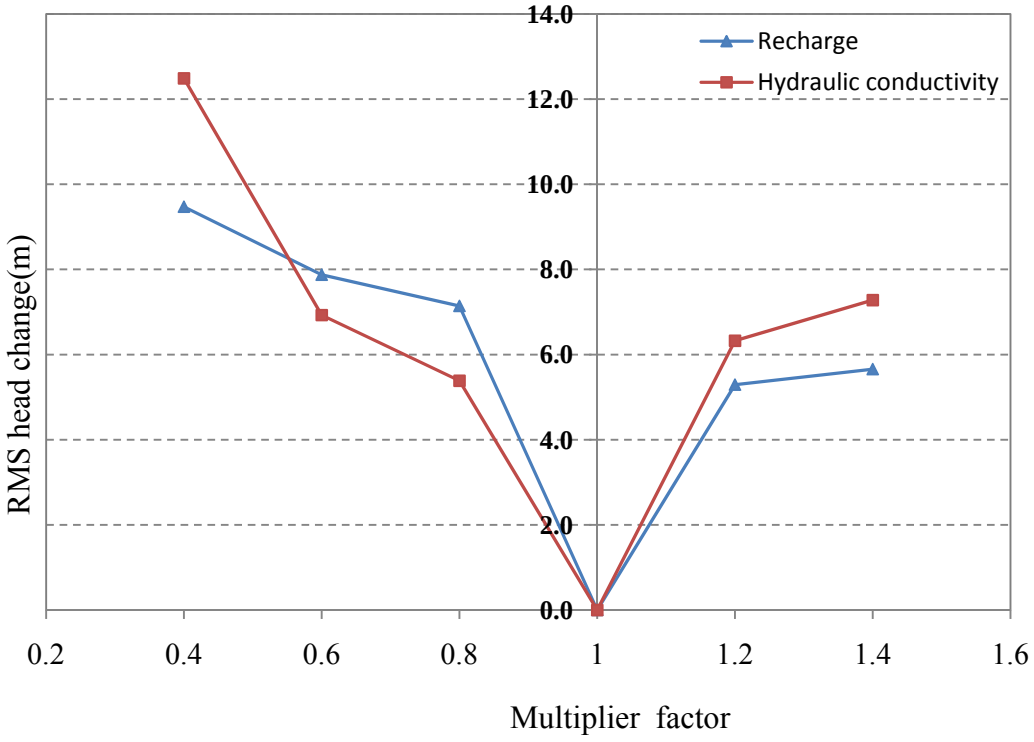

Figure 5.11 Sensitivity analyses of recharge and hydraulic conductivity

6. Pumping scenario analysis

Pumping scenarios were used to evaluate the response of the groundwater system under variable groundwater abstraction rates. The system response was compared with resulting changes in water level and groundwater outflow from the model domain. For this analysis, irrigation boreholes that tap the alluvial aquifer on the valley floor were used. Among the inventoried boreholes, only few of them are being used for the irrigation at present while others kept capped. No recorded data was available concerning how the groundwater has been utilized currently. However, based on the information obtained from project area, some estimation was performed as it was discussed in chapter five, section 5.2.3. Therefore, the actual abstraction rates are uncertain at this level. Forty irrigation and two water supply boreholes were used as discharging wells for the purpose of this analysis (Figure 5.13). They were treated in two stages as scenario-one and scenario-two under steady-state condition. Based on the information obtained (Table 5.1), it was estimated that 18.6 m^3d^{-1} of groundwater was utilized to satisfy the crop water demand for every 1 ls^{-1} of well yield.

Accordingly, 21 boreholes which have different yield, were assigned for scenario- one and the remaining 21 boreholes were assigned for scenario-two (Table 6.1 – 6.2). In scenario - one a total of about 6.3 Mm^3y^{-1} of abstracted water was used to see the effect of pumping on the calibrated model. The data of each well were set into the model and processed using the well package of the MODFLOW program.

In scenario-two a total of 13.2 Mm^3y^{-1} of groundwater was assumed to be abstracted from 42 boreholes i.e., including the 21 boreholes used in scenario-one were used to analyze the effect of increased groundwater discharge over the model domain as compared to the calibrated model result.

Table 6.1. The estimated amount of abstracted water used in scenario-one

Well ID	X	Y	Q (ls^{-1})	Estimated abstracted water (m^3d^{-1}) *
THG1	576389	1336995	40	530
THG2	575845	1334499	50	937
THG3	576000	1333000	50	937
THG4	575449	1331350	50	937
PHG5	571410	1335231	50	937
PHG6	571823	1334961	50	937
PHG7	572284	1334915	50	937
PHG8	570553	1334123	45	810
PHG9	570154	1333909	50	937
PHG10	569657	1333976	50	937
HG1	568082	1338941	50	937
HG2	569450	1338823	50	937
HG3	569659	1338130	20	372
HG4	569354	1339493	50	937
HG5	571782	1333845	50	937
HG6	567804	1339909	50	937
HG7	568283	1340339	50	937
HG8	567346	1340010	28	521
HG9	569905	1339618	10	186
HG10	570348	1339366	34	635
K33**	567405	1339719	40	1152

* it was estimated based on the crop water demand per season (6 months)

** water supply borehole for kobo town (average 8hrs pumping/day)

The amount of water abstracted in scenario- two was increased by 52% from the amount used in scenario- one. In scenario- two, rather than increasing the amount of discharge on the existing boreholes, additional pumping boreholes were used to increase the amount of water abstracted from the aquifer (Table 6.2).

Table 6.2. The estimated amount of water abstracted from additional boreholes used in scenario-two

Well ID	X	Y	Q (ls^{-1})	Estimated amount of water abstracted from BHs (m^3d^{-1}) *
PK1	568066	1340931	50	937
PK2	568476	1341101	50	937
PHG1	567688	1338578	50	937
PHG2	567801	1337977	45	842
PHG3	568356	1337982	50	937
PHG4	566854	1339244	45	810
TK7	569334	1341467	50	937
PK6	569299	1341890	40	747
PK7	569892	1341651	40	747
PK8	569814	1341065	50	937
PK9	570100	1340420	50	937
HG11	571055	1335915	50	937
HG12	572295	1335804	50	937
HG13	571683	1336365	50	937
HG14	571067	1336466	50	937
HG16	574865	1331232	25	467.5
HG17	574673	1331879	50	937
HG18	574474	1332360	50	937
Zeleke1	570187	1338097	50	937
Zeleke2	570658	1337490	50	937
K34**	568463	1339475	40	1152

* it was estimated based on the crop water demand per season (6 months)

** water supply borehole for kobo town (average 8hrs pumping/day)

The model simulation result for scenario-one has shown that for a total of 1.73×10^4 m^3d^{-1} of abstracted water from 21 boreholes per crop season was resulted in an average decline of water level by 8m for the entire model area. However, the decline in head exceeds 14m at the boreholes close to the northern boundary of the valley (Table 6.3). According to the model simulated water budget, this area relatively receives low in-flow through the head dependent boundary.

In scenario-two, for a total of 3.61 x 10^4 m^3d^{-1} of abstracted water from 42 boreholes per crop season, the model simulation resulted in an average decline of water level by 13m for the entire model domain (Table 5.8). However, this value exceeds more than 25m in area where the wells are close together and more in number at northern and northwestern part of the valley. Generally, the effect of increased groundwater abstraction is more pronounced in the northern and northwestern part of the valley floor, where there are more boreholes at close distance and the in-flux is relatively low (Figure 5.13).

Table 6.3. Estimated groundwater abstraction rate and the average decline in groundwater level for the two different pumping scenarios

	Number of boreholes	Total discharge (m^3d^{-1}) utilized for a crop season	Average decline in head for the whole model domain (m)
Scenario-1	21	1.73 x 10^4	8*
Scenario-2	42	3.61 x 10^4	13**

* the head dropped more than 14m at pumping wells located north and northwest of the valley

** the water level dropped more than 25m where the wells are close together and more in number (Northern part of the valley)

The model generated groundwater contour maps for both pumping scenarios (Figure 6.1 and 6.2) show that the regional groundwater flow direction of the model domain remains the same, except some local effects near the northern boundary of the valley floor.

In order to minimize such significant decline in water level particularly near the northern boundary of the valley floor, it is recommended to decrease the current abstraction rate and if there is further plan to develop additional wells in this vicinity, it is advisable to locate boreholes at distance than the existing condition. According to the information obtained from the project office, one of the irrigation borehole (HG8) located northwest of the valley floor was faced a decrease in discharge from 50 ls^{-1} to 28 ls^{-1}. Such type of effects may probably associated with the above-assumed causes.

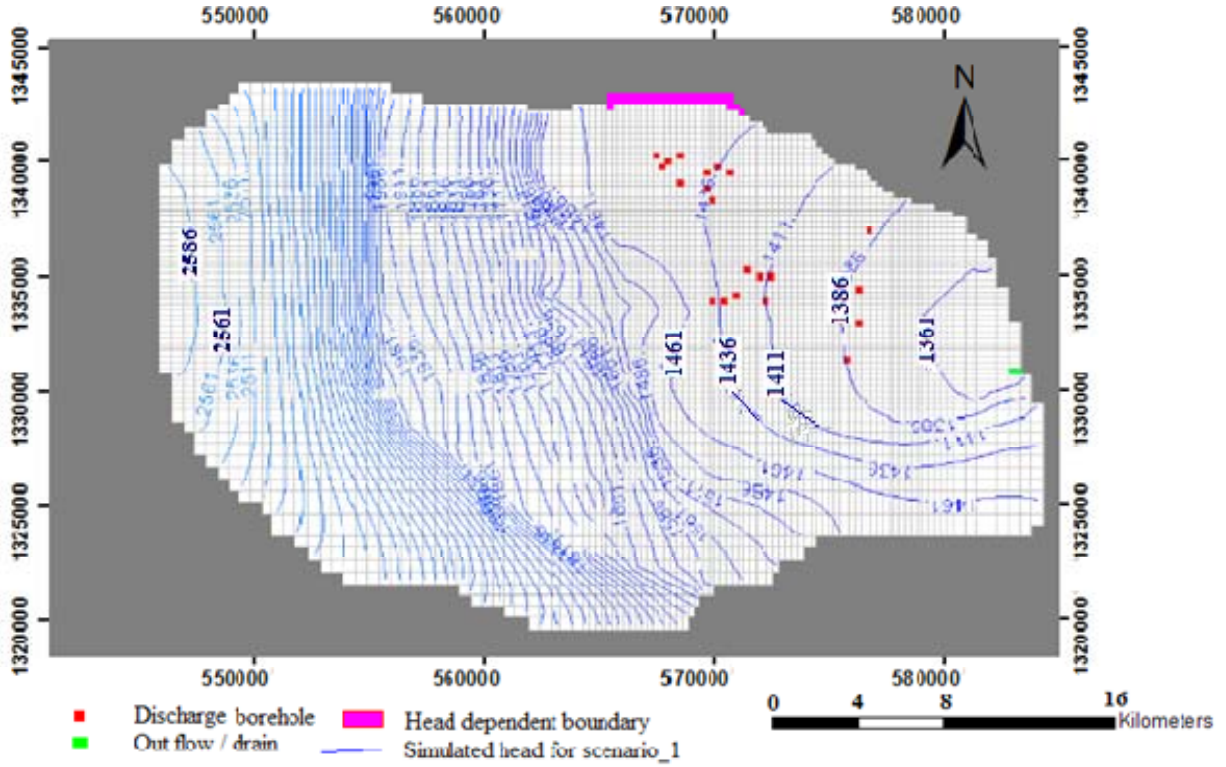

Figure 6.1 The model simulated groundwater heads for pumping scenario_1

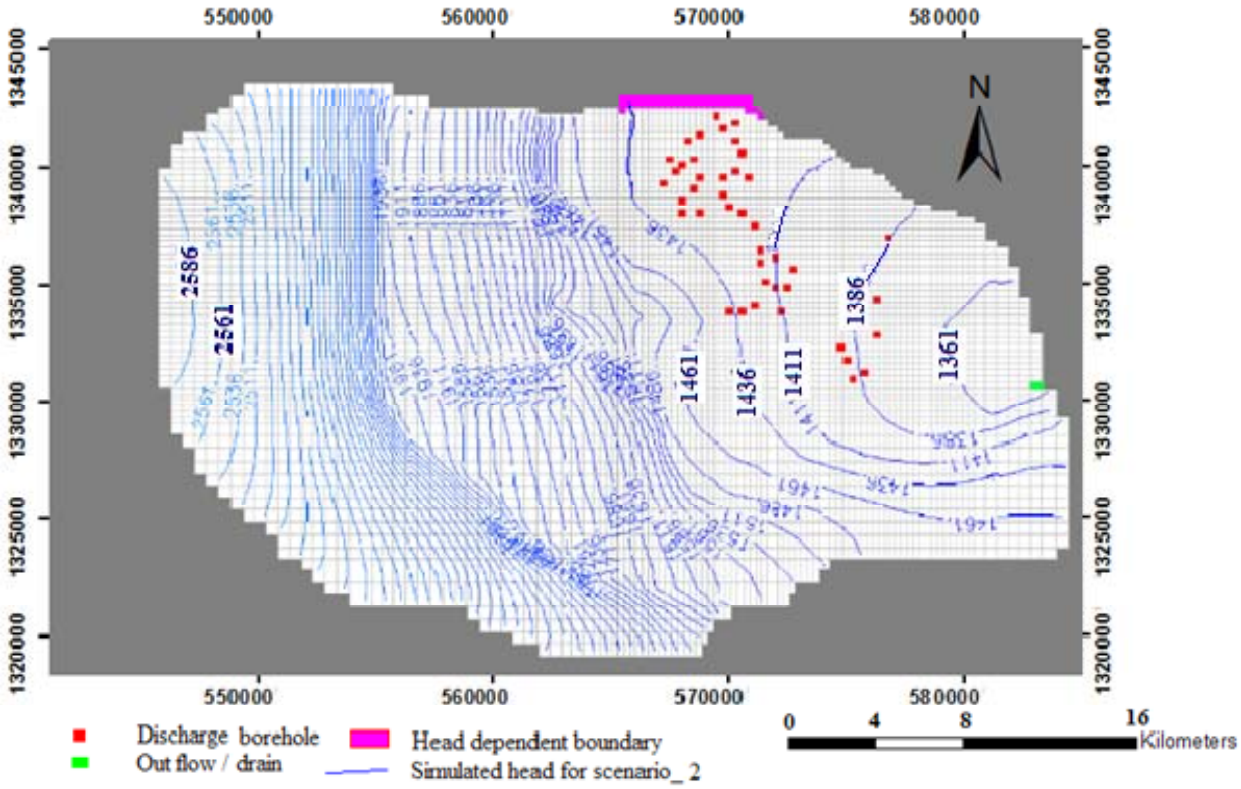

Figure 6.2 The model simulated groundwater heads for pumping scenario_2.

6.1. Model simulated groundwater budget for different pumping scenarios

Because of the irrigation area and the pumping wells are limited to the valley floor only, the model simulated groundwater budgets of the pumping scenarios were processed for the valley part of the model domain. The simulated model results for non-pumping and pumping scenarios are shown in Table 6.4.

Table 6.4. Simulated water budget of the valley (Kobo-valley) for different scenarios

Scenario	FLOW TERM	IN	OUT	IN - OUT
Non- pumping	Horizontal exchange	36.83	13.33	23.50
	Recharge	3.34	0.00	3.34
	River leakage	7.23	34.38	-27.15
	Head dependent boundary	0.32	0.00	0.32
	Total	47.71	47.71	0.00
Scenario _ 1 (with 1.73 x 10^4 m^3d^{-1} abstraction)	Horizontal exchange	36.98	12.97	24.02
	Wells	0.00	6.32	-6.32
	Drains	0.00	0.19	-0.19
	Recharge	3.46	0.00	3.46
	River leakage	8.82	30.32	-21.50
	Head dependent boundary	0.54	0.00	0.54
	Total	49.81	49.80	0.0
Scenario _ 2 (with 3.61 x 10^4 m^3d^{-1} abstraction)	Horizontal exchange	37.83	12.93	24.91
	Wells	0.00	13.19	-13.19
	Drains	0.00	0.19	-0.19
	Recharge	3.46	0.00	3.46
	River leakage	10.47	26.33	-15.85
	Head dependent boundary	0.88	0.00	0.88
	Total	52.64	52.64	0.0

6.2. Graphical comparison of the hydraulic heads simulated under different pumping scenarios

As shown in Figure 6.3, model generated hydraulic heads under three different scenarios: non-pumping, pumping in scenario_1 and pumping in scenario_2 were plotted together in order to compare the variation in head distribution.

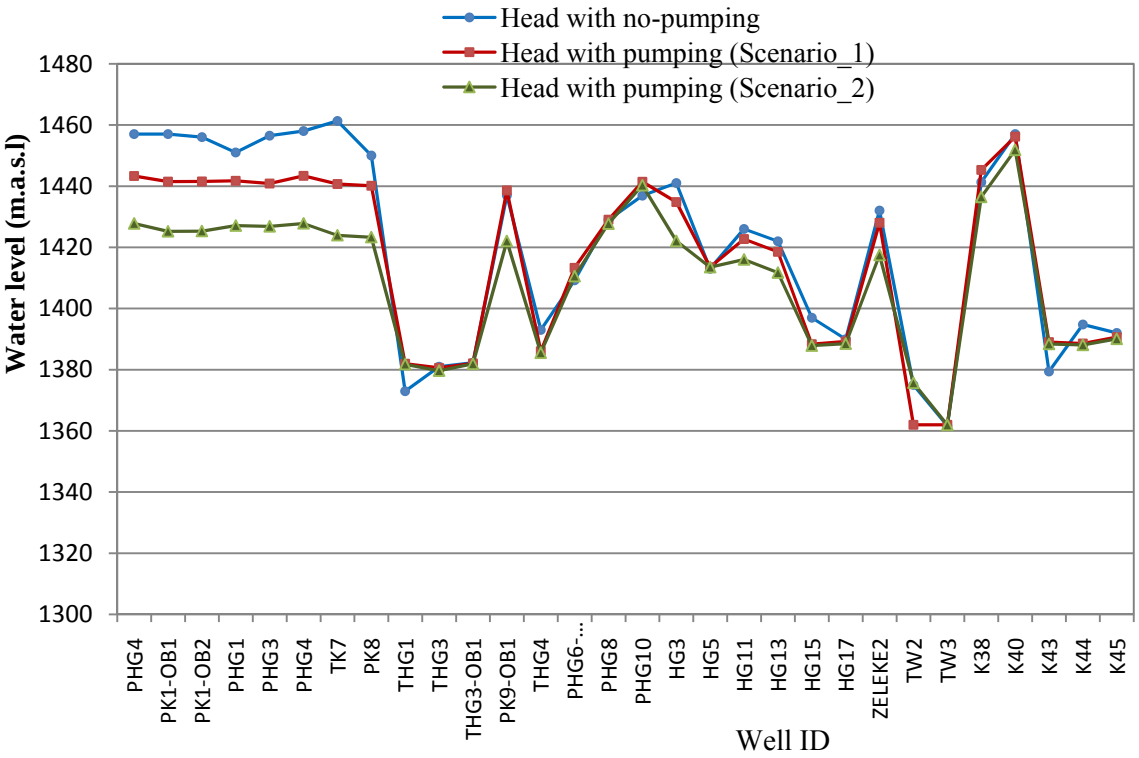

Figure 6.3 Comparison between the observed and simulated heads of different scenarios.

The decline in hydraulic head under both scenarios was more pronounced near the northern boundary of the valley floor, where there are relatively large numbers of discharging boreholes, which are closer to each other. In addition, the simulated water budget result indicates that the in-flow through the general head boundary (north part) was found very low to replenish the pumped water. The head in the remaining area of the model domain was less affected by pumping.

Similarly the scatter plot (Figure 6.4) also shows that the deviation of simulated heads below the straight line, i.e. the decline in head with respect to the observed head. The decline in heads near the pumping wells was associated to the formation of local cone of depression.

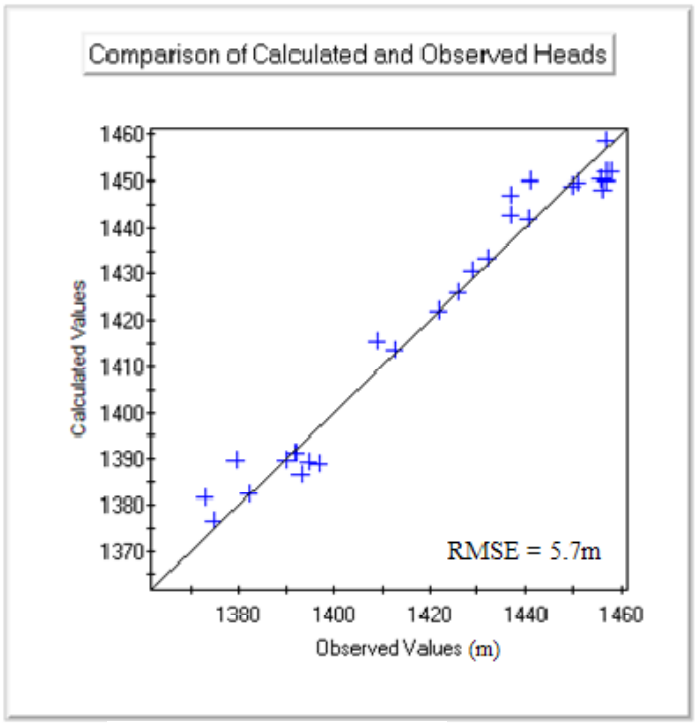

Non-pumping scenario

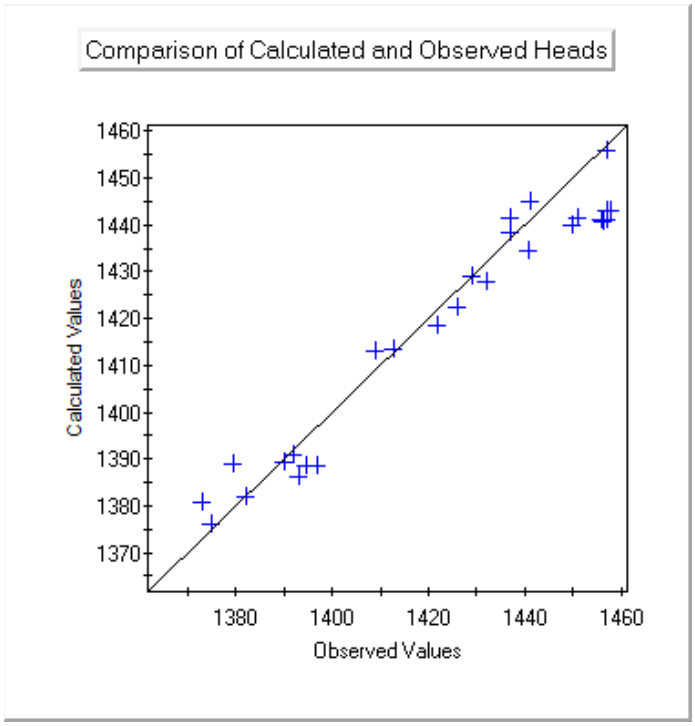

Pumping scenario_1

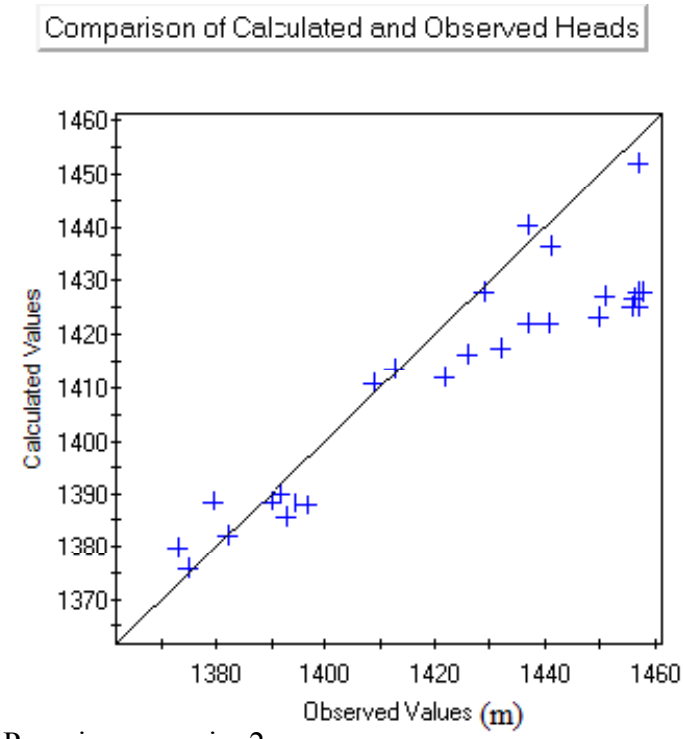

Pumping scenario_2

Figure 6.4 The scatter plots of simulated versus observed heads for pumping and non-pumping scenarios.

7. Results and discussion

In this chapter, the results from the water balance and model simulation with their respective limitations were explained and discussed.

7.1 Results from the water balance method

The water balance method was applied in this study for the estimation groundwater recharge with very limited data and interpolation techniques. As explained in chapter 4, the results were classified into three different recharge zone values (Table 4.6). According to the estimation analysis performed in chapter four, the following results were obtained.

The highland volcanic, the valley escarpment, and the valley floor receive estimated groundwater recharge of 56, 15 and 52 mmy^{-1} respectively. These values were used as initial model input in the numerical modeling. In other words, the water balance results were 29.13 Mm^3y^{-1} and 7.28 Mm^3y^{-1} for the highland volcanic and valley floor including the escarpment respectively. The model simulated total recharge (both from direct and indirect recharge) for the highland volcanic aquifer and the alluvial sediment aquifer including the underlying top most fractured basalt were 30.7 Mm^3y^{-1} and 47.7 Mm^3y^{-1} respectively. The recharge estimated by the water balance method for highland volcanic aquifer agrees with the model-simulated recharge. However, for the valley part of the basin there is significant difference between the recharge from the water balance method and model simulated. This is because of the water balance method does not consider the horizontal flux from the volcanic aquifer which is the important component in the model simulated recharge (in this context, recharge refers to the total in-flow to the aquifer).

Limitations in the water balance method

The water balance method used in this study was computed based on very few data which are limited to the valley floor. For the highland volcanic part, the meteorological data were interpolated from the stations that lie along the western highlands of the Afar rift escarpment. The highland volcanic of the study basin is also part of the western end of

the Afar rift. The runoff coefficient was adopted from the previous studies. The estimated recharge value of the valley fill sediments aquifer does not consider the in-flow from the volcanic aquifer.

7.2. The result of the numerical groundwater flow modeling

The model results were achieved after the model was calibrated through trial and error approach until the simulated hydraulic heads values fit the observed head values to a satisfactory degree. The model calibration was resulted a reasonable match between observed and calculated heads with RMS error of 5.7m (Figure 5.8 and 5.10). The results of the calibrated model were shown in Table 7.1.

Table 7.1 Summary of the model output parameters

Zone of the study area	Recharge estimated from the water balance method (mmy^{-1})	Model calibrated recharge (mmy^{-1})	Range of estimated hydraulic conductivity (md^{-1})	Calibrated hydraulic conductivity (md^{-1})
The highland volcanic aquifer	56	46	0.01 - 2	0.01 - 2.5
The valley fill sediments aquifer	44	32	1.5 - 30	2 - 18

During the modeling process, the estimated recharge from the water balance was used as initial input of model. However, the simulation result from the initial input recharge resulted in extremely exaggerated hydraulic head values. To correct these results, the model was treated in two ways: by adjusting the input recharge and changing the input hydraulic conductivity values within acceptable ranges. Since the water balance method applied for this study has many limitations as discussed above in section 7.1 of this chapter, the recharge estimated from this method might be over estimated.

The hydraulic conductivity values of the calibrated model results are almost in agreement with the input hydraulic conductivity values. However, there are few over estimated hydraulic conductivity values of the alluvial sediments aquifer obtained from the pumping test analysis.

Generally, both the hydraulic conductivity results have uncertainties due to the following reasons.

- The hydraulic conductivity values for the volcanic aquifer were adopted from literature and very limited borehole data which cannot represent the entire model area,
- Since the observed hydraulic heads were limited only to the valley floor of the studied basin, values in hydraulic conductivity outside this area can be changed significantly without affecting the calibration criterion for head values.

Groundwater flow system

Groundwater flow system is a set of flow paths used for defining groundwater flow directions. The flow systems indicate the direction of the recharge and discharge areas. Accordingly, the model simulated hydraulic heads contour map (Figure 5.10), shows that the groundwater flows from west to east in the highland volcanic aquifer, and then converges from all sides towards the south-east of the model area i.e towards the outlet. The general hydraulic gradient in both aquifers (the highland volcanic and the valley fill sediments) fairly follows the surface topography and the gradient is towards east and south-east for the highland and valley respectively. It is in agreement with the flow system defined by the conceptual model of the area. Relatively deep groundwater level was assumed for the highland volcanic aquifer because of the absence of shallow groundwater conditions along deep cut valley escarpments.

7.3 Sensitivity analysis

The sensitivity analysis is useful in determining which parameters most influence model results. These parameters should be emphasized in future data collection attempting to improve model accuracy. The analysis result shows that the hydraulic conductivity and recharge have significant impact on water level, and the model is sensitive to both parameters. The model is more sensitive with decrease of the recharge and hydraulic conductivity values and relatively less sensitive with increase of both parameters values. The analysis was conducted by using the calibrated model as a reference measure.

7.4. Water budget of the model domain

Water budget computation involves the identification and quantification of all flows in and out of the aquifer structure. The water budget of the model domain is one of the methods to quantitatively evaluate the amount of groundwater flow through an aquifer system. The summary of the entire model area water budget showed that the model calculated inflow and outflow terms are in balance (Table 5.3). The in-flow and the outflow components of the of the groundwater system which are the most difficult parameters to calculate directly were computed by the model. The result from the steady state model run shows that the total in-flow of the entire model area was 48mmy^{-1}. Since steady state condition was assumed the out-flow was also 48mmy^{-1}. Similarly, the water budget for the sub-regions: the highland volcanic and the valley were estimated using the model (Table 5.4 and 5.5). For the highland volcanic, the model estimated total in-flow from the recharge and river leakage was 54 mmy^{-1} and discharge it (out-flow) as horizontal flux to the alluvial aquifer and very few to river. For the valley part, the model estimated total in-flow from horizontal exchange, recharge and head dependent boundary was 52 mmy^{-1} and it discharges (out-flow) to the river.

7.5. Pumping scenario

The model was run for two pumping scenarios and the result was analyzed. In scenario-one with a total of 1.73 x 10^4 m^3d^{-1} abstracted water resulted in an average decline of water level by 8m. While, in scenario-two, a total of 3.61 x 10^4 m^3d^{-1} was pumped and resulted in an average decline of the water level by 13m. The decline in head is more pronounced where the wells are large in number and at close distance from each other (Figure 6.1 and 6.2).

7.6. Model limitations

Due to simplifications and assumptions used during modeling made numerical groundwater flow model to have limitations in the representation of the real world system. The degree of uncertainty in the model was raised due to the lack of data and

poor quality of the existing data. The interpretation in the modeling process such as, converting the real world into conceptual model and the conceptual model into numerical model may each step introduce errors. The available measured hydraulic heads were used for calibration. No independent measured heads were available to validate the model. Thus, the model was calibrated but not verified. Because of this the model results should not be interpreted as a perfect simulation, rather as a system response within fairly realistic model input parameters. The model may not be readily used for the detail groundwater management purposes because of the stated limitations. The results should be interpreted and applied considering all the limitations and drawbacks associated to the input parameters.

7.7 Discussion of the model

The main objective of modeling the study area was to have a better understanding of the groundwater system in the studied basin. As it was described in the result, there are still uncertainties concerning the groundwater flow system in the basin. The uncertainties can be minimized through comprehensive data collection together with continued processing of numerical models. The groundwater circulation in the area is much more complex than was previously assumed.

The model can be used for analysis of contaminant transport in the future. Provided that groundwater flow directions are a crucial aspect of the numerical model, it is obvious that more data collection is required to expand the knowledge relating to boundary conditions of the model domain.

8. Conclusion and Recommendation

8.1 Conclusion

The study was intended to obtain a better understanding of the groundwater flow system of the Hormat – Golina basin (the Kobo Valley and the highland volcanic) by applying numerical flow modeling. The following conclusions can be draw from the results obtained in the study.

In order to simplify the computation and for the purpose of analysis, the basin was divided into two regions: the highland volcanic aquifer and the valley fill sediments aquifer. All the previous studies were limited to the valley fill sediments.

The study was set better approach for the defining of the conceptual model which was transferred to the numerical model that has capability to imitate the field data with relatively good accuracy. The field observation together with the model result can be used to realize the aquifers systems under steady state condition despite of the uncertainties of the results. The uncertainties can be minimized by extended data collection that allows the model to be refined in detail for better accuracy. It is also important to simulate transient conditions and make a thorough validation prior to use for predictions and management.

The calibrated steady-state groundwater flow model of this study was able to reasonably simulate the hydraulic heads that fit the measured heads particularly for the valley part of the basin. In addition, the model simulated heads contour map shows that the general hydraulic gradient in the basin pursues the surface topography and the gradient is towards east for the highland volcanic and towards southeast for the valley area. It was in agreement with the groundwater flow system defined in the conceptual model.

The water balance method used for this study has many limitations, thus the recharge estimated from this method might be over estimated. Although this method has many drawbacks, the recharge from the water balance method was used as initial model input.

The boundary conditions defined for the model area were well simulated by the model to reflect the real conditions. The calibrated model simulated water budget result shows that

the valley fill sediments aquifer gets more in-flow (23.50 Mm^3y^{-1}) from the highland volcanic aquifer by horizontal flux, 3.34 Mm^3y^{-1} from recharge and insignificant in-flow (0.32 Mm^3y^{-1}) from the head dependent boundary. For the steady state assumption, the basin discharged the same amount of water to the river. The effect of very low in-flow condition along the general head boundary in the northern boundary of the valley may have contribution on the significant decline in discharge of the irrigation well close to this boundary.

Based on the analysis of field data together with the pumping test data analysis, the alluvial aquifer is not entirely unconfined type. Some part of the valley particularly near the valley center shows confined aquifer type. This is presumably due to relatively thick clay horizons, which was verified from borehole lithological logs.

The sensitivity analysis showed that the model is sensitive to both the horizontal hydraulic conductivity and the recharge. Both parameters have significant influence on the model simulated hydraulic heads.

The steady state model with pumping scenarios depicts that groundwater abstraction of 1.73×10^4 m^3d^{-1} and 3.61×10^4 m^3d^{-1} from the alluvial sediments aquifer resulted in a maximum groundwater head decline of 14m and 27m respectively in the pumped wells close to the northern boundary of the valley. The simulated heads contour maps of both pumping scenarios showed that the general groundwater flow direction was remain unchanged except with some local change near the northern boundary of the valley.

The study concludes that the steady-state numerical groundwater flow model together with the conceptualized model can be used to visualize the groundwater response of the study basin for the stresses applied (recharge and withdrawal) despite of the limited data.

8.2 Recommendation

Since all the previous studies were limited to the valley only, the current study can be used as a base for the regional groundwater flow modeling of the entire Hormat- Golina basin which comprises the valley (Kobo valley). For detail modeling in the future, further refinement of the model is possible, which is expected to improve the accuracy of the model, if additional data and further comprehensive field-based observation become available.

The model was calibrated but not verified. Hence, the results obtained here should not be considered as a perfect simulation, rather as a system response within reasonable model input parameters. Thus, the model should be applied with caution for detail groundwater management use. The results should be interpreted and used considering all the limitations and drawbacks related to the input parameters.

To improve the calibration values, groundwater level and abstraction rates should be monitored at a set of monitoring wells that are properly distributed in the area. In order to minimize measuring error, the observation wells have to be fitted with automatic water level measuring device. Once an improved steady-state model is developed and the necessary data are obtained, a transient model for the pumping scenario should be made for better predictions of pumping effect and for better recharge simulation, as recharge and groundwater outflow are strongly time dependent.

In this study, the thickness of the volcanic aquifer was assumed from the selected cross-section. However, for a better accuracy it needs further investigation as it has impact on the model simulation. The thickness of the alluvial aquifer was inferred from the existing borehole data and the alluvial aquifer was assumed to be hydraulically connected with the underlying fractured volcanic aquifer. This assumption needs further field verification through drilling.

The hydraulic conductivity to which the model is highly sensitive requires better characterization. Recharge, as the most sensitive parameter of the model, should also be estimated in a more precise way, because when converting to transient condition it is necessary to have knowledge on the spatial and temporal distribution of recharge.

In order to determine rational water budget of the basin that can be used for independent calibration of the model simulation result, the necessary data gaps over the entire basin have to be filled. Accordingly, the following hydro-meteorological stations have to established within the basin;

Depending on the criteria set for the establishment of gauging stations that can be required for a given catchment at least two stations have to be installed for the highland part of the basin,

River discharge measuring stations have to installed at three places: where the two main streams (Golina and Hormat) that drain the highland join the valley floor and at the out-let of the basin.

For further groundwater resource development plans in the valley, it is important to take into account the balance between the groundwater recharge and the intended abstraction rates both for irrigation and domestic water supply to ensure the sustainability of the resource in the valley. Moreover, it is also important to revise the boreholes' separation distance.

References

Allen, G.R., Pereira, L.S., Raes, D. and Smith, M., (1998) Crop evapotranspiration-guidelines for computing crop water requirements. FOA Irrigation and drainage paper 56. FAO, Rome, Italy, pp.300.

Anderson, M. P., and Woessner, W. W. (1992) Applied Groundwater Modeling. Acad. Press, San Diego, USA.

Bear, J., (1979) Analysis of flow against dispersion in porous media- Comments. Jour. Hydrology, 40(3-4): 381- 385.

Chiang, W.H., and Kinzelbach, W.,(2003) Processing MODFLOW Pro (Version 7.0.17), A simulation system for modeling groundwater flow and pollution.

Chiang, W.H., Kinzelbach, W. and Rauch, R.,(1998) Aquifer simulation model for Windows ASMWIN 6.0: Groundwater flow and transport modeling, an integrated program. Gebruder Borntraeger Berlin etc., 137 pp.

Co-SAERAR (1999). Feasibility study report for the Kobo-Girana Valley Development Study Project, Volume III: Annex C: Hydrogeology. The Commission for Sustainable Agriculture and Environmental Rehabilitation in Amhara Region.

Daniel Gemechu (1977) Aspects of climate and water budget in Ethiopia. Addis Ababa University Press, Addis Ababa.

Dereje Ayalew, D., Bourdon, E., Ebinger, C., Wolfenden, E., Yirgu, G., Grassineau, N., (2005). Temporal compositional variation of early sin-rift rhyolites along the western margin of the Southern Red Sea and Northern Main Ethiopian Rift. Addis Ababa University, Department of earth science and Royal Holloway University of London, Department of Geology, Egham, UK.

Dessie Nadew (2003). Aquifer characterization and hydrochemical investigation in Raya Valley, northern Ethiopia, Ph.D. Thesis, Institute of Applied Geology, Universität für Bodenkultur Wien.

Fetter, C.W., (1994) Applied hydrogeology. Prentice Hall Inc. New Jersey, USA. 604pp.

Freeze, R.A. & Cherry, J.A., (1997) Groundwater. Prentice-Hall, Englewood Cliffs, N.J., USA. 604pp.

Fujinaw, K. (1977) Finite element analysis of groundwater flow in multiaquifer systems, 2. A quasi three-dimensional flow model. *Jour. Hydrology*, 33, 349.

References

German Agency for Technical Co-operation (1977) Kobo-Alamata agricultural development program. Volume II: Annexes pedology and water development . German consults.

Jyrkama, M.I., and Sykes, J.F., (2007) The impact of climate change on spatially varying groundwater recharge in the grand river watershed (Ontario). Jour. Hydrology, 338(3-4): 237-250.

Kresic, N. (1997) *Hydrogeology and Groundwater Modeling*. CRC Press LLC, USA.

Kruseman, G.P. and de Ridder, N.A., (1992). Analysis and evaluation of pumping test data. International Institute for Land Reclamation and Improvement /ILRI, Netherlands, 377pp.

McDonald, M. G., and Harbaugh, A. W. (1988) A modular three-dimensional finite-difference groundwater flow model. Techniques of Water-Resources Investigations 06-A1, USGS, 576pp.

Mesfin Aytenfisu and Engida Zemedagegnehu (2003). Review and appraisal of the hydrogeological feasibility study report. Amhara National Regional State Kobo-Girana Valley Development Program.

Molla Demlie, Tenalem Ayenew and Wohnlich, S., (2007) Comprehensive hydrological and hydrogeological study of topographically closed lakes in highland Ethiopia. Jour. Hydrology 339, pp149.

RVDP, (1997). Hydrogeological study phase II feasibility draft report. Raya Valley Development study Project Tigray National Regional Government.

Seifu Kebede, Travi, Y., Asfawessen Asrat, Tamiru Alemayehu, Tenalem Ayenew, and Zenaw Tessema (2007) Groundwater origin and flow along selected transects in Ethiopian rift volcanic aquifers. *Hydrogeology Journal*.

Shaw, E. M. (1988). Hydrology in practice (2nd ed.). London: Van Nostrand Reinhold (International) Co. Ltd.

Shibasaki, N., (1999) Study on Methodology of Practical Parameter Estimation for Groundwater Modeling Based Hydrogeological Classification. *Jour. Geosciences*, Osaka City University, Vol. 42, Art. 2, 21-43.

Sileshi Mamo (2007). Raya hydrogeology and isotope hydrological investigation project, final report. Ministry of Mines and Energy Geological Survey of Ethiopia.

References

Simmers, I., (1988). Estimation of natural groundwater recharge. NATO ASI Series C: Mathematical and Physical Sciences; 222. D. Reidel, Dordrecht etc., 510pp.

Simmers, I., Hendrickx, J.M.H., Kruseman, G.P. and Rushton, K.R., (1997). Recharge of phreatic aquifers in semi-arid areas. International contributions to hydrogeology : IAH International Association of Hydrogeologists; 19. Balkema, Rotterdam etc., 277pp.

Tenalem Ayenew and Tamiru Alemayehu (2001). Principle of hydrogeology. Addis Ababa University, Addis Ababa, Ethiopia.

Tenalem Ayenew (2001). Numerical groundwater flow modeling of the central main Ethiopian rift Lakes basin, SINET: Ethiopian. Journal of Science 24 (2), 167 – 184.

Tenalem Ayenew (1998). The hydrogeological system of the Lake district basin, central main Ethiopia rift. Ph.D Thesis, Free University of Amsterdam.

Todd, D.K., (2005). Groundwater hydrology. Wiley, Hoboken, NJ, 636pp.

Tyson, H. N., and Weber, E. M. (1964) Groundwater management for nation's future-computer simulation of groundwater basins. *Jour. Hydraulics Div., Proc. Amer. Soc. Civil Engrs.*, 90, HY4, 57.

Wilson, J. L., and Guan, H. (2004) Mountain-block hydrology and mountain-front recharge. New Mexico Institute of Mining and Technology, Socorro, New Mexico.

Yeh, H.-F., Lee, C.-H, Chen, J.-F. and Chen, W.-P., (2007). Estimation of groundwater recharge using water balance model. Water Resources, 34(2): 153-162.

Zanettin, B., Nicoletti, M. & Petrucciani, C., (1978). The evolution of the Checha escarpment and the Ganjuli graben (lake Abaya) in the Southern Ethiopia Rift. Neues Jahrbuch fur Geologie und Palaontologie, 8: 473-490.

Zanettin, B., Justin – Visentin , E., Niccoletti, M. & Piccirllo, E.M., (1980). Correlation among Ethiopian volcanic formations with special references to the chronological and stratigraphic problems of the Trap series. Rome, Italy, Accademia Nazionale dei Lincei, 47: 231-252.

Appendices

Appendix 1. Meteorological data

Appendix 1.1 Monthly rainfall data

Monthly rainfall (mm) at Kobo station

Year	Jan	Feb	Mar	Apr	May	Jun	Jul	Aug	Sep	Oct	Nov	Dec	Annual
1996	79	0	31	75	133	53	147	205	67	18	64	0	872
1997	0	0	43	58	48	52	111	94	37	169	49	0	660
1998	54	32	24	39	12	4	326	312	51	6	0	0	860
1999	316	226	2	12	48	34	0	20	107	25	0	0	790
2000	1	0	2	76	42	5	227	268	49	88	24	83	865
2001	0	0	71	19	16	2	231	220	98	8	4	2	671
2002	5	0	0	0	13	3	100	296	117	16	0	67	616
2003	41	33	35	66	33	11	138	248	42	0	0	43	689
2004	30	0	28	88	3	26	116	162	9	74	36	10	583
2005	8	0	34	158	126	3	125	191	23	9	65	0	742
Mean	53	29	27	59	47	19	152	202	60	41	24	21	735

Monthly rainfall (mm) at Waja station

Year	Jan	Feb	Mar	Apr	May	Jun	Jul	Aug	Sep	Oct	Nov	Dec	Annual
1996	20	0	83	121	166	26	94	195	54	15	48	5	827
1997	10	0	90	20	27	4	60	55	7	230	79	0	581
1998	76	31	47	27	38	0	311	345	92	8	0	0	975
1999	41	0	71	36	4	40	92	324	47	0	1	43	699
2000	74	0	0	56	19	7	154	259	7	37	30	8	651
2001	0	0	60	20	26	23	150	197	37	10	0	0	523
2002	63	0	22	64	0	7	65	158	55	0	0	82	516
2003		61	42	93	0	8	113	329	51	0	1	43	740
2004	32	44	31	88	6	22	50	113	25	4	43	8	465
2005	0	8	17	134	88	7	148	169	21	1	0	0	593
Mean	35	14	46	66	37	14	124	214	40	30	20	19	657

Monthly rainfall (mm) at Alamata station

Year	Jan	Feb	Mar	Apr	May	Jun	Jul	Aug	Sep	Oct	Nov	Dec	Annual
1996	133	0	69	123	115	25	77	250	36	8	58	0	895
1997	46	0	125	27	29	22	87	54	72	192	139	0	792
1998	179	23	26	35	20	0	348	272	64	18	0	0	984
1999	44	0	21	9	7	1	211	432	67	55	0	0	847
2000	0	0	10	44	74	0	246	450	68	15	83	73	1063
2001	0	0	158	13	30	17	225	244	25	10	10	3	733
2002	98	0	18	112	8	4	73	214	46	14	0	90	675
2003	76	70	42	94	25	13	112	234	23	0	0	67	754
2004	33	16	40	168	14	50	117	243	41	8	21	20	770
2005	21	1	110	132	66	24	142	167	33	6	0	0	702
Mean	63	11	62	76	39	15	164	256	47	32	31	25	821

Monthly rainfall (mm) at Korem station

Year	Jan	Feb	Mar	Apr	May	Jun	Jul	Aug	Sep	Oct	Nov	Dec	Annual
1996	36	1	98	242	165	68	137	281	63	11	73	0	1175
1997	10	2	98	51	93	64	172	56	59	323	164	1	1091
1998	160	39	27	28	80	12	397	356	212	46	0	0	1356
1999	66	0	3	50	13	32	235	350	112	45	2	0	908
2000	0	0	4	48	76	9	318	321	91	133	66	94	1159
2001	2	3	130	22	36	51	283	380	62	13	2	13	998
2002	65	1	34	107	16	3	137	229	90	8	0	93	782
2003	13	24	74	75	24	20	168	381	78	2	4	30	892
2004	14	6	41	55	2	54	144	249	66	35	22	10	697
2005	8	0	106	223	163	28	253	298	41	37	0	0	1157
Mean	37	8	61	90	67	34	224	290	87	65	33	24	1022

Monthly rainfall (mm) at Maichew station

Year	Jan	Feb	Mar	Apr	May	Jun	Jul	Aug	Sep	Oct	Nov	Dec	Annual
1996	9	1	123	146	141	66	117	246	42	4	57	0	952
1997	16	0	52	59	38	83	166	64	64	206	80	0	828
1998	65	33	35	39	116			214	223	11	0	0	737
1999	45	0	11	22	16	12	176	253	78	109	0	2	725
2000	0	0	6	18	65	12	195	194	126	151	61	75	903
2001	0	2	93	9	35	26	212	283	84	25	0	11	780
2002	84	0	34	68	41	21	67	188	93	19	0	34	649
2003	24	38	93	194	13	14	107	325	32	5	2	18	864
2004	13	5	20	128	1	60	141	247	27	38	3	0	683
2005	6	3	51	61	98	18	120	219	23	22	20	20	660
Mean	26	8	52	74	56	35	145	223	79	59	22	16	778

Appendix 1.2 Monthly maximum temperature

Monthly T_{max} (^{o}C) at Kobo station

Year	Jan	Feb	Mar	Apr	May	Jun	Jul	Aug	Sep	Oct	Nov	Dec	Annual
1996				30.4	30.1	32.1	31.7	30.2	30.4	29.7	27.1	26.1	29.8
1997	25.4	28.0	29.3	30.3	33.1	33.4	31.9	31.7	32.4	27.9	27.1	27.2	29.8
1998	25.4	26.7	29.1	32.4	33.5	36.0	30.9	28.7	29.8	29.3	28.3	27.6	29.8
1999	26.9	30.4	29.0	32.1	34.2	35.3	30.5	29.7					31.0
2000		29.2	30.4	31.2	33.0	34.7	32.1	30.3	30.5	28.6	27.4	26.1	30.3
2001	25.5	28.1	28.7										27.4
2002					34.3	35.0	34.0	30.9	29.9	30.1	29.5	26.3	31.3
2003	25.9	29.0	30.2	30.9	34.0	34.6	32.1	30.0	30.8	30.3	29.2	26.8	30.3
2004	27.6	28.0	30.2	30.8	34.6	34.2	32.7	31.5	31.9	30.0	29.7	27.1	30.7
2005	26.9	30.2	31.3	31.6	31.7	35.0	32.7	32.2	30.7	30.8	29.4	28.3	30.9
Mean	26.2	28.7	29.8	31.2	33.2	34.5	32.1	30.6	30.8	29.6	28.5	26.9	30.1

Monthly T_{max} (°C) at Waja station

Year	Jan	Feb	Mar	Apr	May	Jun	Jul	Aug	Sep	Oct	Nov	Dec	Annual
1996	27.4	30.9	30.3	30.6	30.6	33.0	32.0	31.4	32.0	31.4	29.0	28.1	30.6
1997	27.6	29.5	29.7	30.6	33.7	33.9	33.1	33.6	34.6	30.3	28.6	29.0	31.2
1998	27.9	29.2	29.8	31.4	33.6	37.4	31.5	29.4	30.3	30.2	29.3	29.1	30.8
1999	27.6	30.5	29.2	32.7	34.3								
2000		27.0	27.7	26.8	28.5	29.6	26.5	24.7	24.7	23.3	23.4		26.2
2001	20.9	23.0	23.4	24.6	27.1						29.0	29.4	
2002	29.8	29.8	31.7	34.0	35.2		35.3	30.6	33.1	31.3	29.7	28.7	31.7
2003		29.9	30.5	31.8	33.9	36.4	34.0	30.8	31.6	31.5	30.0	27.9	31.7
2004	29.2	28.9	30.0	30.1	34.2	34.1	33.3	31.7	31.6	29.9	29.7	26.8	30.8
2005	28.0	31.1	31.1	32.0	31.6	35.9	32.3	31.1	32.2	30.4	29.4	27.9	31.1
Mean	27.3	29.0	29.3	30.5	32.3	34.3	32.2	30.4	31.3	29.8	28.7	28.4	30.0

Monthly T_{max} (°C) at Alamata station

Year	Jan	Feb	Mar	Apr	May	Jun	Jul	Aug	Sep	Oct	Nov	Dec	Annual
1996		29.5	30.9	30.8	30.8	32.6	32.4	31.2	31.6	31.2	29.0	28.4	30.8
1997	27.4	29.9	28.9	30.3	34.4	34.5	33.1	33.9	33.3	29.8	28.6	28.7	31.4
1998	27.0	27.7	30.5	34.5	34.5	36.1	31.8	28.8	30.7	30.8	30.4	29.8	31.4
1999	28.8	32.4	31.0	34.1	35.8		30.9	30.1	30.1	30.1	30.0	29.2	31.4
2000	29.7	31.6	32.8	34.2	35.2	36.8	33.2	30.5	30.5	29.3	29.0	26.8	31.8
2001	27.5	30.4	30.5	31.7	34.1	33.8	31.2	28.9	29.6	30.0	27.9	27.5	30.5
2002	24.7	28.0	29.8	30.4	33.7	34.3	33.6	30.6	29.4	30.7	28.8	26.3	30.5
2003	25.8	28.5	29.0	30.1	33.2	34.2	31.4	29.4	30.1	29.9	28.4	26.0	30.0
2004	27.1	27.1	29.5	28.6	33.4	32.8	31.9	29.6	29.5	29.1	28.4	26.3	29.7
2005	25.9	29.4	29.6	29.8	30.3	33.4	31.0	29.9	30.0	29.3	28.4	27.2	29.9
Mean	27.1	29.4	30.3	31.5	33.5	34.3	32.1	30.3	30.5	30.0	28.9	27.6	30.7

Monthly T_{max} (°C) at Korem station

Year	Jan	Feb	Mar	Apr	May	Jun	Jul	Aug	Sep	Oct	Nov	Dec	Annual
1996	19.0	22.1	22.4	22.3	22.4	23.7	22.8	23.5	24.5	23.9	21.2	19.9	22.3
1997	19.8	21.6	22.3	22.4	24.9	24.7	23.3	24.1	24.9	21.4	21.0	21.1	22.6
1998	19.7	20.8	22.1	24.0	24.4	26.1	22.5	21.9	23.3	21.5	20.1	19.9	22.2
1999	19.3	22.3	21.7	24.2	25.9	27.3	22.0	22.7	24.3	25.1	24.6	21.5	23.4
2000	21.6	22.4	23.0	23.5	25.3	27.2	22.9	21.6	22.2	22.1	20.0	18.7	22.5
2001	18.0	20.3	20.3	22.5	24.4	24.5	22.7	21.6	22.1	21.3	19.6	19.9	21.4
2002	17.9	20.5	21.6	22.5	25.6	26.2	25.2	22.4	21.8	22.1	21.7	20.1	22.3
2003	20.3	22.4	22.4	22.6	24.6	25.5	22.4	21.7	22.3	21.4	20.9	19.4	22.2
2004	21.1	20.8	22.2	22.8	26.1	25.1	23.5	22.6	23.0	21.4	20.9	19.5	22.4
2005	19.9	22.9	22.7	22.8	23.0	25.3	22.8	23.2	23.2	22.1	21.1	20.3	22.4
Mean	19.7	21.6	22.1	23.0	24.7	25.6	23.0	22.5	23.2	22.2	21.1	20.0	22.4

Monthly T_{max} (°C) at Maichew station

Year	Jan	Feb	Mar	Apr	May	Jun	Jul	Aug	Sep	Oct	Nov	Dec	Annual
1996	19.0	21.4	21.8	22.1	22.2	23.1	22.4	22.4	23.2	21.7	19.5	18.4	21.4
1997	19.1	21.1	22.2	23.4	24.4	24.9	22.5	22.4	24.2	20.3	19.1		22.1
1998	19.9	19.6	22.1	24.4	21.4	22.4	21.2	20.7	20.2				21.3
1999	19.2	22.8	22.0	24.3	25.8	26.9	20.8	21.4	22.0	20.1	20.8	19.2	22.1
2000	20.5	21.8	23.0	22.9	25.1	26.4	22.8	21.9	22.1	20.3	19.4	18.5	22.1
2001	18.5	21.1	20.7	22.9									
2002	24.1	23.6	25.8	25.4	25.2	23.0	21.8	21.8	21.1	19.3			23.1
2003	20.3	22.4	22.3	23.0	24.8	25.5	23.1	22.3	23.0	21.5	20.8	19.2	22.4
2004	21.2	21.1	22.4	22.1	25.8	24.9			23.0	21.3	21.1	20.0	22.3
2005	19.9	23.1	22.8	23.3	23.4	25.9	22.7	23.2	23.5	21.6	20.6	20.3	22.5
Mean	20.2	21.8	22.5	23.4	24.2	24.8	22.2	22.0	22.5	20.8	20.2	19.3	22.0

Appendix 1.3 Monthly minimum temperature

Monthly T_{min} at Kobo station

Year	Jan	Feb	Mar	Apr	May	Jun	Jul	Aug	Sep	Oct	Nov	Dec	Annual
1996				17.2	16.5	17.4	18.2	17.5	15.7	12.0	11.7	10.2	15.1
1997	13.2	12.3	15.9	16.2	17.7	18.7	18.5	17.8	16.3	15.5	15.6	11.9	15.8
1998	15.4	15.3	17.2	18.1	17.9	20.7	17.9	17.3	16.1	14.5	10.1	8.4	15.7
1999	11.6	11.1	15.5	16.0	17.5	18.2	17.3	16.2					15.4
2000		10.6	14.1	16.5	16.1	15.9	14.9	11.8	7.1	9.4	7.7	7.2	11.9
2001	7.1	7.4	11.6										8.7
2002					16.9	19.6	19.6	17.6	16.9	13.0	12.1	15.2	16.4
2003	13.5	15.0	16.4	17.0	17.6	19.3	19.9	17.3	16.9	12.6	12.5	11.2	15.8
2004	14.7	13.5	14.4	16.8	16.5	18.3	18.1	17.5	15.5	13.2	12.7	13.9	15.4
2005	13.9	14.1	17.1	17.2	18.1	18.7	18.7	17.8	17.2	13.5	12.5	9.6	15.7
Mean	12.8	12.4	15.3	16.9	17.2	18.5	18.1	16.8	15.2	13.0	11.9	10.9	14.60

Monthly T_{min} at Waja station

Year	Jan	Feb	Mar	Apr	May	Jun	Jul	Aug	Sep	Oct	Nov	Dec	Annual
1996	14.4	12.4	16.2	16.2	15.7	16.6	17.8	17.2	15.2	11.2	10.9	9.0	14.4
1997	12.8	11.6	15.4	15.6	15.7	17.0	17.0	17.5	16.0	16.1	15.6	12.1	15.2
1998	15.2	14.2	16.7	15.3	15.1	17.7	18.4	17.0	15.7	13.8	9.5	6.3	14.6
1999	10.7	9.1	14.4	14.4	16.1								12.9
2000		8.5	11.8	15.5	15.5	16.9	17.5	16.2	15.1	13.1	13.6		14.3
2001	10.4	11.0	11.7	12.2	12.3						9.0	8.4	10.7
2002	11.7	10.4	12.9	17.3	16.6		16.2	15.4	12.1	10.2	9.1	8.1	12.7
2003		10.1	9.9	9.7		16.3	19.3	17.3	15.8	11.3	11.2	10.5	13.1
2004	14.0	12.6	13.2	16.6	13.8	17.1	18.5	20.7	20.6	18.0	15.6	11.6	16.0
2005	13.4	12.4	16.3	14.8	17.0	17.2	17.7	17.0	14.9	10.9	15.5	6.0	14.4
Mean	12.8	11.2	13.8	14.8	15.3	17.0	17.8	17.3	15.7	13.1	12.2	9.0	13.8

Monthly T_{min} at Alamata station

Year	Jan	Feb	Mar	Apr	May	Jun	Jul	Aug	Sep	Oct	Nov	Dec	Annual
1996		12.9	16.0	16.4	16.1	16.1	16.7	16.3	15.5	13.9	12.7	11.5	14.9
1997	12.9	12.9	15.8	16.2	17.6	18.6	17.6	17.5	17.0	15.9	16.2	12.8	15.9
1998	14.9	15.0	16.6	17.9	18.1	19.9							17.1
1999	12.4	11.9	13.3	17.3	20.2		18.8	16.7	10.2	5.7	3.9	1.90	12.0
2000	2.3	5.3	6.6	7.9	10.1	11.4	11.6	9.2	8.7	7.9	6.5	6.3	7.8
2001	3.9	6.1	8.3	10.1	12.2	13.9	11.8	10.7	10.4	10.8	7.8	6.9	9.4
2002	9.5	14.4	17.0	17.7	18.6	20.0	19.7	16.7	16.7	15.9	15.4	16.0	16.5
2003	14.3	15.7	17.4	18.0	20.3	20.0	19.4	17.0	17.4	15.9	15.0	12.9	16.9
2004	14.6	8.8	10.1	16.1	18.0	19.5	18.7	17.8	17.1	15.4	15.2	15.1	15.5
2005	14.4	15.3	17.2	17.7	17.9	19.1	18.9	16.3	16.6	15.6	12.0	12.1	16.1
Mean	11.0	11.8	13.8	15.5	16.9	17.6	17.0	15.4	14.4	13.0	11.6	10.6	14.2

Monthly T_{min} at Korem station

Year	Jan	Feb	Mar	Apr	May	Jun	Jul	Aug	Sep	Oct	Nov	Dec	Annual
1996	7.9	5.7	9.9	10.2	7.6	8.5	11.8	12.0	9.2	4.1	4.5	3.2	7.9
1997	5.7	5.7	9.2	8.7	8.7	11.3	12.4	11.4	7.1	8.7	10.0	4.2	8.6
1998	8.5	7.5	9.6	9.3	10.2	9.8	11.9	11.8	10.2	7.0	1.1	-0.6	8.0
1999	3.4	1.7	6.5	7.4	8.6	9.7	11.6	10.6	8.4	6.9	0.4	2.3	6.5
2000	2.5	1.8	5.6	9.5	8.9	10.8	12.3	11.5	8.5	6.8	5.3	4.4	7.3
2001	3.3	3.3	8.5	7.2	9.2	11.8	12.3	11.9	8.2	6.8	2.5	2.0	7.3
2002	6.3	4.5	8.3	8.6	7.1	11.0	11.7	11.1	8.3	4.5	3.0	7.2	7.6
2003	4.3	2.2	3.8	10.1	9.8	11.2	13.1	12.1	9.9	4.1	4.5	2.8	7.3
2004	6.7	5.8	7.4	10.6	7.8	11.3	12.5	12.1	8.0	6.0	5.0	6.2	8.3
2005	6.7	5.8	7.4	10.6	7.8	11.3	12.5	12.1	8.0	6.0	5.0	6.2	8.3
Maen	5.5	4.4	7.6	9.2	8.6	10.7	12.2	11.7	8.6	6.1	4.1	3.8	7.7

Monthly T_{min} at Maichew station

Year	Jan	Feb	Mar	Apr	May	Jun	Jul	Aug	Sep	Oct	Nov	Dec	Annual
1996	8.5	8.4	11	11	11	13	12	13	10	7.7	7.4	6.3	9.94
1997	8	6.9	11	11	12	13	13	12	11	10	10	7	10.41
1998	9.7	9.2	11	12	13	7.3	5.2						9.63
1999	6.5	6.9	9.1	9.9	12	13	10	11	10	9.3	5.3	5.9	9.08
2000	6.1	6.3	8.1	11	12	14	14	12	10	8.6	7.7	6.8	9.72
2001	5.7	6.1	10	9.9	12	13	13	14	12	9.1	5.8	6	9.72
2002	8.1	7.7	10	11	11	14	15	13	9.5	8.1	7.3	9	10.31
2003	7.8	9.2	10.4	11.5	11.7	13.4	13.4	12.7	11.6	7.6	7.1	6.3	10.2
2004	8.9	7.8	9.0	11.7	11.9	13.6	13.6	13.1	10.2	8.1	7.4	7.9	10.3
2005	7.9	8.6	10.7	11.6	12.4	13.8	13.7	13.1	11.6	7.8	4.7	4.7	10.1
Mean	7.7	7.7	10.0	11.1	11.9	12.8	12.3	12.7	10.7	8.5	7.0	6.7	9.9

Appendix 1.4 Monthly relative humidity (RH) (%)

Monthly relative humidity (%) at Kobo station at 1800

Year	Jan	Feb	Mar	Apr	May	Jun	Jul	Aug	Sep	Oct	Nov	Dec	Annual
1996				46.9	56.3	49.1	53.3	56.8	52.3	43.0	48.4	45.8	50.2
1997	64.5	34.4	43.3										47.4
1998				35.4	30.7	27.0	52.4	63.8	58.9	47.2	33.3	42.9	43.5
1999	56.2	56.9											56.5
2000													
2001													
2002						20.8	32.9	50.0	55.1	38.4	32.8	58.7	41.2
2003													
2004	56.0	42.3	32.9	48.9	21.9	24.2	44.0	55.1	45.5	42.7	36.7	50.6	41.7
2005	53.6	36.6	45.6	38.8	47.4	28.7	46.6	42.3	51.1	37.8	39.2	33.0	41.7
Mean	57.6	42.5	40.6	42.5	39.1	30.0	45.8	53.6	52.6	41.8	38.1	46.2	46.0

Monthly relative humidity (%) at Kobo station at 1200

Year	Jan	Feb	Mar	Apr	May	Jun	Jul	Aug	Sep	Oct	Nov	Dec	Annual
1996		44.0		47.2	56.5	48.6	44.7	50.4	43.8	35.8	35.0	47.0	45.3
1997	58.1	44.0	37.6										46.6
1998		44.0		39.5	33.6	24.3	51.5	60.3	49.7	39.5	35.0	47.0	42.4
1999	56.6	44.0									35.0	47.0	45.6
2000													
2001													
2002		44.0				21.1	29.5	42.6	51.1	30.8	35.0	47.0	36.7
2003													
2004	49.8	44.0	32.6	42.9	22.2	26.4	32.8	44.2	40.8	36.4	35.0	47.0	37.8
2005	51.1	37.3	43.0	39.4	44.3	25.8	41.2	43.6	42.1	36.6	39.0	32.5	39.7
Mean	53.9	43.0	37.7	42.3	39.1	29.2	39.9	48.2	45.5	35.8	35.7	44.6	42.0

Monthly relative humidity (%) at Kobo station at 0600

Year	Jan	Feb	Mar	Apr	May	Jun	Jul	Aug	Sep	Oct	Nov	Dec	Annual
1996	87.0			75.0	86.1	53.0	72.2	84.8	89.1	82.5	79.2	81.2	79.0
1997	88.0	74.1	83.4	75.0		53.0							74.7
1998	87.0			75.0	60.0	53.0	77.0	90.0	93.1	83.3	72.4	76.7	76.7
1999	87.0	83.1		75.0		53.0							74.5
2000													
2001													
2002	87.0			75.0		53.0	66.2	82.4	89.5	78.3	72.0	87.1	75.4
2003													
2004	87.0	82.6	66.8	75.0	50.7	53.0	66.1	79.4	81.8	80.5	75.9	84.0	73.6
2005	84.8	70.3	78.4	72.7	84.7	59.0	71.6	80.8	83.7	77.1	75.2	74.1	76.0
Mean	86.8	77.5	76.2	74.7	70.4	53.9	70.6	83.5	87.5	80.3	75.0	80.6	75.7

Monthly relative humidity (%) at Maichew station

Year	Jan	Feb	Mar	Apr	May	Jun	Jul	Aug	Sep	Oct	Nov	Dec	Annual
1995	53.7	67.3	66.7	73.0	72.3	37.3	65.3	71.3	62.7	55.0	54.7	69.0	62.4
1996	74.7	57.0	70.3	66.0	65.0	51.0	61.0	63.7	55.3	54.3	59.7	58.3	61.4
1997	68.3	52.3	66.3	60.3	51.3	51.0	63.0	58.3	53.7	68.3	76.7	66.0	61.3
1998	80.0	72.3	68.0	54.0	62.0	39.0	71.0	65.7	63.3	52.3	44.0		61.1
1999	59.3	37.3	56.0	44.0	38.0	31.7	66.0	67.3	66.3	72.0	55.3	61.0	54.5
2000	51.3	39.3	43.7	45.3	43.0	35.7	64.3	70.7	64.0	74.0	70.0	68.7	55.8
2001	67.7	53.3	67.7	55.0	52.3	50.0	67.3	72.7	67.0	64.3	59.7	56.7	61.1
2002	76.0	56.3	63.0	56.0	41.0	39.3	50.7	62.3	63.7	57.3	55.0	76.0	58.1
2003	67.0	72.0	58.0	47.0	40.0	38.0	61.0	68.0	64.0	60.0	56.0	70.0	58.4
2004	65.0	56.0	50.0	69.0	34.0	42.0	56.0	66.0	58.0	60.0	60.0	66.0	56.8
Mean	66.3	56.3	61.0	57.0	49.9	41.5	62.6	66.6	61.8	61.8	59.1	65.7	59.1

Appendix 1.5 Mean monthly sunshine hours

Mean monthly sunshine hours at Kobo station

Year	Jan	Feb	Mar	Apr	May	Jun	Jul	Aug	Sep	Oct	Nov	Dec	Annual
1996	6.8	5.3	7.9	9.6	9.9	8.5	4.0	5.1	6.8	9.6	9.9	8.8	7.7
1997	8.0	7.3	9.3	6.9	9.4	6.2	3.1	5.1	7.3	9.5	9.7	8.1	7.5
1998	6.3	7.5	8.9	9.5	9.2	6.8	6.7	7.4	6.0	7.1	9.0	7.0	7.6
1999	6.9	4.4	8.7	6.6	9.1	6.3	6.1	6.5	7.0	9.6	10.1	9.3	7.6
2000	9.3	7.2	6.1	7.6	9.1	5.1	5.2	5.1	5.1	8.2	9.3	8.7	7.2
2001	8.0	7.4	8.9	7.9	9.8	8.3	3.4	6.6	7.1	7.9	8.1	7.9	7.6
2002	7.8	8.6	8.7	9.7	6.5	5.7	4.0	5.8	7.7	8.9	9.1	8.5	7.6
2003	8.7	10.2	8.1	9.0	6.8	6.4	8.3	7.1	6.7	7.3	8.6	9.0	8.0
2004	8.1	8.7	9.0	6.8	7.2	6.1	7.3	5.6	6.2	8.1	9.9	9.4	7.7
Mean	7.8	7.4	8.4	8.2	8.6	6.6	5.3	6.0	6.7	8.5	9.3	8.5	7.6

Mean monthly sunshine hours at Maichew station

Year	Jan	Feb	Mar	Apr	May	Jun	Jul	Aug	Sep	Oct	Nov	Dec	Annual
1996	7.4	7.5	6.4	7.7	7.8	7.6	5.8	5.7	7.2	6.6	7.1	7.4	7.0
1997	7.9	8.8	5.5	7.2	8.2	6.2	5.5	6.2	6.7	6.2	6.6	8.4	7.0
1998	5.2	6.3	7.4	8.7	8.7	6.9	4.2	4.3	7.3	8.5	9.0	9.3	7.2
1999	7.4	9.8	7.2	10.2	9.7	7.3	3.9	4.9	7.0	6.0	8.9	7.7	7.5
2000	9.0	9.8	9.7	7.3	9.2	6.3	5.2	5.5	5.9	7.1	7.8	6.3	7.4
2001	4.4	7.9	4.4	6.2	7.2	12.1	4.6	5.0	7.0	7.9	6.9	8.3	6.8
2002	8.2	8.2	7.6	9.4	9.3	6.3	6.1	6.3	6.7	7.8	7.7	6.7	7.5
2003	6.4	8.0	6.3	9.9	9.0	6.0	4.7	4.4	7.3	9.4	8.0	7.9	7.3
2004	6.9	8.0	8.6	7.6	10.5	5.9	5.2	5.4	6.3	8.0	8.3	7.4	7.3
Mean	7.0	8.3	7.0	8.2	8.8	7.2	5.0	5.3	6.8	7.5	7.8	7.7	7.2

Appendix 1.6. Mean monthly wind speed (m/s) at 2m height

Mean monthly wind speed (m/s) at Kobo station

Year	Jan	Feb	Mar	Apr	May	Jun	Jul	Aug	Sep	Oct	Nov	Dec	Annual
1996	2.6	2.0	2.1	2.0	1.6	1.8	2.1	1.7	1.2	1.3	1.5	1.6	1.8
1997	1.8	2.0	2.1	2.0	2.2	1.9	2.0	1.7	1.6	1.4	1.3	1.4	1.8
1998	1.6	1.7	2.0	2.2	2.0	2.5	2.2	1.6	1.1	1.3	1.4	1.5	1.8
1999	1.6	1.8	2.2	2.1	2.1	2.3	2.0	1.5	0.0	0.0	0.0	0.0	1.3
2000	1.6	1.8	2.2	1.8	1.7	2.2	2.2	2.0	1.5	0.0	0.0	0.0	1.4
2001	1.5	1.7	1.7	1.4	1.2	1.4	0.5	0.8	0.2	1.6	1.7	1.8	1.3
2002	1.8	1.8	1.9	1.8	1.4	2.3	2.1	1.8	0.9	1.0	1.3	1.5	1.6
2003	1.6	1.7	2.0	1.9	1.5	2.0	2.0	1.4	1.0	1.1	1.3	1.3	1.6
2004	1.7	1.9	2.0	2.0	1.8	2.1	2.2	1.5	1.5	1.2	1.3	1.6	1.7
2005	2.0	2.1	2.2	2.0	1.6	1.9	2.0	1.8	1.2	1.2	1.3	1.5	1.7
Mean	1.8	1.9	2.0	1.9	1.7	2.0	1.9	1.6	1.0	1.0	1.1	1.2	1.6

Mean monthly wind speed (m/s) at Maichew station

Year	Jan	Feb	Mar	Apr	May	Jun	Jul	Aug	Sep	Oct	Nov	Dec	Annual
1996	1.1	1.3	1.3	1.3	1.3	2.9	3.8	2.7	1.2	1.2	1.2	1.2	1.7
1997	1.1	1.3	1.3	1.3	1.5	1.9	3.1	2.0	1.3	1.2	1.0	1.0	1.5
1998	0.9	1.0	1.2	1.4	1.4	1.9	3.6	2.6	1.2	1.2	1.3	1.3	1.6
1999	1.2	1.4	1.4	1.5	1.6	2.0	3.3	2.2	1.1	0.9	1.1	1.1	1.6
2000	1.2	1.3	1.3	1.4	1.4	2.2	3.4	2.8	1.1	0.9	0.9	1.0	1.6
2001	1.2	1.3	1.3	1.0	1.2	2.4	3.2	2.5	1.1	1.2	1.1	1.1	1.6
2002	0.9	1.2	1.2	1.3	1.3	2.4	2.5	2.5	1.1	1.2	1.2	1.1	1.5
2003	1.1	1.3	1.3	1.3	1.3	1.8	3.4	2.7	1.4	1.2	1.2	1.1	1.6
2004	1.2	1.3	1.3	1.2	1.6	1.9	3.2	2.3	1.2	1.2	1.2	1.2	1.6
2005	1.1	1.2	1.3	1.4	1.3	3.0	3.0	2.7	1.2	1.2	0.9	1.0	1.6
Mean	1.1	1.3	1.3	1.3	1.4	2.2	3.3	2.5	1.2	1.1	1.1	1.1	1.6

Appendix 1.7 Meteorological stations used for the Interpolation

Longitude [°]	Latitude [°]	Altitude [m]	Distance [km]	Direction	Direction	Station Name
39.6	11.81	1960	24	163	S	WALDIA
39.68	12.51	2200	57.2	16	N	ALAMATA
39.58	11.28	2040	82	176	S	HAIK
39.53	12.76	2380	82.7	0	N	MAICHEW
39.66	11.16	2540	96.2	172	S	DESE
39.56	12.91	2580	99.5	2	N	ADISHOHO
39.71	11.08	1916	105.8	170	S	COMBOLCHA
39.53	13	2500	109.4	0	N	BETEMERA
38.03	11.88	2410	164.2	265	W	DEBRE-TABOR

Appendix 1.8 Mean monthly temperature obtained from the interpolation

Longitude	[°]	39.533
Latitude	[°]	12.016
Altitude	[m]	2790
Method	Nearest Neighbour	

	Best Estimate	Low Estimate	High Estimate	Standard Error	Bias	Vertical Gradient	Long. Gradient	Lat. Gradient	Dir.	
T_Mean	[°C]	[°C]	[°C]	[°C]	[°C]	[°C/100m]	[°C/100km]	[°C/100km]	Degrees	
Jan	13.65	11.92	15.39	1.74	-0.34	-0.43	-1.81	0.37	281.49	W
Feb	13.66	11.74	15.59	1.92	-0.32	-0.51	-1.17	0.06	272.77	W
Mar	14.57	12.12	17.01	2.45	-0.26	-0.4	-1.33	1.02	307.34	NW
Apr	15.61	13.69	17.53	1.92	-0.22	-0.45	-0.64	0.8	321.48	NW
May	16.4	14.19	18.61	2.21	-0.28	-0.47	-0.09	1.35	356.07	N
Jun	16.62	14.35	18.89	2.27	-0.29	-0.51	1.31	1.53	40.63	NE
Jul	15.7	13.86	17.54	1.84	-0.57	-0.73	2	0.81	68.06	E
Aug	15.51	14.18	16.83	1.32	-0.44	-0.67	1.51	0.8	62.21	NE
Sept	15.14	13.29	16.99	1.85	-0.49	-0.68	0.94	1.01	43.08	NE
Oct	13.39	11.07	15.71	2.32	-0.48	-0.66	0.35	0.79	23.84	NE
Nov	13.07	10.98	15.16	2.09	-0.43	-0.54	-0.47	1.13	337.59	N
Dec	12.92	11.26	14.59	1.66	-0.39	-0.57	-0.44	0.86	332.95	NW
Mean	14.12	12.72	16.65	1.97	-0.38	-0.55	0.01	0.88	0.94	N

Appendix 1.9 Mean monthly precipitation obtained from the interpolation

Longitude	[°]	39.428
Latitude	[°]	12.02
Altitude	[m]	2945

Method Nearest Neighbour

Prec.	Best Estimate [°C]	Low Estimate [°C]	High Estimate [°C]	Standard Error [°C]	Bias [°C]	Vertical Gradient [°C/100 m]	Longitudinal Gradient [°C/100km]	Latitudinal Gradient [°C/100km]	Direction Degrees	
Jan	0	0	23.58	23.58	0.34	-5	7.4	-5.14	124.79	SE
Febr	4.18	0	21.02	16.84	-0.75	-3.56	10.37	-3.29	107.6	E
Mar	24.3	0	72.31	48.01	-12.8	-5	26.11	-2.42	95.29	E
Apr	53.05	29.19	76.91	23.86	-1.6	-5	17.8	-10.15	119.7	SE
May	48.87	19.88	77.86	28.99	-0.23	-5	-26.81	-16.68	238.11	SW
Jun	76.93	61.69	92.18	15.25	-1.4	3.82	-84.83	-19.59	257	W
Jul	275.52	257.46	293.58	18.06	3.15	3.89	-156.76	-51.71	251.74	W
Aug	299.2	282.99	315.41	16.21	1.71	2.85	-134.98	-43.2	252.25	W
Sep	61.45	24.65	98.26	36.81	7.29	-2.5	-60.96	-44.38	233.95	SW
Oct	23.14	0.95	45.34	22.19	0.93	-2.54	-21.62	-12.31	240.34	SW
Nov	17.59	0	35.43	17.84	-0.56	-3.04	-2.87	0.13	272.51	W
Dec	0	0	17.42	17.42	-0.21	-2.87	0.17	-3.49	177.17	S
Mean	72.27	48.52	96.03	23.75	-0.34	-2	-35.58	-17.69	243.57	SW

Appendix 2 Pumping test analysis curves

Appendix 2.1 Neuman unconfined curves

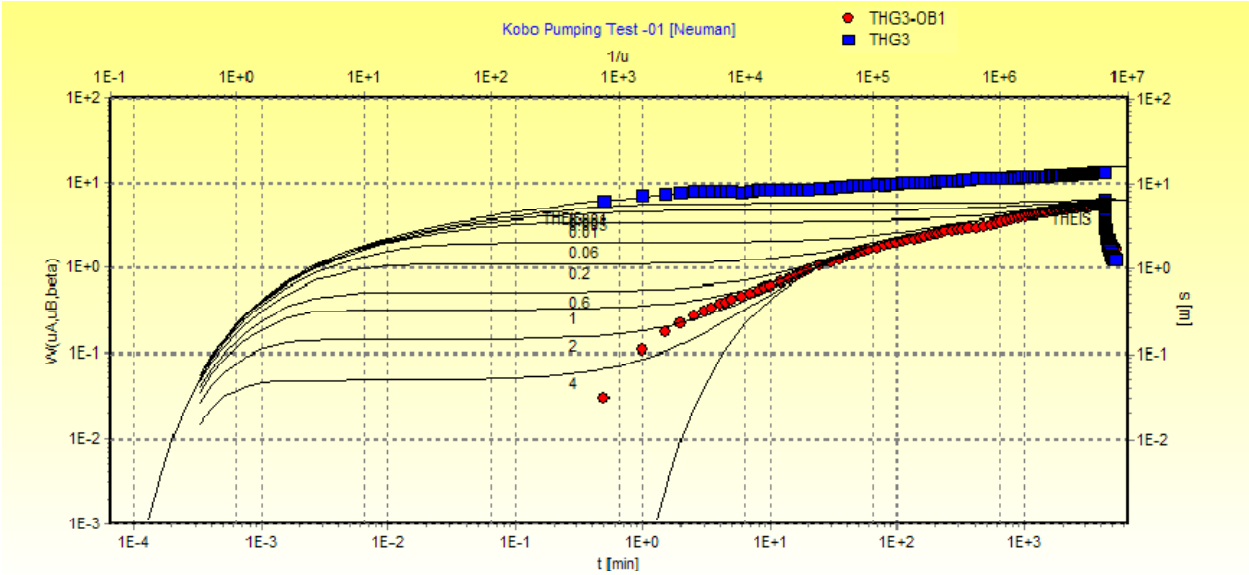

Transmissivity: 3.83E+2 m²/d
Conductivity: 6.38E+0 m/d

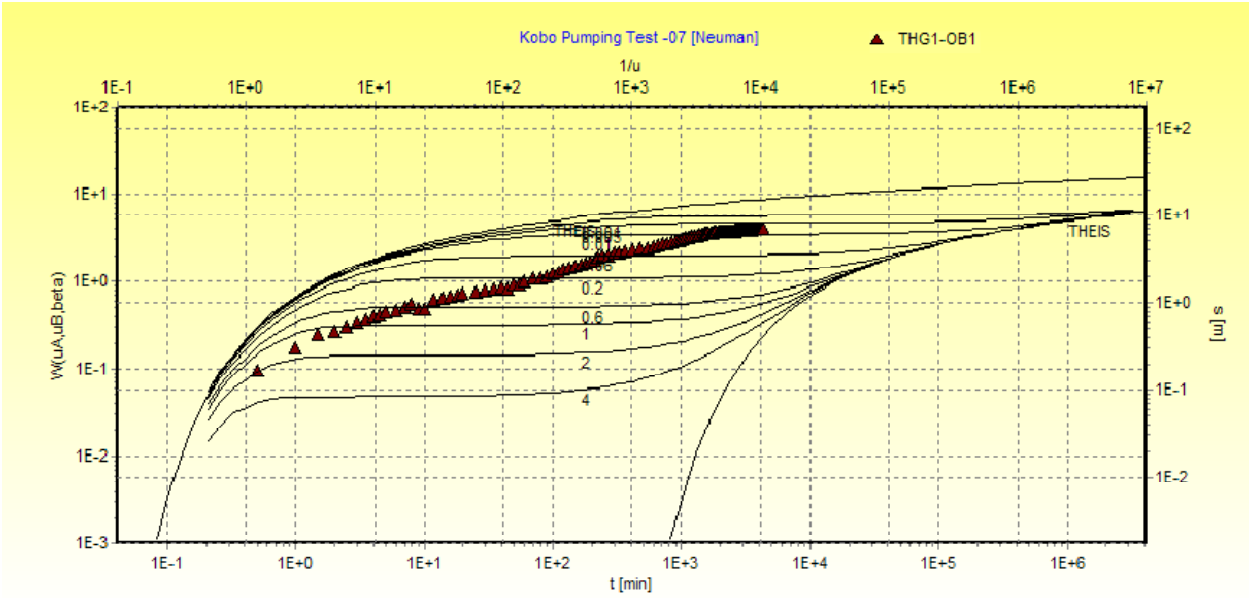

Transmissivity: 1.14E+2 m²/d
Conductivity: 3.81E+0 m/d
Storativity: 6.16E-14
Specific Yield: 6.16E-10

Appendix 2.2 Theis constant graphs

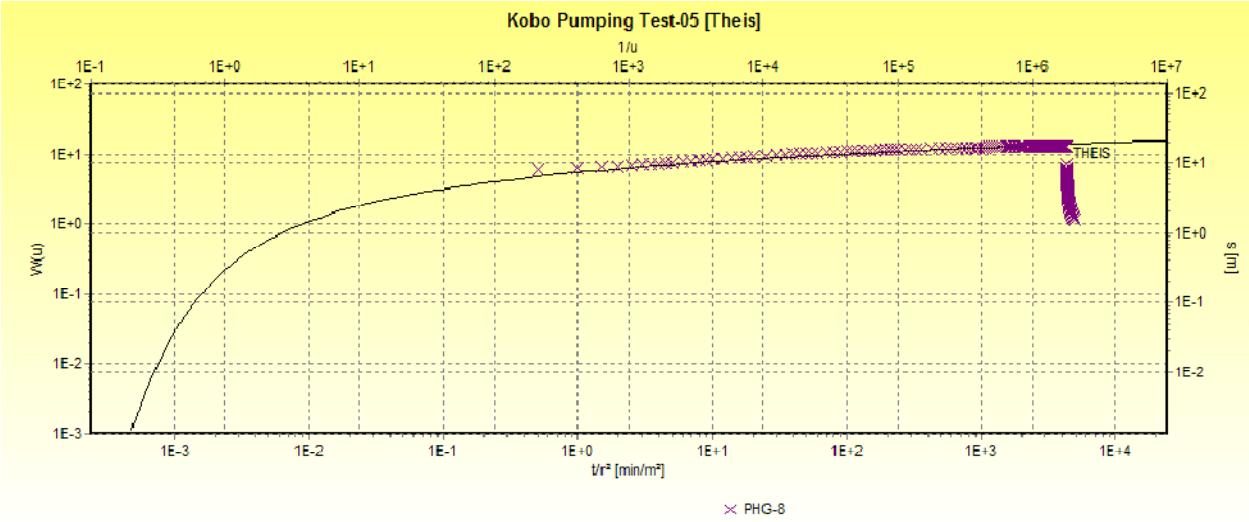

Transmissivity: 2.38E+2 m²/d Storativity: 1.58E-3
Conductivity: 4.96E+0 m/d

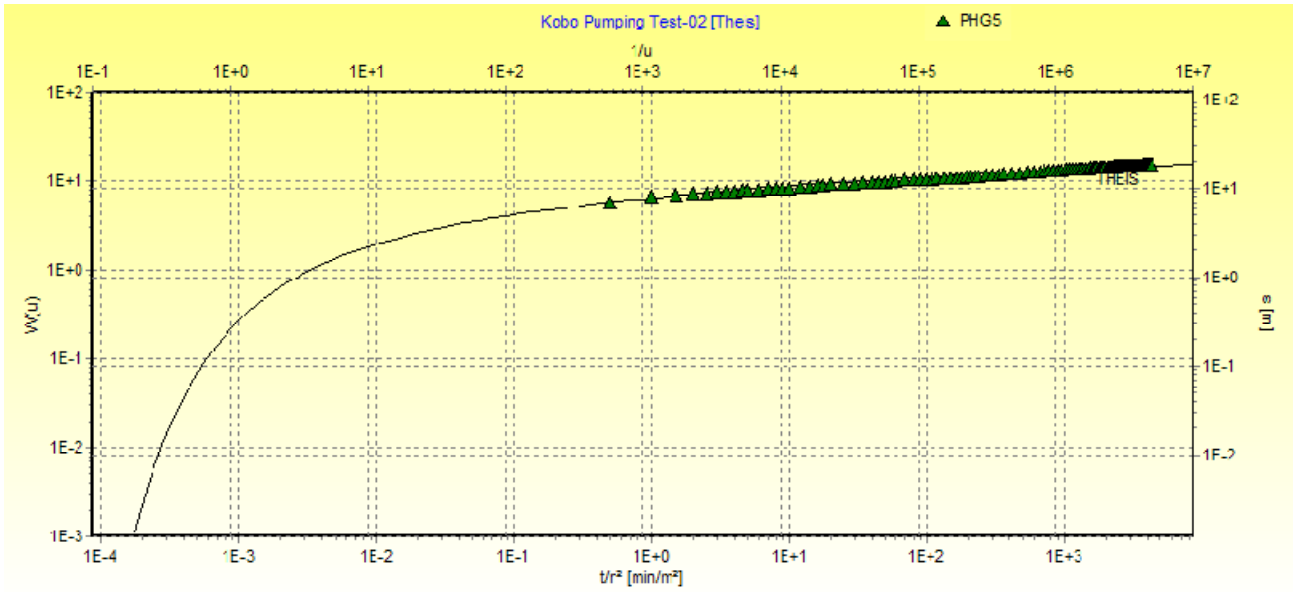

Transmissivity: 3.25E+2 m²/d Storativity: 7.83E-4
Conductivity: 7.73E+0 m/d

Appendix 2.3 Theis recovery graphs

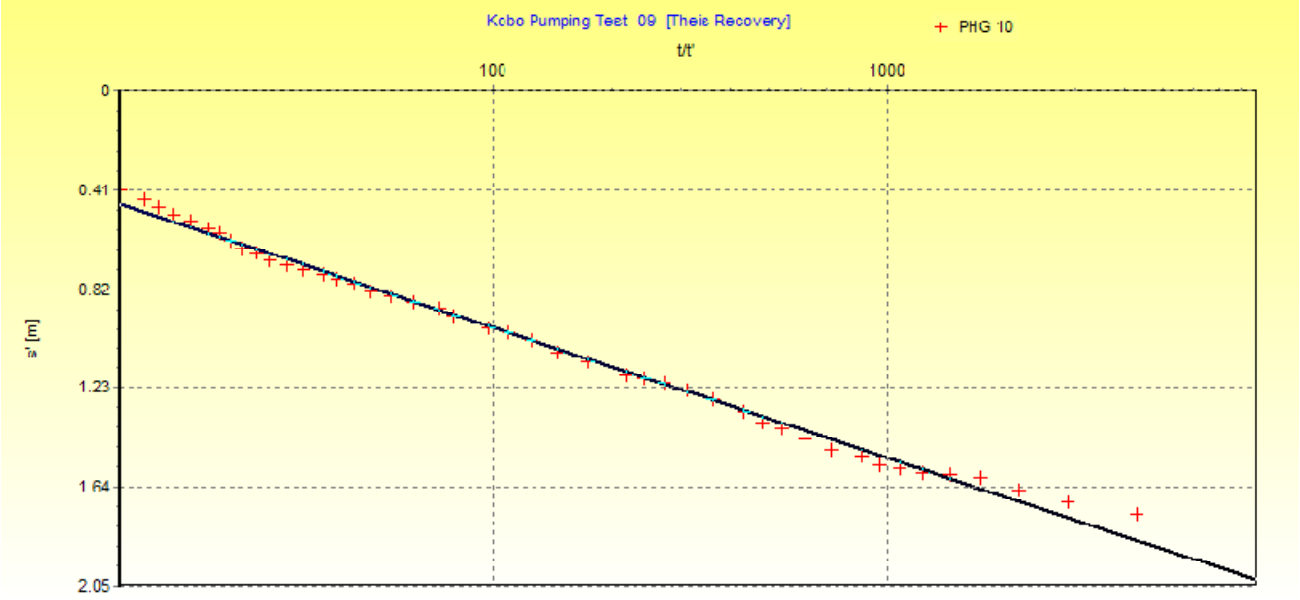

Transmissivity: 1.74E+3 m²/d
Conductivity: 3.87E+1 m/d

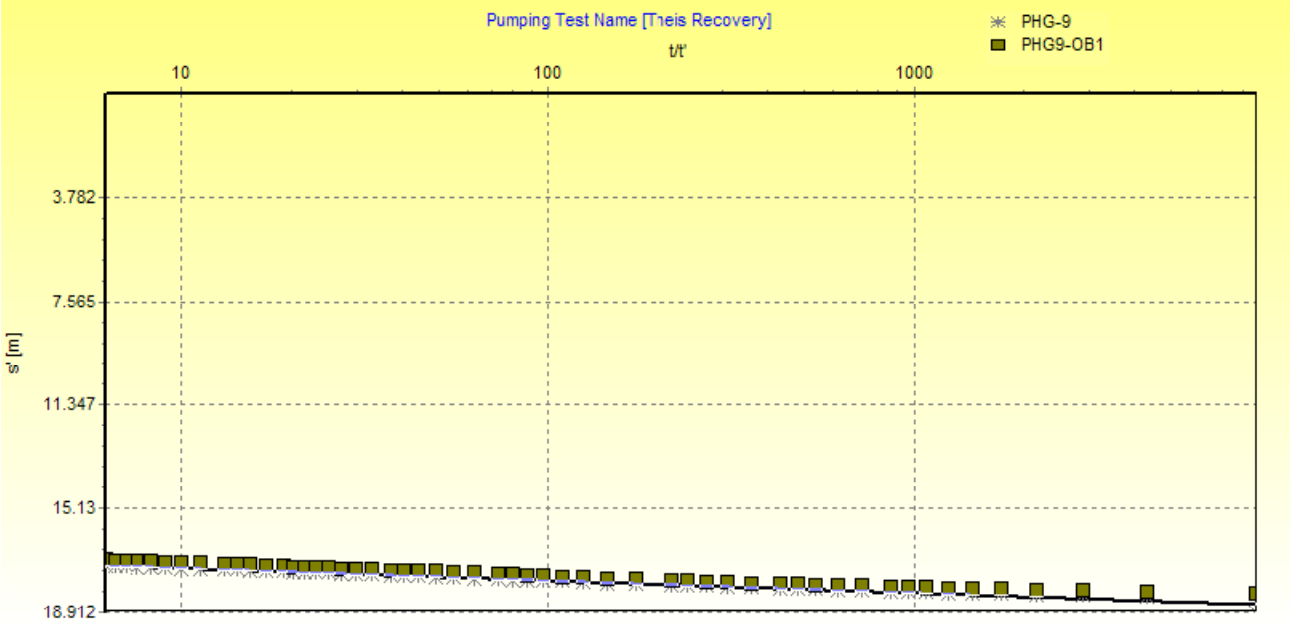

Transmissivity: 1.91E+3 m²/d
Conductivity: 3.98E+1 m/d

Appendix 3. The head difference between the observed and model simulated heads

Obsrev. Name	X	Y	Calculated head (m)	Observed head (m)	Residual head (m)
PHG4	566854	1339244	1451.82	1457	5.177
PK1-OB1	568085	1340948	1450.19	1457	6.808
PK1-OB2	568016	1340878	1450.25	1456	5.751
PHG1	567688	1338578	1449.55	1451	1.454
PHG1-OB1	567981	1338232	1455.00	1460.16	5.16
PHG3	568356	1337982	1448.21	1456.5	8.289
PHG4	566854	1339244	1451.83	1458	6.172
TK7	569334	1341467	1449.27	1461.3	12.029
PK8	569814	1341065	1448.67	1450	1.333
THG1	576389	1336995	1381.62	1373	-8.622
THG3	575804	1333200	1382.20	1381	-1.2
THG3-OB1	575802	1333150	1382.37	1382.29	-0.075
PK9-OB1	570100	1340420	1447.00	1437	-10.004
THG4-OB1	575471	1331124	1388.00	1395	7.00
THG4	575449	1331350	1386.75	1393	6.249
PHG7	572289	1334951	1395.00	1401	6
PHG6	571821	1334963	1413.00	1409	-4
PHG6-OB1	571868	1335028	1415.48	1409.2	-6.277
PHG8	570553	1334123	1430.50	1429	-1.503
PHG9	570154	1333909	1432.00	1434.00	2
PHG10	569657	1333976	1442.72	1436.9	-5.817
HG3	569659	1338130	1441.98	1441	-0.97
HG5	571782	1333845	1413.61	1413	-0.608
HG11	571055	1335915	1426.04	1426	-0.04
HG12	572295	1335804	1399.00	1400	1
HG13	571683	1336365	1422.03	1422	-0.03
HG14	571067	1336466	1415.00	1419	4
HG15	574997	1330600	1388.98	1397	8.02
HG17	574673	1331879	1389.68	1390	0.321
ZELEKE1	570187	1338097	1433.00	1431	-2
ZELEKE2	570658	1337490	1433.43	1432	-1.434
TW2	577087	1334495	1376.50	1375	-1.504
TW3	579090	1332043	1362.11	1361.69	-0.416
K38	568228	1336496	1450.10	1441.3	-8.8
K40	568020	1335266	1458.63	1457	-1.631
K43	574975	1334515	1389.59	1379.4	-10.189
K44	575015	1330461	1389.21	1394.8	5.588
K45	574378	1331442	1391.13	1392	0.869